LITHOFACIES, DIAGENESIS, AND PETROPHYSICAL PROPERTIES OF SELECTED SANDSTONES FROM THE MORROWAN KEARNY FORMATION OF SOUTHWESTERN KANSAS

by

Richard H. Franz
B.A., Wittenberg University, 1980

Submitted to the Department of Geology and the Faculty of the Graduate School of the University of Kansas in partial fulfillment of the requirements for the degree of Master of Science.

Anthony W Walton
Professor in Charge

Committee Members

For the Department

ACKNOWLEDGEMENTS

First, I would like to express my gratitude to my parents, Mr. and Mrs. Richard J. Franz, and family for their never-ending support and encouragement. I would like to thank Dr. A. W. Walton, Dr. W. R. Van Schmus, and Dr. D. Green for their assistance and efforts in reviewing this manuscript. I express my gratitude to Marvin D. Woody for his help in getting me started on this project. I also wish to thank Cities Service Company (Tulsa, Oklahoma) for obtaining isotope data and for the use of core Williams D-2, and G. James of the Kansas Geological Survey for his assistance in obtaining X-ray diffraction data. In addition, I express my gratitude to the Tertiary Oil Recovery Project and to the Kansas Geological Survey for their financial support, and for the use of materials and equipment.

TABLE OF CONTENTS

LIST OF TABLES

LIST OF FIGURES

ABSTRACT

A knowledge of lithofacies and their diagenetic modifications and petrophysical properties is essential to successful exploration and enhanced oil recovery. Five general lithofacies comprise the bulk of eight cores from the Kearny Formation. Lithofacies A is a glauconitic, fossiliferous, cross-bedded sandstone, which occurs in the lower part of the Kearny. Oil production has come from lithofacies B, C, and D. Lithofacies B of the upper Kearny is a feldspathic-lithic (shale clast) cross-bedded sandstone. Lithofacies C is a glauconitic, non-fossiliferous sandstone of the lower Kearny. Lithofacies D, from the lower and upper Kearny, is variable but is generally described as fine-grained, rippled sandstone with shale laminae. Bioturbated sandstone (lithofacies E) constitutes another facies from the lower Kearny Formation.

Diagenesis involved three general stages, and was important in controlling petrophysical properties. Early diagenesis included the formation of chlorite grain coatings in lithofacies C, D, and E. As a whole these coatings did not act to prevent quartz overgrowth cementation. Low porosity and permeability in lithofacies A is largely a consequence of mainstage cementation by ferroan calcite. Late stage diagenesis involved the formation of ferroan dolomite-ankerite, kaolinitization of K-feldspar, and dissolution of ferroan dolomite and feldspar. Dissolution was important in creating secondary porosity in lithofacies B. Liquid saturation porosity ranges from 0 to 21% and brine permeability ranges from 0 to 248 md. Relatively high permeability occurs in lithofacies B, C, D and E, and is associated with high porosity, good sorting, and coarse pore size distribution.

CHAPTER I

INTRODUCTION

Purpose and Significance of Study

It is generally recognized that in order to meet the petroleum needs of the future, enhanced oil recovery (EOR) methods will be necessary. EOR involves processes designed to extract oil remaining in reservoirs after primary drive production. This includes means of freeing the oil so it becomes mobile, drive mechanism to move the oil through the reservoir to the production well, and methods to increase permeability. Various fluids are injected into the reservoir to achieve this, including fresh water, brines, acids, and surfactants and polymers. In some cases it may be necessary to block off high permeability zones with gels first, in order that fluids contact oil remaining in low permeability areas. Success of EOR, depends upon a good understanding of how these processes work, and the nature of the reservoir as a permeable, potentially interactive medium. The potential for recovery is very good. In Kansas it has been estimated that the potential for production of oil from single pay fields through enhanced recovery is two to three billion barrels (Ebanks, 1975, p. 22). This underscores the importance of the Tertiary Oil Recovery Project (TORP) at the University of Kansas, under which this thesis was largely funded.

In order for EOR projects to succeed there must be a forehand knowledge of the geologic characteristics of the reservoir, because they control reservoir geometry and fluid flow (Ebanks, 1977, p. 92-107). Geologic characteristics include depositional environment and subsequent geometry and distribution of

sand bodies, distribution of textural parameters, and diagenetic modifications. TORP has incorporated geologists to provide input on the geological parameters that are of importance to reservoir engineering. This input serves to provide a basic understanding of how geological parameters correlate with petrophysical parameters. Porosity, permeability, and pore-size distribution are examples of petrophysical parameters. Ideally, this geological input along with the integration of petrophysical data will also be of use in the future in the case of attempted EOR projects in Kansas.

The purpose of this study of the Kearny, therefore, is fundamentally twofold. First, it is an attempt to demonstrate the geological controls of petrophysical properties of this formation, and with application to general understanding. Secondly, the aim is to provide geological and petrophysical information that will be of use in the future for enhanced recovery projects attempted in the Kearny Formation.

A number of geological properties influence petrophysical properties (Pettijohn et al., 1972, p. 525). Diagenetic mineralogy (cements) can be of great importance. Authigenic minerals occurring in the pore systems of reservoirs block such pores, and may react with injected EOR fluids resulting in their breakdown and possibly the precipitation of material in the pores (Peterson et al., 1982 p. 14-19). It is therefore important to be aware of the diagenetic character of a reservoir before initiating enhanced recovery. Because of the importance of diagenesis this thesis has focused on this aspect, and the relationships of diagenesis to petrophysical properties. An additional purpose, beyond description, is to interpret the diagenetic history of the Kearny Formation. This detailed petrographic study of the Kearny Formation is of

further significance because it contributes to our knowledge of the geology of the Lower Pennsylvanian in southwestern Kansas.

Study Area

Eight cores from the Kearny Formation in southwestern Kansas were used in this study (Table 1) (Fig. 1). All but one are part of the collection of the Kansas Geological Survey. Selection of these cores was made primarily on the basis of availability within a reasonable study area. An effort was made to represent different stratigraphic intervals within the formation. From these cores 117 samples were taken for thin sections and 91 for petrophysical analysis. Samples were chosen to represent different lithofacies, cement types, sedimentary structures, and grain sizes.

Previous Works

Two previous studies have concentrated on diagenesis and petrophysical aspects of Morrowan Stage sandstones. Adams (1964) recognized two types of marine sandstones in the lower Morrowan Stage sandstones in northwestern Oklahoma and the Texas Panhandle. Each type represents a distinct diagenetic facies. Sandstone type A is a well-sorted, non-glauconitic, non-calcareous, high energy nearshore facies (Adams, 1964, p. 1568). Diagenesis in these sandstones is characterized either by extreme pressure solution or by minor to moderate pressure solution and quartz overgrowths (Adams, 1964, p. 1569). Sandstone type B is an argillaceous, poorly-sorted, glauconitic, calcareous, and fossiliferous facies thought to represent deposition under lower energy conditions (Adams, 1964, p. 1568). Minor quartz overgrowths, calcite or dolomite cement (approach-

TABLE 1

CORES USED IN THIS STUDY

	CORE	LOCATION	DEPTH (meters)	STRATIGRAPHIC INTERVAL
1.	Williams D-2 (WD2)(Cities Service Co.)	19-33S-42W Morton Co.	1389-1402	upper Kearny
2.	1 Jones B (1JB)(KGS)	9-33S-41W Morton Co.	1562-1572	upper Kearny
3.	1 Low G (1LG)(KGS)	6-33S-40W Morton Co.	1661-1672	upper Kearny
4.	5 Low A (5LA)(KGS)	8-33S-40W Morton Co.	1741-1754	lower Kearny
5.	2 Gaskill A (2GA)(KGS)	10-33S-38W Stevens Co.	1845-1886	lower Kearny
6.	1 Nell A (1NA)(KGS)	19-33S-37W Stevens Co.	1871-1893	lower Kearny
7.	1 Pennington (1P)(KGS)	16-34S-32W Seward Co.	1839-1853	lower Kearny
8.	1 Bolan (1B)(KGS)	6-33S-29W Meade Co.	1774-1786	lower Kearny

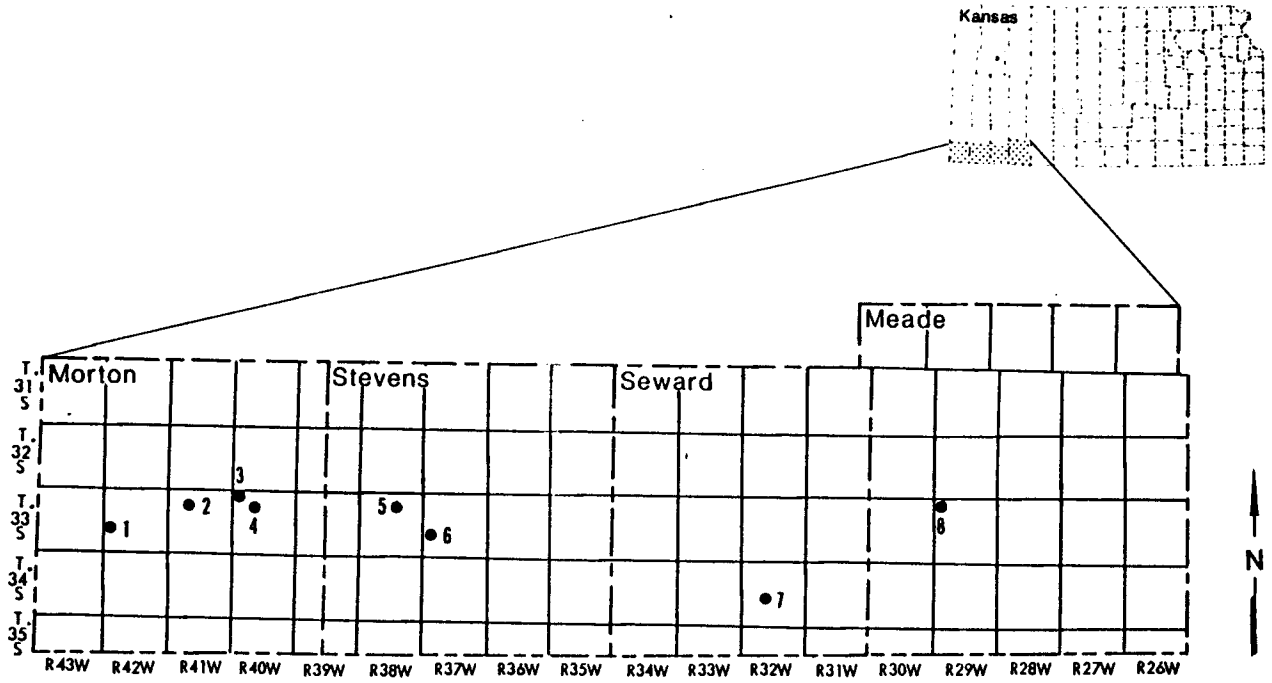

Fig. 1 Location of cores used in this study.

ing 50% of total rock volume), and authigenic chlorite and kaolinite characterize this diagenetic facies (Adams, 1964, p. 1577).

Porosity and permeability in these two sandstones were apparently controlled largely by diagenesis, with grain-size as an indirect control. Type A sandstones have original porosity and are permeable, if medium- to coarse-grained, and impermeable if fine-grained (Adams, 1964, p.1568). Numerical values for porosity and permeability were not given in the study. Adams believes more extreme pressure solution and the lesser amounts of cement required to destroy porosity are the factors responsible for the impermeable nature of the fine-grained rocks (Adams, 1964, p. 1577). In type B sandstones porosity is generally the result of dissolution of carbonate cement, which is sufficient to create commercial permeabilities (Adams, 1964, p. 1578). The results presented in Adams' study suggest a correlation between diagenetic facies and "petrophysical facies."

Kasino and Davies (1979) examined some upper Morrowan Stage sandstones from Cimmarron County, Oklahoma. They recognized the following diagenetic sequence: calcite and silica cements; compaction of ductile grains; dissolution of feldspar, rock fragments, cements, and matrix; silica overgrowths, with kaolinite and chlorite cements; calcite and ankerite cements; and partial removal of late-stage calcite and ankerite (Kasino and Davies, 1979, p. 189).

Effective porosity in these sandstones is secondary, and resulted from the dissolution of carbonate cement. Primary porosity was reduced by compaction of detrital clays, mica, and rock fragments. Porosity and permeability range from about 4 to 24 percent and 0 to 200 md, respectively. The authors suggest that the scatter of points found on their plot of porosity against permeability

reflects the secondary nature of the pores. They further believe, however, that porosity and permeability are directly related, which indicates the secondary pores are largely interconnected. Porosity and permeability are independent of grain size, which is also consistent with the secondary origin of the pores (Kasino and Davies, 1979, p. 189-193).

CHAPTER II

GEOLOGY OF THE KEARNY FORMATION

Nomenclature

In Kansas the Lower Pennsylvanian Series is equivalent to the Morrowan Stage. Rocks of this age occur in the state in the subsurface of western Kansas (Fig. 2). Such rocks were first reported and named the Kearny Formation in 1944 on the basis of the presence of the fusulinid Millerella (Zeller, 1968). The Kearny Formation was later expanded by McManus (1959). Throughout the mid-continent rocks of Morrowan age are most commonly known simply as the Morrow, or as the Morrow Formation.

Stratigraphy

The Kearny Formation consists of those rocks present between the generally oolitic limestone of Mississippian age and the overlying dark limestones and shales of the Atokan Stage. The upper boundary is usually easily picked on electric logs because of the distinctive "Thirteen Finger Limestone" of the Atokan. A coal bed commonly marks the start of Atokan rocks. The Kearny in Kansas is present within a depth interval of approximately 1300 m and 1900 m, and it ranges in thickness from 0 to 185 m. The formation thickens and occurs deeper to the south into the Anadarko Basin. In the basin deep Morrowan Stage rocks reach a depth of 3,720 m and a thickness of over 930 m (Swanson, 1979).

The Kearny Formation is not formally subdivided, but most workers recognize lower and upper portions. This applies to Morrowan Stage rocks in the Anadarko Basin and the Hugoton Embayment, as the stratigraphy is generally

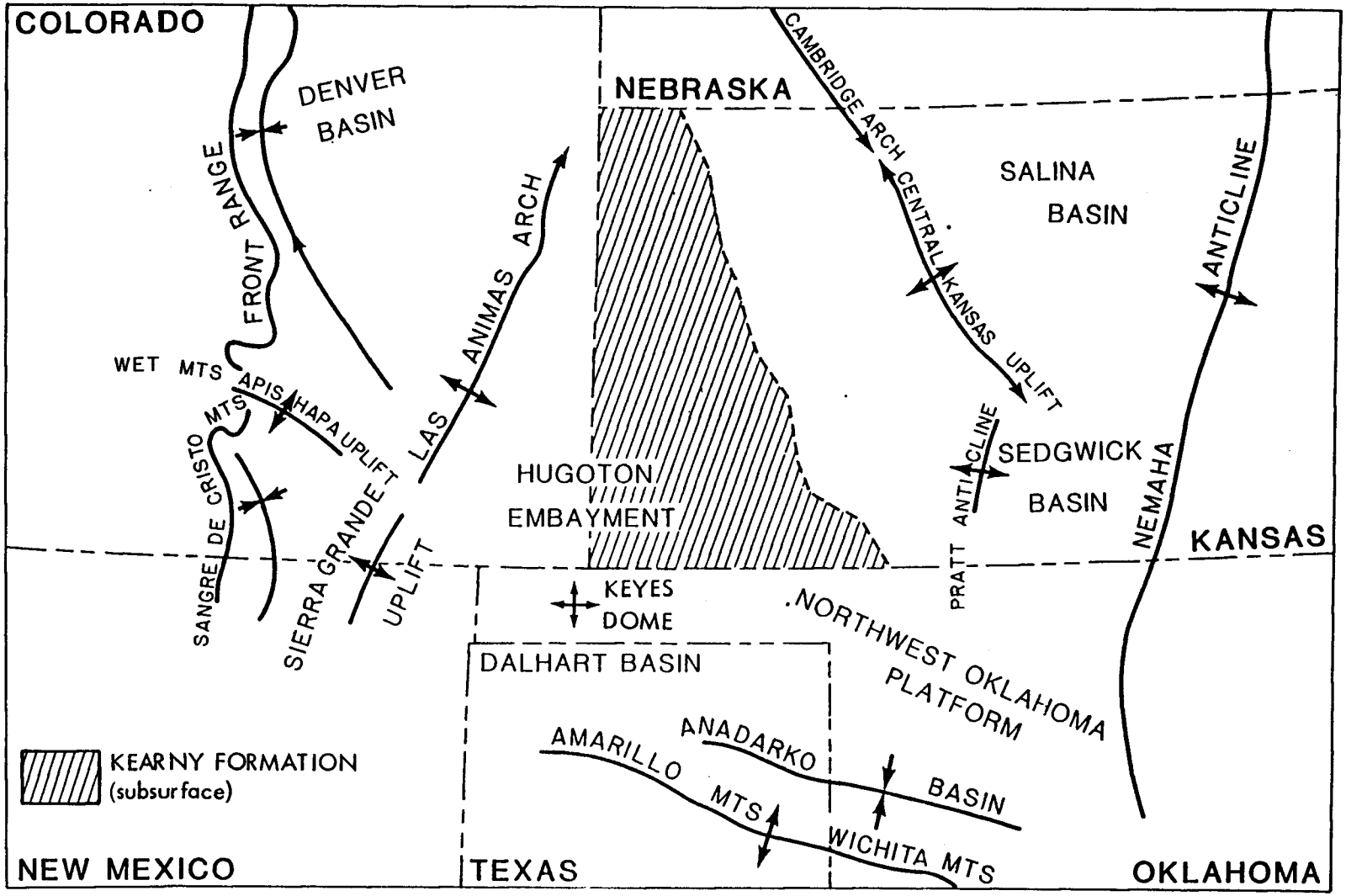

Fig. 2 Occurrence of the Kearny Formation and tectonic features of the southern mid- continent (after Merriam, 1955, McManus, 1959).

similar. A type log is shown in Figure 3. The lower Kearny consists of black shales and discontinuous limestones, sandstones, and fossiliferous sandstones. The upper Kearny is characterized mainly by black shales, carbonaceous shales and discontinuous, coarse-grained sandstones. Sandstones of different stratigraphic intervals have locally been assigned informal names or letter designations. The basal unit is generally known as the Keyes sandstones. Upper Morrowan sandstones have been referred to as the Purdy sands. The stratigraphy and lithologies of the Kearny Formation are presented in McManus (1959), which is a comprehensive reference on Morrowan stage rocks in western Kansas.

Structural Setting and Depositional History

During Morrowan time western Kansas was part of the Hugoton Embayment, which was an extension of the Anadarko Basin (Fig. 2). The confining uplifts included the Central Kansas Uplift, Sierra Grande Uplift, and the Las Animas Arch. These exposed areas and the Ancestral Rockies are considered possible source areas for Kearny Formation sediments (Swanson, 1979).

Deposition of the Kearny began with the trangression of marine waters northward out of the Anadarko Basin. Shallow marine environments prevailed throughout much of lower Morrowan time and into the upper Morrowan. Much sandstone and limestone was deposited as offshore bars and shoals along with some beach sedimentation. Subsurface analysis suggests cyclic trangression and successive shoreline stands through northwestern Oklahoma and southern Kansas (Busch 1961, Khaiwka 1968). During stillstands shoreline sequences developed along with offshore bars. Much of the coarse-grained sediments of the lower Kearny were deposited in structural or erosion lows, forming channel-fill and strike-valley sandstones (Busch, 1961).

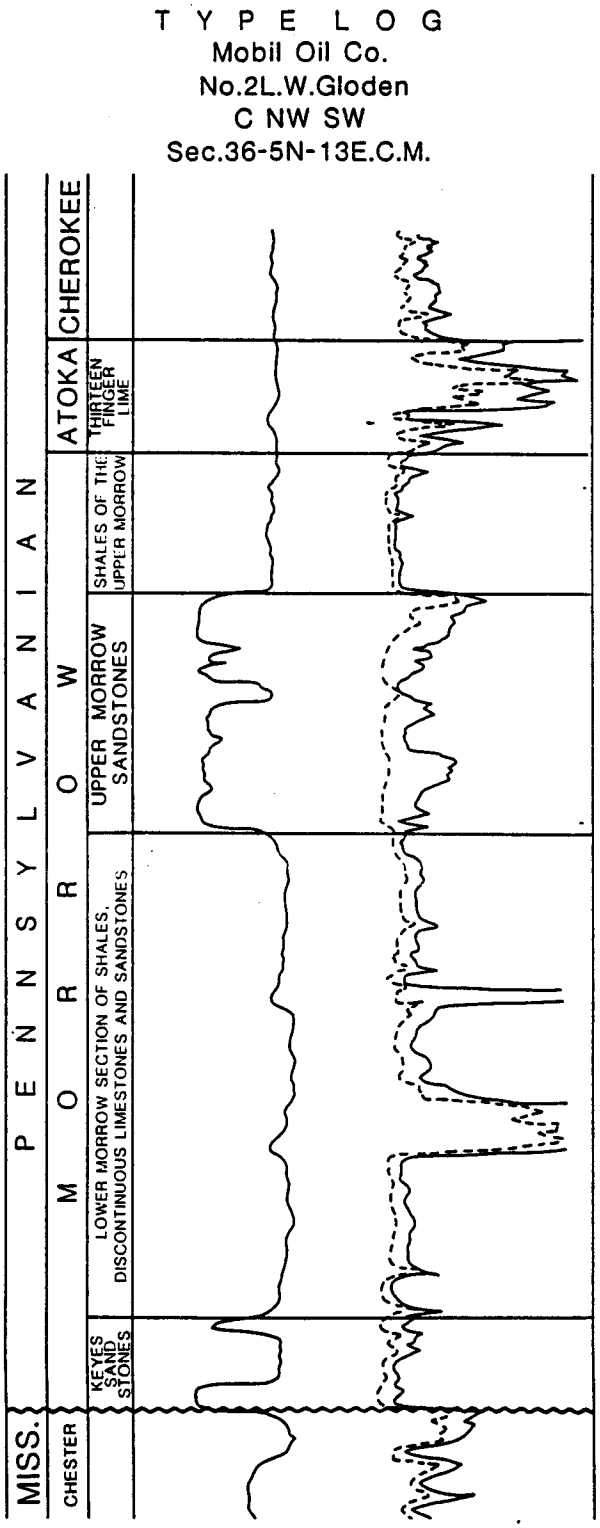

Fig.3 Typical electric log of Morrowan Stage and adjacent rocks in the Anadarko Basin (after Arro, 1965).

Late Morrowan time was characterized by a major deltaic progradation southeastward from Colorado into Oklahoma (Swanson, 1979). Fluvial-deltaic environments predominated although marginal-marine sedimentation also took place (Kasino and Davies, 1979). Oil production largely comes from stream-mouth bar, distributary channel-fill, and point bar sandstones of the upper Kearny. Minor transgression took place late in Morrowan time. The contact of the Kearny with the overlying Atokan rocks is in part an unconformity, but some sedimentation to the southwest and into the basin was continuous into the Atokan.

Petroleum Geology of the Morrow

Sandstone and conglomeratic deposits of late Morrowan age are most important as reservoirs in the Anadarko Basin and Hugoton Embayment (Swanson, 1979). Production also comes from sandstone deposits of early Morrowan time. The first discoveries in late Morrowan deposits were made in 1951 in Morton County, Kansas, and Ochiltree County, Texas. Subsequent early discoveries were made in Meade and Seward Counties, Kansas, and Ochiltree County, Texas. Some of the more prominent producing areas include the Interstate field in Morton County, Kansas, and the Camrick area of Texas County, Oklahoma. Most production has been wet gas with distillate, although pools of oil exist throughout the basin (Swanson, 1979).

Late Morrowan reservoirs represent point bars, distributary channel fills and stream-mouth bar deposits (Swanson, 1979). Other late Morrowan reservoirs include estuarine, tidal flat, beach and offshore bar deposits (Kasino and Davies, 1979).

Recent discoveries have been made in Morrowan Stage rocks in southeastern Colorado. Production comes from the lower Morrow Keyes sandstone and lower, middle, and upper sandstones of the upper Morrow. Reservoir rocks were deposited mostly in fluvial delta plain and tidal channel environments, and are erratically distributed. Individual sandstone bodies have widths up to 1 mile (1.6 km) and a maximum thickness of 42 feet (13m)(Avis and Boothby, 1982).

The majority of oil production from Morrowan Stage rocks in Kansas comes from the southwestern corner of the state (Morton, Stevens, Seward counties). Most comes from late Morrowan deposits at depths on the order of 4,000 to 5,200 feet (1240 to 1612m) and with reservoir thicknesses of generally 2 to 40 feet (0.6 to 12.4 m). The oil produced is fairly light (38-42 API) (Paul and Bahnmaier, 1981).

Enhanced recovery projects that have been employed to date in the Kearny Formation have been mostly by controlled waterflooding. Untreated brines, but mostly mixtures of fresh water and brine, have been used in waterflooding (Paul and Bahnmaier, 1982).

CHAPTER III

DESCRIPTION AND INTERPRETATION OF LITHOFACIES

Seven major, general sandstone and sandstone-shale lithofacies are represented in the cores used in this study. In addition, one major limestone and three shale lithofacies are present in the cores. Lithofacies are rock units that are objectively described (Reading, 1978, p. 4). These units are not meant to correspond to informal or formal subdivisions of a formation. Descriptions of each lithofacies are given first, followed by interpretations of depositional settings. Each lithofacies exhibits a range of characteristics and some overlap exists. Variations within lithofacies are discussed and related to particular cores. Simplified graphical core descriptions are compiled in Appendix A.

Description

Lithofacies A

Lithofacies A is a gray to brown, fossiliferous, cross-bedded sandstone (Fig. 4. It is distinguished as a lithofacies on the basis of the abundant fossil content. It is the most abundant sandstone type, amounting to about 23 percent of the total thickness of sandstone used in this study. Lithofacies A is present in four cores: 1NA, 2GA, 1P, and 1B. It is glauconitic and well cemented by carbonate. Lithofacies A is poorly to well sorted, with a majority (estimated modal) grain size of fine-medium to coarse, with coarsest grains ranging up to pebble size. Less abundant shale clasts up to 16 mm long are also present. Grain sizes and distributions are variable. A poorly sorted unimodal distribution occurs with a range from somewhat finer than the modal size to the coarsest size

Fig. 4 Lithofacies A. Structureless and high-angle cross-bedded. Scale is 10 centimeters.

Fig. 5 Lithofacies B. High-angle cross-bedded with textural laminations.

fraction. Improved sorting also occurs and the distribution is bimodal with a fine to medium quartz fraction and a coarse to very coarse quartz and skeletal fraction. Pelmatozoan and brachiopod shell fragments are the predominant fossil types. Some moderately-well to well sorted strata (less than 1 to 30 cm thick) of the finer and coarser fractions are also present, as are poorly sorted, conglomeratic zones. Bed surfaces may be marked by clay laminae. Both normally and inversely graded beds are present. There is some uncertainty about the nature of some grading because of difficulty in delineating bed boundaries. Several 10 cm, normally graded units occur in core 2GA; these range from very-coarse sand-granule size at the base to fine sand at the top. Some bedding surfaces are recognized by their uneven, erosive appearance. Such surfaces are immediately overlain by coarse to pebble size sediment containing clasts of blackl shale and either chert or phosphate. These beds probably represent storm deposition. A variation of this lithofacies occurs in core 1P where black, pyrite-bearing shale laminations are abundant.

Sedimentary structures in this lithofacies are also variable and include structureless intervals, horizontal stratification to low-angle crossbedding (less than 10^{o}) and relatively high angle cross-bedding (greater than 10^{o}). High angle bedding is most common. The angles measured on slabbed surfaces are commonly on the order of $10\text{-}15^{o}$, but it is likely that angles are higher based on observations of unslabbed surfaces. It is difficult to recognize vertical sequences of angle changes and individual cross-bed sets. In core 1P lithofacies A is horizontally-bedded to relatively low-angle cross-bedded. Core 1B is similar to 1P but is also characterized by somewhat wavy-bedding planes.

Upper and lower contacts are either transitional, erosional or abrupt. Underlying lithofacies can be either biotrubated sandstone (lithofacies E), interlaminated sandstone-shale (lithofacies F), sandy limestone, or black shale. Overlying lithofacies include very fine to fine grained cross-bedded sandstone (lithofacies D) or black shale.

Following the petrographic classification scheme of Folk (1980, p. 153-155), lithofacies A is generally described as a poorly to well sorted, medium to coarse sandstone: dolomite or calcite cemented submature to mature, glauconitic, fossiliferous subarkose to quartzarenite. Point counts indicate that skeletal material is about 10 to nearly 50 percent of the detrital mineralogy. Glauconite pellets constitute 3 to 23 percent of the detrital grains.

Lithofacies A is interpreted to have been deposited in a shallow marine environment under moderately high but fluctuating energy conditions. Fossils and authigenic mineralogy are strong indicators of depositional environment (Reading, 1978, p. 229-232). Pelmatozoans, brachiopods, mollusks, and bryozoans constitute an assemblage characteristic of normal marine salinity and shallow depth (less than 200m) (Reading, 1978, p. 229). Glauconite pellets are generally believed indicative of a marine environment (Reading, 1978, p. 231-232). Porrenga (1967) suggests glauconite is most common in a depth range of 30 to 700 m. Phosphate is present in lithofacies A as organic and inorganic grains. Phosphates are also most common in marine deposits (Reading, 1978, p. 230). Abundant glauconite is unlikely to be preserved in high energy shoreline settings (Spearing 1975, p. 114). Therefore it is probable that lithofacies A was deposited in the offshore environment.

Relatively coarse grain size (medium to coarse) and high angle cross-bedding suggest moderate to high flow velocities (40 cm/sec or greater) (Southard, 1975, p. 21). Sediment was most likely deposited as sand waves or dunes (Southard, 1975, p. 21, 24-25). The wide variation in grain sizes present in lithofacies A, alternating size-sorted strata, and other variations in sorting indicate that energy conditions fluctuated, and were episodic in nature. Normal grading can be interpreted as an indication of decaying currents (Pettijohn et al., 1972, p. 112). This may reflect waning storm conditions. Bagnold (1954) presented the concept of dispersive pressure to explain coarsening upwards (inversely graded) avalanche-face cross-strata.

Lithofacies B

Lithofacies B is brown, poorly to well sorted, feldspathic-lithic cross-bedded, medium sandstone to conglomeratic sandstone, which is slightly dolomitic (Fig. 5). It differs from lithofacies A by lacking fossils and is distinguished by its feldspar and lithic constituents. It occurs in three cores: 1JB, WD2, and 1LG, equaling about 18.5 percent of all sandstone lithofacies in this study. The modal grain size is medium to coarse and the coarsest grains are 9 mm pebbles. Most coarser grains range to 3-4 mm granules. Overall sorting is poor in that a wide range of grain sizes occurs throughout. Individual strata, however, are often moderately-well to well-sorted. Beds are usually 1-5 cm thick but in core WD2 they reach 10-13 cm thick, and these thicker zones are often more poorly sorted. The better sorted strata are commonly composed of the coarser fraction although they can be composed of the modal grain size. Conglomeratic layers sometimes overlie apparent erosional surfaces and occur at the base of the lithofacies. Normal or inverse grading is present in some beds.

A uniform, vertical grain size sequence, such as fining-up, is not present in lithofacies B. Less common features of this lithofacies include black shale laminae and carbonaceous streaks. Rare glauconite (WD2) and pelmatozoan fragments (1LG) are also present.

Lithofacies B is structureless or exhibits relatively high-angle cross-bedding (10-20 degrees). It is difficult to recognize sets or a particular vertical sequence of structures. In core 1JB, however, cross-bedding appears to be organized in 0.3 m thick units that trend upwards from relatively low to higher angle inclination. These units may be individual cross-bed sets.

Lithofacies B occurs as single intervals in three cores. It is 4.3m thick in 1JB, 7m thick in 1LG, and 7.3m thick in WD2. In each case it abruptly overlies interlaminated (or intercalated) silt-to fine sandstone and shale (lithofacies F) or carbonaceous, black shale. In core 1LG lithofacies B is in erosional contact with an overlying very-fine to fine-grained rippled sandstone (lithofacies D). In the other cores the overlying lithofacies is an interlaminated silt- to very-fine sandstone and shale (lithofacies F). The overlying contact is abrupt. In core 1JB two units of lithofacies B, 12.7 cm and 0.4 m thick, occur in the upper part of the core (Appendix A).

Petrographically lithofacies B is quite variable. It may be described as a poorly to well sorted medium to conglomeratic sandstone: dolomite- and quartz cemented submature to mature arkose to feldspathic litharenite. In core 1JB lithofacies B is an arkose, with detrital components including about 25 to 36 percent feldspar, (plus igneous rock fragments) and 2 to 8 percent rock fragments. In WD2 the composition ranges from arkose to lithic arenite to feldspathic litharenite. Feldspar and rock fragments ranging from about 21to 31

percent, and 7 to 29 percent. Shale clasts in core 1LG ranging from about 1 to 16 percent, with feldspar amounting to about 3 to 15 percent of the detrital grains. Such a composition places lithofacies B in core 1LG within the subarkose to predominantly sublitharenite range.

Lithofacies B in cores 1JB and WD2 are interpreted to have been deposited in a non-marine environment as sand waves or dunes under moderately high flow velocities. Lack of fossils and glauconite and associated lithofacies of probable non-marine origin suggest a non-marine environment for lithofacies B in these two cores. Non-calcareous shale that contains plant fragments and slickensides is associated with lithofacies B. This type of shale was most likely deposited in a marsh or floodplain environment (Potter et al., 1980, p. 33, 61).

Texture and the sequence of lithofacies in cores 1JB and WD2 are similar to other upper Morrow cores interpreted as deltaic in origin (Swanson, 1979). Upwards trending sequences consisting of non-carbonaceous shale; intercalated fine sand and shale; non-fossiliferous, coarse, cross-bedded sandstone; and laminated clay, silt and fine sand or carbonaceous shale are typical of Swanson's cores, 1JB, and WD2. In core WD2 carbonaceous shale underlies lithofacies B. The coarse sandstone lithofacies is interpreted by Swanson to be a stream-mouth bar or distributory channel deposit. Rare glauconite in these cores implies some minor marine influence or reworking.

Grain sizes and variations, and high angle cross-bedding are interpreted to represent similar flow conditions to those for lithofacies A. For lithofacies B, however, these upper flow regime conditions probably occured in a fluvial channel with episodes being related to periods of flooding.

In core 1LG lithofacies B is similar in character to that in 1JB and WD2 with the exception that it contains rare pelmatozoan fragments. This suggests a marine origin for the deposition of these sediments. This is discussed further under the section on interpretation.

Lithofacies C

Lithofacies C is a gray, moderately-well to very-well sorted, fine to coarse, slightly carbonate cemented, glauconite, cross-bedded sandstone (Fig. 6). Lithofacies C differs from A in that it contains few fossils. Cores 5LA and 2GA contain it, representing about 16 percent of the total thickness of sandstone lithofacies used in this study. It is moderately-well to very-well sorted, with the modal grain size being generally medium to coarse. As in lithofacies A and B, a coarser-grained fraction is present but to a lesser degree. Quartz, feldspar, black grains (phosphate, chert), and shale clasts in this coarser fraction range from coarse sand to pebbles up to 1 cm (shale clasts). Coarser grains tend to be more abundant in the lower portions of this lithofacies. Sorting decreases in association with this coarser fraction. In core 5LA this decrease in sorting is also evident in the upper one-fourth of the unit where it is overlain by bioturbated muddy sandstone (lithofacies E) containing abundant coarse to pebble size grains.

Lithofacies C is also characterized by well-sorted laminae and beds, a nearly bimodal grain size distribution in places, and graded beds similar to lithofacies A and B. Black clay laminae are abundant in this lithofacies, particularly in 5LA. These laminae define beds (1-5 cm) and are commonly developed into stylolites. High-angle (10 to 25 degrees) cross-bedding is the characteristic structure. It is difficult to recognize with certainty vertical

Fig. 6 Lithofacies C. High-angle cross-bedded with clay laminae (right).

Fig. 7 Lithofacies D. Rippled with clay laminae.

sequences within structures (angle changes). Some burrows are also present. Lithofacies C ranges in thickness from 1 to 8.5 m, and is overlain and underlain transitionally or abruptly by black shale or muddy bioturbated sandstone (lithofacies E).

A general petrographic classification of lithofacies C is: moderately-well to very well-sorted medium to coarse sandstone: calcite, dolomite, and quartz-cemented submature to mature glauconitic subarkose. Detrital constituents include an average of about 7 percent feldspar, 3 to 25 percent glauconite and less than one percent fossils.

Lithofacies C was deposited in a shallow marine environment generally similar to that under which A was deposited. Glauconite, grain size, and sedimentary structures suggest deposition on a marine shelf under moderately high energy conditions as sand waves or dunes. Storm related episodes of sedimentation occurred. Abundant glauconite and clay laminae are unlikely to be preserved in continual high energy shoreline settings (Spearing 1975, p. 114). As glauconite and clay laminae are abundant in much of this lithofacies, it is further likely that they were deposited in an offshore shelf environment.

Lithofacies C shows an upward sequence of improved sorting and lesser amounts of clay laminae. Because the upper portion of this lithofacies is cleaner and better sorted, a transition is inferred to have occurred from moderately high, variable energy conditions to somewhat higher energy, more continuous flow conditions. Offshore bars typically show characteristics reflecting an increase in energy conditions upwards, usually grain size increases upwards (Brenner and Davies, 1974; Spearing, 1975). Although lithofacies C does not

coarsen upwards, it seems to reflect increasing energy conditions in the upper portion. It therefore may represent deposition as an offshore bar.

Lithofacies D

Lithofacies D is brown to gray-green, very-fine to fine grained, carbonate and quartz-cemented, glauconitic, rippled sandstone (Figs. 7, 8, 9). Lithofacies D is delineated on the basis of fine grain size and the presence of abundant shale. Black, sometimes micaceous, shale laminae are characteristic and occur in abundances sufficient to describe this lithofacies as flaser bedded in part. "Flaser bedded" is used here to describe the relative abundance of sand (about 75%) and shale (about 25%) (Ruby et al., 1981, p. 43). Nearly equal amounts of sand and shale would be considered wavy bedded. Well developed lenses of mud, however, are not common. Most shale laminae are fairly continuous and wavy. In some instances it is possible to interpret this type of interbedding to have been generated under wave conditions because of associated ripple surfaces (Fig. 7). It is present in four cores (1B, 1LG, 1NA, 2GA) totaling about 15 percent of all sandstone types studied. In each core this lithofacies is distinctive. In core 2GA lithofacies D occurs as a 1.8 m interval overlain and underlain by lithofacies A. This unit is rippled with some bidirectional (?) current ripples and horizontal to slightly inclined planar lamination. A 7.5 cm interval of medium size sand occurs within this unit. Several wood fragments are notable constituents in this unit. This sandstone is further classified as a well-sorted, very-fine grained sandstone: quartz, mature, glauconitic quartzarenite. Glauconite pellets range from 14 to 20 percent of the framework grains and impart a green color to this unit.

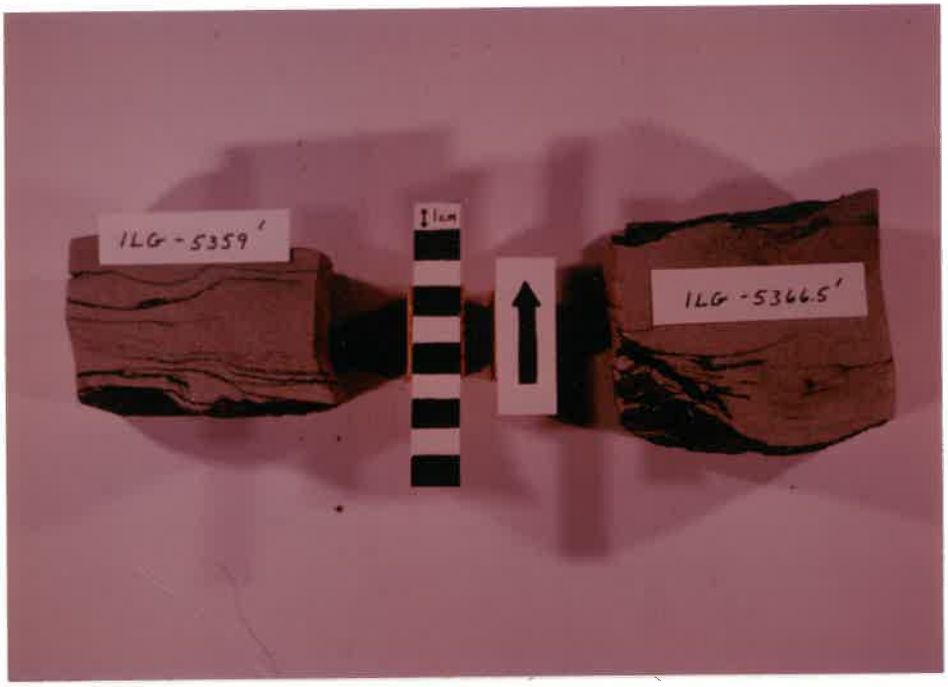

Fig. 8 Lithofacies D. Rippled.

Fig. 9 Lithofacies D. Cross-bedded with abundant clay laminae.

In core 1NA lithofacies D is distinctive in that it is cross-bedded with minor ripple cross-lamination and bioturbation. It is grouped with this lithofacies on the basis of textural similarities. Black clay laminations are abundant. Calcite cementation is also notable as patches associated with shell debris or as bands (Fig. 9). Petrographically this sandstone is a well-sorted, fine sandstone: calcite and quartz cemented mature glauconitic quartzarenite. Glauconite ranges from 14 to 17 percent of the detrital grains; skeletal and phosphatic grains range from 1 to about 1.8 percent each. Fossils and phosphatic grains are medium sand size.

Two units of lithofacies D are present in core 1NA, one of which is 2.2 m thick and is overlain and underlain by lithofacies A. The upper contact is somewhat gradational, the lower one is abrupt. The other unit is 1.2 m thick and is in abrupt contact above and below with intercalated glauconitic, fine sandstone and black shale (lithofacies F).

Lithofacies D is also present in cores 1B and 1LG. In 1B it is ripple cross-laminated with abundant pyrite-bearing black shale laminae. Rippled surfaces are rounded and symmetric. This unit is described as flaser bedded where black shale increases in abundance. Horizontal burrows are abundant. Petrographically this is a well-sorted, very-fine to fine sandstone: quartz cemented mature glauconitic quartzarenite. Glauconite content is 6 to 9 percent. Bioturbation has produced some mixing of sand and clay resulting in a less mature sandstone in places.

Two intervals of lithofacies D, 2.3 m and 3.6 m thick are present in core 1B. These intervals are separated by a meter of more extensively bioturbated sandstone (lithofacies E). The abrupt basal contact of the lower interval is with

lithofacies A. The upper contact is somewhat gradational with an interlaminated very-fine sandstone and black shale (lithofacies F).

In core 1LG lithofacies D is a unit 4.3 m in erosional contact with lithofacies B below. Sedimentary structures are similar to those in core 1B: ripple cross-lamination that grades into flaser bedding where black shale is more abundant. Throughout much of the unit, black shale laminae are less common than in core 1B. Some intercalation of black shale, silty shale, and very-fine sand occurs in the upper meter (wavy-bedded).

Although texturally and structurally similar in a general way to other units of lithofacies D, the section in 1LG is petrographically quite distinctive. It is classified as a very-fine to fine grained sandstone: immature micaceous, glauconitic, shale clast-bearing subarkose. Detrital matrix consists of silty, micaceous clay ranging from 23 to 30 percent (mean - 26.6 percent). Feldspar is predominantly microcline and ranges from about 0 to 11 percent of the detrital mineralogy. Glauconite ranges from about 0 to 0.8 percent, mica from 0 to 1.4 percent, and shale clasts from about 0 to 3.5 percent. The sand-size fraction is moderately-well sorted with some scattered medium-grained quartz present. Granule to pebble-size quartz grains are common in a 0.7 m interval beginning 0.7 m from the base of the unit. These coarser grains are in part concentrated in layers.

Lithofacies D is interpreted to have been deposited in a shallow marine environment under low and variable flow conditions. Evidence for a marine origin is similar to that for lithofacies A: fossils, glauconite and phosphatic grains. The presence of carbonaceous material may indicate a nearshore setting. Fine grain size and ripples imply low flow velocities (20-25 cm/sec) (Southard,

1975, p. 21). In core 1NA this lithofacies is cross-bedded, which suggests higher energy flow conditions. Abundant shale interbeds indicate that energy conditions fluctuated and at times were low enough to permit clay minerals to settle out. Ripple sets with planar bounding surfaces in core 2GA resemble current-produced ripples (Reineck and Singh, 1973, p. 30). Such currents may originate in a nearshore marine environment by tides. Rounded and symmetric rippled surfaces (core 1B) are characteristic of wave dominated environments (DeRaaf, Boersma, and Van Gelder, 1977).

Lithofacies E

Lithofacies E is glauconitic, bioturbated sandstone (Fig. 10). This lithofacies is distinct from the others because of the abundant bioturbation. Bioturbated sandstone is present in three cores (5LA, 1P, 1B) and comprises about 13 percent of the total sandstone lithofacies. Burrows are predominantly horizontal, circular to ovoid, less than 1 cm in diameter, and widespread throughout a given interval. Vertical burrows are also present (core 1B). Lithofacies E is subdivided into muddy and clean bioturbated sandstone (Fig. 10). In core 1B this unit is present as a muddy, extensively bioturbated version of lithofacies D. It is otherwise very similar to lithofacies D as it is characterized in core 1B, the two lithofacies being somewhat gradational. Three intervals are present: a 2.2 m basal section overlain by sandy limestone, a 0.5 m section above and below which lies lithofacies A, and a section 1 m thick separating two units of lithofacies D. In core 5LA muddy bioturbated sandstone is present as two units, 0.7 m and 2 m in thickness. Both are overlain and underlain by lithofacies C with relatively abrupt contacts. This sandstone is poorly-sorted

Fig. 10 Lithofacies E. Muddy (left) and clean bioturbated sandstone.

Fig. 11 Lithofacies F.

with a majority grain size of fine to medium and maximum grain size in the granule to pebble range (to 9 mm). Bioturbation has produced a homogenization of sand and clays. Clays are recognized in thin section as matrix: 3.8 percent and 7.9 percent in two point-counted thin sections. A petrographic classification of the bioturbated sandstone of 5LA is: slightly muddy, fine to medium sandstone: quartz cemented submature glauconitic, feldspathic, shale-clast bearing sublitharenite. Average glauconite and feldspar contents are 2.9 percent and 3.6 percent. Shale clasts comprise 5 to 10 percent of the detrital mineralogy.

Clean bioturbated sandstone is present in core 1P as a unit 7.2 m thick, underlain by lithofacies A and overlain by black shale. The lower contact is abrupt; the upper one is not present. It is further classified as a moderately-well sorted, very-fine to fine sandstone: calcite and quartz cemented submature slightly fossiliferous, glauconitic quartzarenite. Grain size distribution and texture are uniform throughout except for the lower 1.5 m. In this section granule- to pebble-size fossils, quartz, and shale clasts are present, in part concentrated over erosional surfaces. Black clay laminae are common to abundant and rarely they mark rippled surfaces. Circular to ovoid horizontal burrows are the predominant structural features. Their diameter ranges from several mm to about 3.5 cm for the long axis of elongate burrows. Burrow walls are not defined by grain size differences. Concentrations of glauconite mostly occur in burrows but may outline burrows. Calcite cementation is extensive but is concentrated in patches, many of which are associated with burrows, as a whole or as outlining features.

Lithofacies E was deposited in a marine shelf setting as is indicated by fossils, glauconite, phosphate, and burrows. Abundant trace fossils are another feature that indicates a marine setting, although not strictly shallow marine shelf (Reading, 1978, p. 230). Most burrows are horizontal and represent grazing activities of organisms, typical of the shelf Cruziana Ichnofacies (Dodd and Stanton, 1981, p. 269). Energy conditions were probably relatively low, permitting the preservation of burrows.

Lithofacies F

A sixth lifthofacies, F, is intercalated micaceous, glauconitic silt to fine sandstone and black shale (Fig. 11). It is similar to lithofacies D in part but is characterized by more abundant shale, which differentiates it from other lithofacies. It is present in five cores (1NA, 1LG, 1JB, WD2, 1B) totaling 9.5 percent of all seven sandstone lithofacies. The sandstone is characteristically moderately-well sorted, very-fine to fine-grained, and glauconitic. Wavy, laminated surfaces, ripples, and burrows are present, as is convoluted bedding. Three units occur with thickness of 1.3 m, 2 m, and 2.5 m. They are overlain and underlain with abrupt contacts by lithofacies A or C. Black shale is somewhat more abundant overall in this lithofacies than in the others, although it is similar to flaser bedded lithofacies D. Lithofacies F in core INA is described as flaser-bedded (less than 25% shale), to wavy-bedded (25 to 50% shale) (Ruby et al., 1981).

A petrographic description of this sandstone is moderately-well sorted very fine sandstone: calcite and quartz cemented submature glauconitic quartzarenite.

Lithofacies F is also present in cores 1JB, WD2, 1LG, and 1B where it is a horizontally interlaminated coarsesilt to veryfine micaceous sandstone and black shale. It ranges from 0.3 m to 1.3 m in thickness and occurs at the bottom or top of a core; sometimes as a transitional lithofacies to black shale. Petrographically this variation of lithofacies F (1JB) is a moderately well-sorted silt to very-fine sandstone: immature micaceous subarkose. A zone of iron-free dolomite replacement (84.2% dolomite), 8 cm thick, is an additional feature in core WD2.

Lithofacies F, in core 1NA, was deposited in a similar marine environment to that of lithofacies D. Greater shale abundance may indicate more prevalent low energy conditions, which permitted the settling of clays. In cores 1JB and WD2 lithofacies F probably represents overbank deposition in a deltaic environment.

Lithofacies G

Sandstone lithofacies G is a unit of interbedded lithofacies A and D that is present in core 1NA. Two units about 0.8 m and 4.4 m thick occur, comprising 4.9 percent of all sandstone. Overlying lithofacies include D or F and the underlying lithofacies is A. All contacts are abrupt. Within lithofacies G, approximately 7 to 15 cm beds of D alternate with 15 to 27 cm beds of A. More skeletal grains occur in lithofacies D than elsewhere in this core, some of which is concentrated in layers. Because it is composed of A and D, lithofacies G was not sampled as a distinct sandstone type.

TABLE 2

DETRITAL COMPOSITION OF LITHOFACIES

	Lithofacies A (7 samples)		Lithofacies B (15 samples)		Lithofacies C (11 samples)	
Grain Type	Mean %	Range %	Mean %	Range %	Mean %	Range %
Monocrystalline Quartz						
Straight Extinction	48.4	40.7 - 55.7	36.0	17.0 - 51.1	55.5	40.3 - 65.7
Slightly Undulose	4.0	2.0 - 6.8	7.5	1.1 - 16.0	11.4	4.8 - 19.8
Strongly Undulose	0.7	0.0 - 2.3	0.2	0.0 - 1.9	1.1	0.0 - 6.7
Semi-Composite Quartz	1.1	0.6 - 2.0	1.2	0.0 - 4.0	2.2	0.4 - 6.0
Composite Quartz						
Straight to Slightly Undulose	1.5	0.0 - 3.2	18.9	8.3 - 43.0	4.3	2.1 - 12.8
Strongly Undulose	0.1	0.0 - 0.4	1.2	0.0 - 6.5	0.3	0.0 - 1.4
Feldspar						
K-feldspar	1.7	0.0 - 3.8	15.8	3.3 - 28.6	7.4	2.8 - 13.0
Plagioclase	----	----	0.1	0.0 - 0.7	0.04	0.0 - 0.4
Igneous Rock Fragment	----	----	7.1	0.0 - 20.0	0.09	0.0 - 0.6
Shale Clast	0.9	0.0 - 2.3	9.7	1.1 - 29.1	2.8	0.0 - 11.9
Chert	0.3	0.0 - 1.1	0.5	0.0 - 2.3	0.3	0.0 - 1.4
Glauconite	13.5	3.0 - 23.3	0.1	0.0 - 0.9	10.3	3.4 - 24.6
Pelmatozoan	19.6	9.5 - 31.7	0.1	0.0 - 1.1	0.3	0.0 - 1.0
Brachipod and Mollusk	5.6	1.1 - 18.8	----	----	0.01	0.0 - 0.4
Byozoan	1.3	0.0 - 4.0	----	----	----	----

TABLE 2

DETRITAL COMPOSITION OF LITHOFACIES (continued)

	Lithofacies A (7 samples)		Lithofacies B (15 samples)		Lithofacies C (11 samples)	
Grain Type	Mean %	Range %	Mean %	Range %	Mean %	Range %
Organic Phosphate Fragment	0.2	0.0 - 1.0	----	----	0.1	0.0 - 0.4
Inorganic Phosphate Grain	0.9	0.0 - 2.0	0.05	0.0 - 0.8	0.3	0.0 - 1.0
Mica	----	----	0.14	0.0 - 1.2	----	----
Metamorphic Rock Fragment	----	----	0.0	0.0 - .3	----	----
Sandstone Rock Fragment	----	----	0.0	0.0 - .6	0.1	0.0 - 0.4
Siltstone Rock Fragment	----	----	----	----	----	----
Detrital Clay Matrix	----	----	0.5	0.0 - 7.5	3.3	0.0 - 25.7
Heavy Minerals	----	----	----	----	----	----

TABLE 2.

DETRITAL COMPOSITION OF LITHOFACIES (continued)

Grain Type	Lithofacies D (10 samples) Mean %	Lithofacies D (10 samples) Range %	Lithofacies E (8 samples) Mean %	Lithofacies E (8 samples) Range %	Lithofacies F (3 samples) Mean %	Lithofacies F (3 samples) Range %
Monocrystalline Quartz						
Straight Extinction	64.3	37.9 - 83.3	72.4	62.5 - 82.5	58.4	49.0 - 63.6
Slightly Undulose	6.6	3.8 - 9.6	5.6	3.0 - 8.1	3.8	5.0 - 11.2
Strongly Undulose	0.1	0.0 - 0.4	0.2	0.0 - 1.2	0.5	0.0 - 1.2
Semi-Composite Quartz						
Composite Quartz	0.7	0.0 - 1.9	0.4	0.0 - 0.9	0.1	0.0 - 0.4
Straight to Slightly Undulose	1.4	0.0 - 11.5	0.9	0.0 - 2.4	3.4	0.6 - 5.7
Strongly Undulose	0.8	0.0 - 7.0	0.2	0.0 - 0.8	0.0	0.0 - 0.0
Feldspar						
K-Feldspar	2.5	0.0 - 9.5	1.0	0.0 - 3.6	4.1	0.4 - 11.3
Plagioclase	0.2	0.0 - 1.4	0.0	0.0 - 0.0	0.7	0.0 - 2.1
Igneous Rock Fragment	0.1	0.0 - 0.6	0.1	0.0 - 0.3	----	----
Shale Clast	0.9	0.0 - 3.5	1.2	0.0 - 3.8	1.8	0.0 - 19.6
Chert	1.0	0.0 - 4.0	0.3	0.0 - 1.2	1.8	0.0 - 4.8
Glauconite	10.8	0.6 - 22.9	8.4	3.6 - 14.5	9.2	0.3 - 19.6
Pelmatozoan	0.2	0.0 - 1.6	1.0	0.0 - 6.0	0.4	0.0 - 1.3

TABLE 2

DETRITAL COMPOSITION OF LITHOFACIES (continued)

Grain Type	Lithofacies D (10 samples) Mean %	Lithofacies D (10 samples) Range %	Lithofacies E (8 samples) Mean %	Lithofacies E (8 samples) Range %	Lithofacies F (3 samples) Mean %	Lithofacies F (3 samples) Range %
Brachiopod and Mollusk	0.3	0.0 - 1.6	1.1	0.0 - 2.8	0.2	0.0 - 0.4
Bryozoan	----	----	0.0	0.0 - 0.4	----	----
Organic Phosphate Fragment	0.0	0.0 - 0.4	0.1	0.0 - 0.4	----	----
Inorganic Phosphate Grain	0.4	0.0 - 2.8	0.4	0.0 - 0.9	----	----
Mica	0.5	0.0 - 1.4	----	----	1.4	0.0 - 4.2
Metamorphic Rock Fragment	----	----	----	----	----	----
Sandstone Rock Fragment	----	----	----	----	----	----
Siltstone Rock Fragment	----	----	0.1	0.0 - 0.6	----	----
Detrital Clay Matrix	8.6	0.0 - 29.8	6.6	0.0 - 17.0	11.8	0.0 - 20.9
Heavy Minerals	0.1	0.0 - 1.2	----	----	----	----

Minor Sandstone Lithofacies

One minor sandstone type present in core 2GA is included for discussion because of its possible significance in terms of depositional environment. It is a carbonaceous, shaly, fine-grained sandstone that contains some coarse to granular shale clasts and shell debris. This facies appears to be similar to others that have been described as rooted. (Ruby et al., 1981, p. 39-40).

Two units are present, one 7 cm thick occurring in the black shale unit in the lower part of the core, and a 20 cm unit in the middle of the core. The latter is underlain by a thin (6 cm) non-clastic limestone, and overlain by lithofacies A. The upper contact is somewhat gradational in that lithofacies A is shaly where it overlies the rooted sandstone. This rooted sandstone indicates a depositional setting where vegetation can develop, such as the back-fringes of a lagoon. In this core it would represent a maximum regressive lithofacies.

Limestone

The major limestone lithofacies present is a sandy pelmatozoan grainstone. It resembles lithofacies A, but is more fossiliferous. Cores 1B and 1P contain 5.9 cm and 1.3 m units of limestone, respectively. In 1B this lithofacies abruptly overlies bioturbated sandstone and is transitional to lithofacies A above. This particular unit contains black shale laminae and has low-angle bedding. In 1P this limestone unit is in transitional contact with lithofacies A above and below, and appears structureless. Fossil content is evidence for a shallow marine environment for this limestone.

Shale

One of the three shale types present is predominant, consituting some or all of the shale in all cores but two (5LA, WD2). This shale is dark-gray to black, laminated, largely non-fossiliferous and well-indurated. This shale is normally also highly calcareous. Pelmatozoan, brachiopod, and fenestrate bryozoan fragments are rare with the exception of some intervals in core 2GA. In this core an interval of shale contains lenses of glauconitic, very-fine, sometimes rippled sand. This shale is marine in origin as indicated by marine fossils and calcareous cement (Potter et al., 1980, p. 48).

In cores 1JB and WD2 a dark-gray to black, laminated, carbonacous, non-calcareous shale occurs. In WD2 6.3 m of this shale underlies lithofacies B. This unit is slightly silty, micaceous, and contains occasional plant fossils and carbonaceous layers. Slickensides are common. In 1JB this shale is present at the top of the core and contains abundant plant fossils. Plant fragments and slickensides are features most characteristic of non-marine marsh or flood plain shales (Potter et al., 1980, p. 33, 61).

A third shale type is a calcareous green shale intercalated with non-elastic gray limestone. It occurs as a 10.2 cm unit at the base of core 5LA, separated from overlying muddy bioturbated sandstone by a 0.3 m gap in the core.

Interpretation of Lithofacies Sequences

The sequence of lithofacies represented in the cores investigated reflects a transition from dominantly shallow marine environments during early Morrowan time, to marginal marine-deltaic environments in later Morrowan time. This is the general model of sedimentation during Morrowan time in the Anadarko Basin

and Hugoton Embayment (Swanson, 1979). A wide variety of environments occurred including: shallow marine shelf, beach, barrier island, lagoonal, tidal channel, tidal flat, estuarine, and fluvial-deltaic (Avis and Boothby, 1982, Swanson, 1979, Kasino and Davies, 1979, Khaiwka, 1968, McManus, 1959).

This variability is in part reflected in the lower Kearny cores studied, making it difficult to construct an overall model of depositional history as represented by sequences. In general, however, sequences of coarse-grained lithofacies (A and C) and fine-grained (D, E, and F) indicate periods of shifting of lower and higher energy shallow marine environments.

Of the upper Kearny cores studied, 1LG is encountered next in the vertical succession. It is distinctly different from the lower Kearny cores but rare pelmatozoan fragments and glauconite indicate a marine setting. The sequence of lithofacies is similar to what might conceivably occur in a tidal channel, estuary, tidal flat environment. Such depositional environments were proposed for upper Morrow lithologies in Cimarron County, Oklahoma (Kasino and Davies, 1979). Lithofacies B and D are somewhat similar to estuarine and possible tidal flat deposits reported by Kasino and Davies. The sequence in core 1LG is: sandy limestone overlain by glauconitic, rippled sandstone and shale in abrupt upper contact with lithofacies B, which is in erosional contact above with lithofacies D. Lithofacies B contains a minor concentration of shale clasts and gravel at its base. This sequence could possibly represent an estuary or tidal channel (lithofacies B) that became reworked in its upper portion and subsequently overlain by tidal flat sands and flaser-bedded sands (lithofacies D).

The uppermost cores studied (1JB, WD2) show sequences similar to those described from other deltaic environments (Swanson, 1979). In particular, the

association of coarse-grained, non-fossiliferous, cross-bedded sandstone (lithofacies B) overlain by interlaminated shale, silt and sand (lithofacies F) and carbonaceous shale is similar to a channel fill, overbank, floodplain-marsh succession. The underlying lithofacies to this sequence may be marine sandstone-shale, shale, or non-marine shale. This would be compatible with deltaic progradation or distributory channel migration. Minor glauconite does occur, notably in lithofacies B of core WD2, which indicates some marine influence or reworking is likely.

CHAPTER IV

SANDSTONE PETROGRAPHY OF THE KEARNY FORMATION

Methods

Authigenic and detritial mineralogy of the Kearny Formation were studied in 117 thin sections made from samples from the eight cores used in the study. Thin section samples are numbered in Appendix A by core abbreviation and depth in feet. All thin sections were impregnated with blue epoxy to aid in recognition of porosity. Some thin sections were stained for carbonate cements using alizarin red-S and potassium ferricyanide following the method given by Dickson (1965). Some thin sections were also stained for K-feldspar and plagioclase feldspar following the method of Bailey and Stevens (1960).

In order to characterize the overall composition and pore types in the various lithofacies represented in the cores, 55 thin sections were point counted. Counts of 400 points were made using a standard rectangular grid system. Fewer points were counted on some coarse samples. Grain size was determined for 19 thin sections during point counting by measuring the long axis of 100 monocrystalline quartz grains (fewer on some coarser grained samples).

Supplemental techniques used in this study include scanning electron microscopy (S.E.M.), X-ray diffraction, isotopic analysis, and electron microprobe analysis. Carbon and oxygen isotopic ratios of four samples of carbonate cement were determined by Cities Service Company in Tulsa, Oklahoma.

Detrital Mineralogy

Quartz

Quartz grains are the most abundant component of the sandstone framework comprising about 37 to 62 percent. These subangular to subrounded grains range in size from coarse silt to pebbles (4 mm). They are dominantly monocrystalline and have straight to slightly undulose extinction. During point counting quartz was empirically classified on the basis of extinction (Folk, 1980, p. 73). Strongly undulose quartz is the rarest type, followed by semicomposite quartz. Polycrystalline quartz is abundant in lithofacies B of the upper Kearny, comprising 12 to 45 percent of the quartz grains. Polycrystalline grains in which the component crystals have straight or slightly undulose extinction formed one category of quartz. This type of grain is quite variable. Some are composed of crystals of approximately the same size and shape (equant). These grains are similar to recrystallized metamorphic grains (Folk, 1980, p. 69). Most of this type of polycrystalline grain is composed of crystals of differents sizes, often one to three medium to granular crystals with several fine to coarse size ones that may occur together. Another class of polycrystalline grains includes those in which the component crystals are strongly undulose or semicomposite, or in which the crystal boundaries are crenulated. Extremely crenulated boundaries characteristic of stretched metamorphic quartz (Folk, 1980, p. 71) are not present. Only one or two grains of quartz were observed that may be volcanic in origin. Such grains have a bipyramidal shape with straight sides, rounded corners, and embayments (Folk, 1980, p. 69).

Vacuoles ("bubble trains") are fairly common as inclusions in quartz grains although they are not particularly abundant. Rutile needles, sillimanite and

feldspar microlites are less common inclusions. Some intragranular porosity occurs in quartz grains, which probably resulted from the dissolution of feldspar microlites.

In lithofacies C, D, and E (core 1P), quartz grains have been coated by chlorite and subsequently mainly cemented by syntaxial quartz overgrowths. Carbonate cementation of quartz grains is most notable in lithofacies A and E, where it follows minor quartz overgrowths. Quartz grains are sometimes etched by carbonate cements.

Feldspar .

Detrital feldspar constitutes from 0 to 23 percent of the framework mineralogy. These fine sand to granule size grains are most abundant in lithofacies B in cores 1LG, 1JB and WD2(upper Kearny), and in lithofacies C in core 5LA. These cores are all from Morton County. Potassium feldspar, particularly microcline, is the predominant type present, and is much coarser than associated plagioclase. Microcline is recognized by its characteristc spindle or gridiron twinning (Scholle, 1979, p. 17). Plagioclase feldspar is recognized by albite twinning. Feldspars as a whole are distinguished from quartz by their somewhat weathered, brownish appearance. Staining was also useful in this study in the recognition of feldspars (Bailey and Stevens, 1960).

Feldspar overgrowths occur but do not appear to be abundant. Alteration of feldspars is common, including including dissolution or replacement by early chlorite, late ferroan dolomite-ankerite, late kaolinite, and sericite. Alteration is most notable in lithofacies B.

Skeletal Grains

Skeletal grains, or fragments of fossils that are made of calcite, range from 0 to 40 percent of the detrital framework and are characteristically very abundant in lithofacies A. These grains are generally coarser than much of the quartz fraction, ranging from medium sand to granule size. Pelmatozoan grains having unit extinction are predominant, many of which are recognized as crinoid fragments (Fig. 17). Crinoid ossicles are recognized by their porous structure and, particularly, their shape (Scholle, 1978, p. 93-95). Brachiopod shell fragments and spines are the next most abundant skeletal grain. These grains are identified by their low-angle parallel fibrous structure (Scholle, 1978, p. 75). Mollusk and bryozoan fragments are also represented. Mollusks are distinguished by crossed-lamelar wall structure and extinction pattern (Scholle, 1978, p. 81). Neomorphosed skeletal fragments are identified as bryozoans on the basis of the shape and orientation of the chambers (zooecia) (Scholle, 1978, p. 67-71). Rare miliolid foraminifera are also present in lithofacies A.

Skeletal grains are usually cemented by a relatively early-formed poikilotopic-overgrowth calcite, ferroan-calcite, or ferroan dolomite-ankerite. Some have been replaced by ferroan calcite and later by ferroan dolomite-ankerite. Others appear to have been dissolved, and the resulting pores filled with sparry ferroan calcite.

Glauconite

Glauconite in the form of rounded, ovoid, green grains (pellets) is abundant in all cores except WD2, 1LG, and 1JB. These pellets constitute 2 to 26 percent of the framework and range from very-fine to coarse sand size. They are recognized optically by their greenish color (sometimes brownish), earthy

texture, and scaly birefringence (Burst, 1958; Folk, 1980). Traditional interpretation of these pellets is that they originated by iron and potassium enrichment of parent illitesmectite (Burst, 1958). Recent work by Odin and Matter (1981) indicates this is the true origin of glauconite only in rare cases. Their interpretation is that glauconite forms by the growth of a glauconite mineral (glauconitic smectite) in the pores of a substrate. the most important factor is the micro-environment. Substrates can be anything that is porous including fecal pellets, skeletal grains, rock fragments, and micas. Some grains observed in the Kearny Formation represent the replacement of pelmatozoan debris. Glauconite formation takes place on the marine shelf (greater than 50 m depth) in areas of slow sedimentation where reducing conditions prevail (Odin and Matter, 1981, p. 636, 639). A semi-confined microenvironment within the substrate is necessary, although exposure to open sea water is also needed to provide a source of ions (Odin and Matter, 1981, p. 639). The structure of the pellets observed in S.E.M. this study resembles smectite or mixed layer smectite-illite According to Wilson and Pittman (1977) the mineral glauconite may morphologically resemble smectite, smectite-illite, or illite. Odin and Matter (1981) report structures that appear distinctive from smectite, but they suggest glauconite minerals may have forms similar to other phyllitic and non-phyllitic minerals (p. 616).

Despite the fact that these glauconite pellets resemble smectite (or the mineral glauconite), there is evidence that they may be dominated mineralogically by chlorite. The birefringence of some pellets suggests they have undergone some alteration to chlorite, in that in these particular grains part or all of the grain has an ultra-blue anomalous birefringence characteristic of chlorite.

Authigenic chlorite coats are better developed on glauconite grains than on any other detrital grains, which may be an indication the grains themselves are chloritic. The strongest evidence, however, comes from X-ray diffraction data obtained on samples of the silt and clay-size fraction. These data reveal that samples particularly rich in glauconite yield very prominant chlorite peaks and minor peaks that may in part reflect the glauconite mineral family (Fig. 12). Glauconite pellets that are composed of equal amounts of chlorite and the mineral glauconite have been documented (Burst, 1958). The chloritic compostion may have arisen in two ways. Chlorite could have formed by the alteration of smectite, as a form of marine diagenesis (Grim, 1968, p. 537). In addition, or alternatively, the mineral glauconite probably has altered to chlorite. Dapples (1967) believes this is a common conversion that represents an advanced stage of shallow burial diagenesis.

Phosphatic Grains

Detrital grains composed of phosphate are present (up to 1.2 percent) in lower Kearny sandstones. Organic phosphate grains (shell fragments) are present (Scholle, 1978, p. 153, Scholle, 1979, p. 40). Some of these grains have been fractured during compaction. Inorganic phosphatic grains range in grain size from very-fine to very-coarse sand and are present in both inclusion free and inclusion-bearing varieties. Quartz grains predominate as inclusions but shell fragments can also occur. Some phosphate grains exhibit a concentric (ooid) structure but the majority are structureless. Inorganic phosphatic grains may have orginated as the alteration product of glauconite-fecal pellets, as intraclasts, or as ooids.

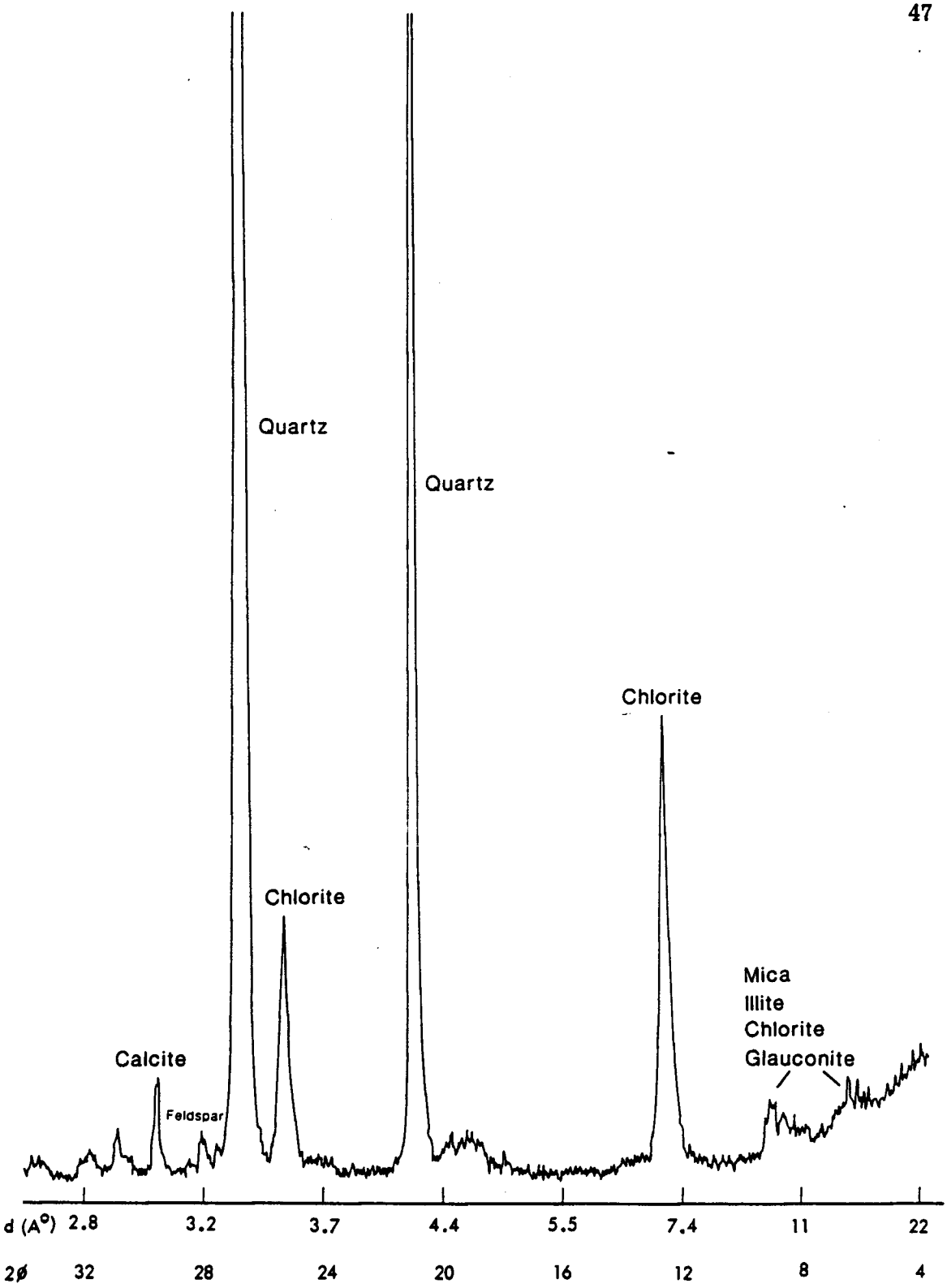

FIG.12

Pressed pellet X-ray diffractogram of silt and clay fraction-lithofacies D(2GA-6029.9)

(Data obtained at the Kansas Geological Survey.)

Lithic Fragments

Rock fragments comprise 0 to 31 percent of the framework grains. Igneous rock fragments and shale clasts are the most abundant types present followed by chert. Metamorphic rock fragments and siltstone fragments are rare and volcanic fragments are not present.

Igneous Rock Fragments

Igneous rock fragments compose 0 to 20 percent of the detrital grains in lithofacies B. These grains are medium sand to pebble size. Several types of these fragments occur, one of which is composed of quartz, K-feldspar, and in some plagioclase crystals in the fine to very-coarse size range (Fig. 13). Another type of igneous rock fragment is composed of finer-grained (microcrystalline to coarse silt) quartz and K-feldspar, and may also contain coarser (fine to medium) crystals of quartz, K-feldspar, or plagioclase (Fig. 14). A few of these grains also contain muscovite. A third type of fragment judged to be igneous is K-feldspar that contains smaller crystals of quartz and sometimes plagioclase. Igneous rock fragments are recognized as such on the basis that they are composed of relatively coarse-grained quartz, feldspars and muscovite (Scholle, 1979, p. 33). These grains differ from volcanic fragments in that they lack lath-shaped feldspars and ferromagnesian minerals (Folk, 1980, p. 85). Some of the greater than sand-sized fragments that are composed of coarser crystals might alternatively be classified as gneiss fragments. The finer-grained, often feldspar-rich, fragments might also be classified as hypabyssal (Dickinson, 1970). Feldspars in some have experienced some dissolution and replacement by sercite and kaolinite.

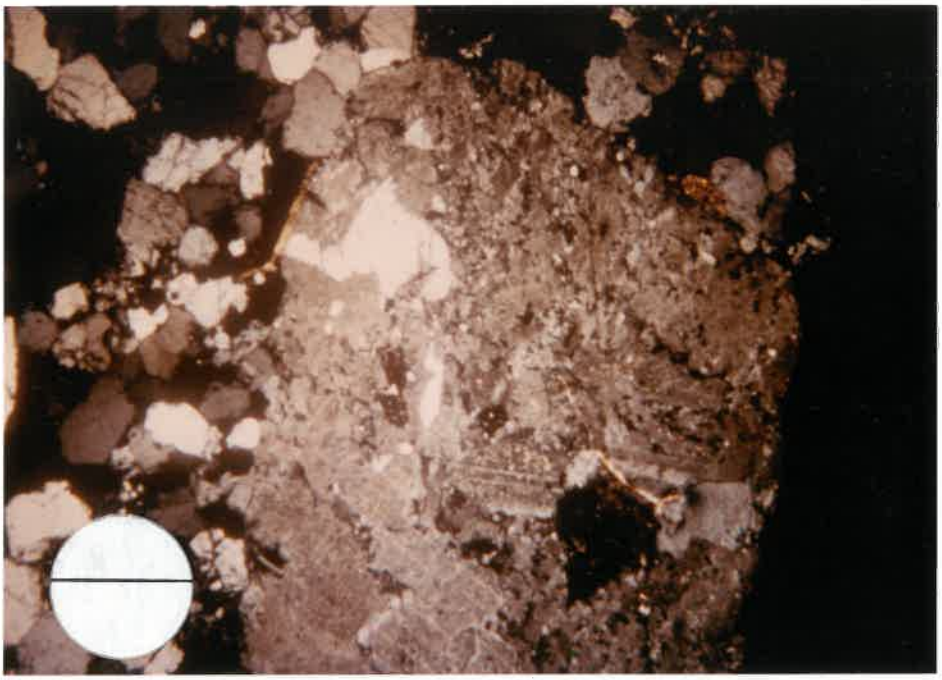

Fig. 13 Coarse-grained igneous rock fragment - lithofacies B.
Bar = 0.8mm. XN.

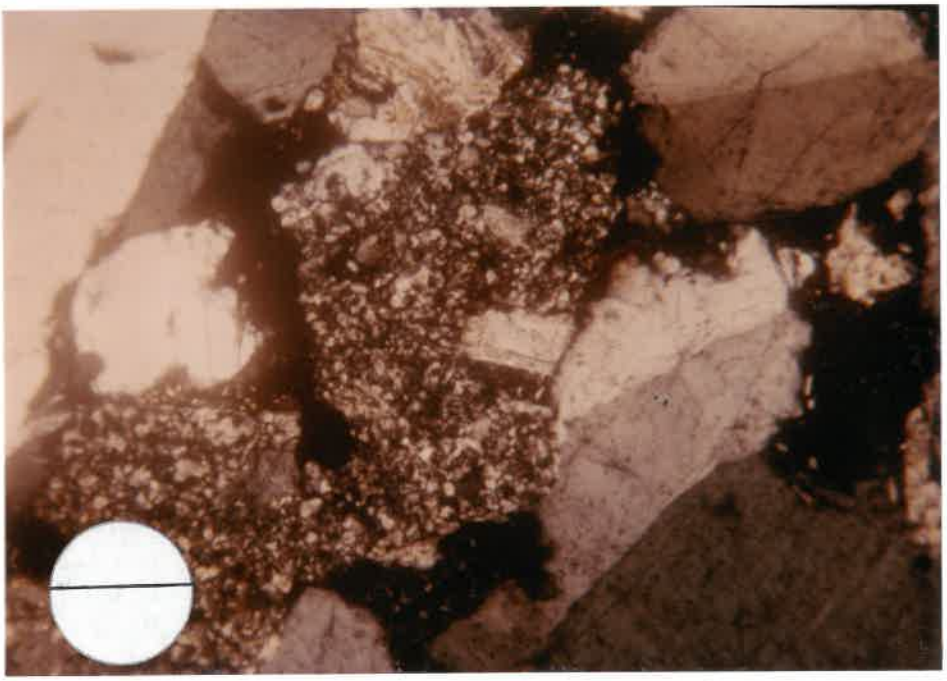

Fig. 14 Fine-grained igneous rock fragment - lithofacies B.
Bar = 0.2mm. XN.

Igneous rock fragments are not listed among the common lithic constituents in sandstones (Pettijohn et al., 1972, p. 187). Presumably igneous rock fragments tend to break down readily and thus are not generally preserved. Their presence in upper Kearny sandstones may suggest relatively short transport.

Shale Clasts

Grains composed predominantly of clay minerals and lesser amounts of quartz silt, and which have a certain degree of structure (fabric) are described here as shale clasts. These grains are present in all sandstone lithofacies and range in percent from 0 to 20. They range in grain size from fine sand to pebble size. Some of these grains may be true sedimentary (shale) rock fragments, particularly those present in the marginal marine-deltaic sandstones of the upper Kearny. Because shale fragments are easily abraded it is believed that they can only survive brief transport (Folk, 1980, p. 88-89). Those grains present in marine Kearny sandstones, and possibly the majority of such fragments, are probably intraclasts. Because of the uncertainty as to the precise origin of these argillaceous grains, they are referred to generally as shale clasts.

Most shale clasts are predominantly composed of clay minerals; many have a preferential orientation (fabric). Quartz silt may or may not be present. Commonly these grains are compacted and squeezed in between more competent grains In this manner they constitute pseudomatrix (Dickinson, 1970). Shale clasts in upper Kearny sandstones may be oxidized in that they appear orange in thin section.

A distinctive type of argillaceous "grain" is present in addition in core 1LG (Fig. 15) (lithofacies B). This material is grain-like in that it bears some indication of a concentric internal structure, and it does not occur dispersed throughout as detrital matrix usually is. These clasts appear oxidized, contain quartz silt, and are replaced by fine-grained carbonate. They usually have undergone dissolution, which makes it difficult in some instances to recognize them as grains as opposed to loose, silty argillaceous detritus.

Because these grains are quite different from other true shale clasts it is appropriate to consider an alternative origin. This material is not compacted as other clasts in the same section are. Thus, possibly they were not deposited with the rest of the detritus that subsequently underwent compaction, but rather were introduced later as mechanically-infiltrated clay matrix. Crone (1974) has shown that mechnical-infiltration below the water table may produce randomly distributed void-filling flocculated aggregates.

Other Types

Chert grains recognized in thin section are generally fine to coarse sand size, composed of microquartz (less than 5 microns) and megaquartz (greater than 20 microns) (Folk, 1980, p. 79). The maximum amount of chert is 1-2 percent. The brownish color of these grains may be attributed to liquid inclusions (Folk, 1980, p. 79). These constitute the only inclusions present. Two metamorphic rock fragments were observed in thin section. These grains are composed of relatively coarse-grained muscovite and are interpreted as schist fragments (Scholle, 1979, p. 31). One siltstone rock fragment was observed in thin section (Scholle, 1979, p. 29).

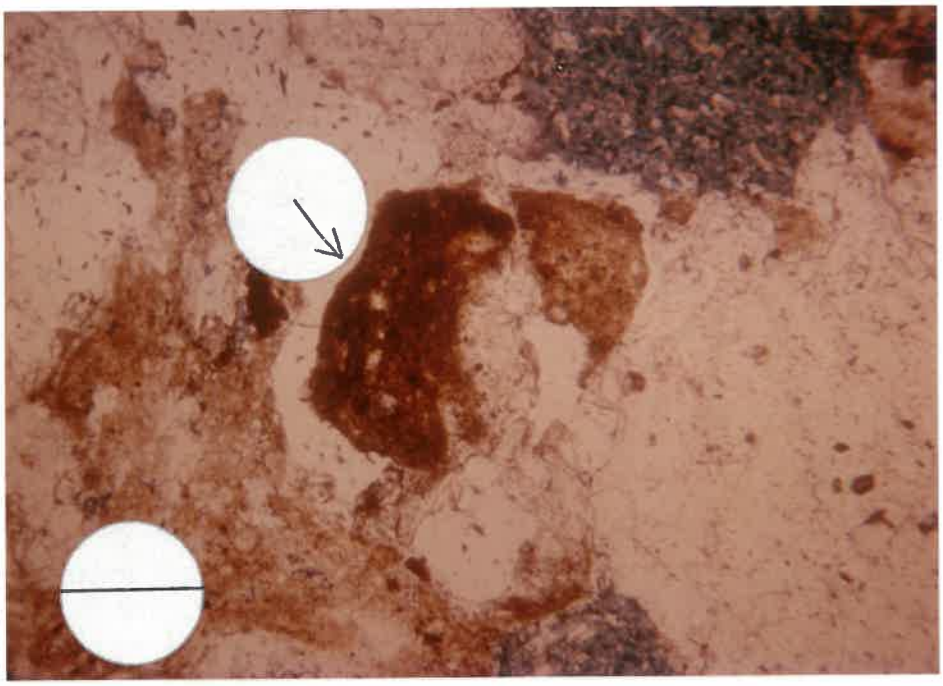

Fig. 15 "Shale clast" (arrow) - lithofacies B.
Bar = 0.2mm. PL.

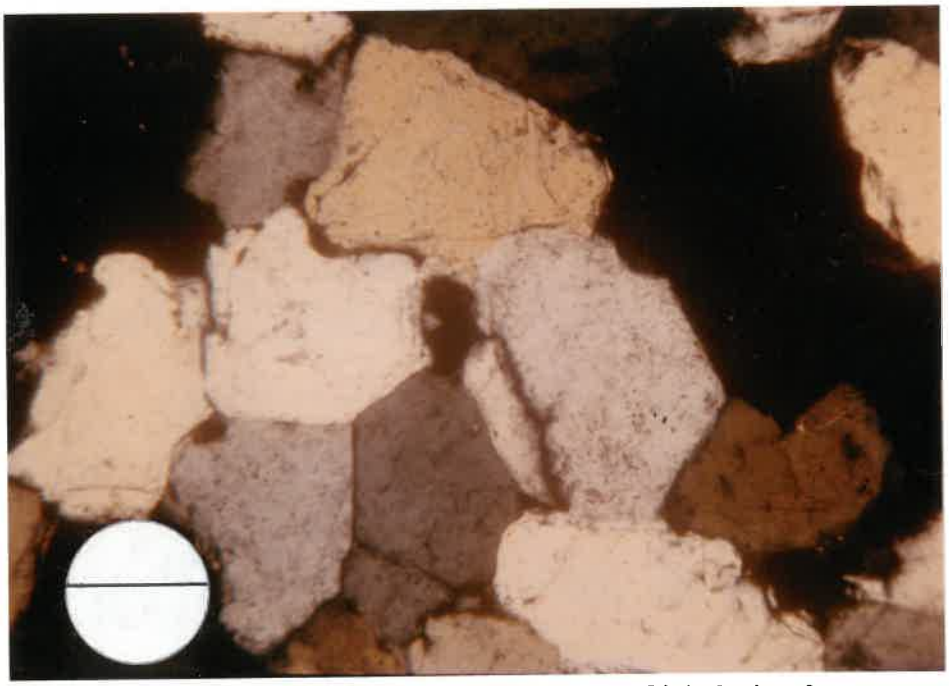

Fig. 16 Interlocking quartz overgrowth cement - lithofacies C.
Bar = 0.2mm. XN.

Accessory Minerals

Minerals occurring in amounts of about one percent or less of the detrital mineralogy include micas, zircon, and tourmaline. Among these, micas (particularly muscovite) are more common. Micas tend to be more commonly associated with detrital clay laminae and matrix, others have sometimes been bent during compaction.

Matrix

True detrital matrix (protomatrix) is recognized as material composed predominantly of clay minerals with quartz silt and mica, and which lacks characterisitcs of shale clasts (Dickinson, 1970). This material is generally well-dispersed throughout the rock, or is present adjacent to shale laminae. Protomatrix is present in the very-fine to fine-grained sandstones of lithofacies D and F. It has also been introduced through bioturbation (lithofacies D and E).

Authigenic Mineralogy

Authigenic minerals present in the Kearny Formation sandstones studied include pore-lining and pore-filling cements, and minerals that occur as replacements or alterations of other grains and cements. A wide variety of diagenetic features occur. A smaller number are of prime importance in this study as they exert some control on porosity and permeability, or have the potential to do so, or might interact with reservoir stimulation fluids. Important authigenic minerals include quartz, ferroan calcite, calcite, ferroan dolomite-ankerite, chlorite, and kaolinite. Authigenic minerals are described in this section; diagenetic history, conditions of formation, and source materials are discussed in a later section.

Quartz

Authigenic syntaxial quartz overgrowths on detrital quartz are present in all sandstone lithofacies, although their abundance has a wide range. Lithofacies C bears the best development with overgrowths ranging from 13.8 to 18.0 percent of the rock (Figs. 16, 17). Lithofacies D and E (in core 1P) are also characterized by extensive quartz cementation. The poorest development of authigenic quartz overgrowths (as low as 0.8 percent) is in lithofacies A where carbonate cementation is more important.

Overgrowths are mainly recognized by "dust-lines" that mark the boundary between detrital grain and authigenic quartz. Such lines are common in Kearny sandstones and this facilitated the recognition of overgrowths. Euhedral grain boundaries and protuberances also indicate authigenic overgrowths. Where chlorite is present it usually pre-dates quartz overgrowths, otherwise they represent the earliest cement. Some chlorite has grown on quartz overgrowths.

Ferroan Calcite

Calcite pore-filling cement containing 0.4 to 2.0 mole percent iron calcite is the predominant authigenic calcite, particularly in lithofacies A where it constitutes 20.8 to 34.8 percent of the rock. Ferroan calcite is recognized after staining as a royal blue or purple color. Lithofacies A in core 1P differs in that it is mainly cemented by ferroan dolomite, with ferroan calcite cement ranging from 3.2 to 6.8 percent of the rock.

Ferroan calcite is clear, generally untwinned, and is present in several morphologies. The major modes of occurrence are as syntaxial overgrowths on pelmatozoans and as poikilotopic cement enclosing quartz grains (Fig. 18).

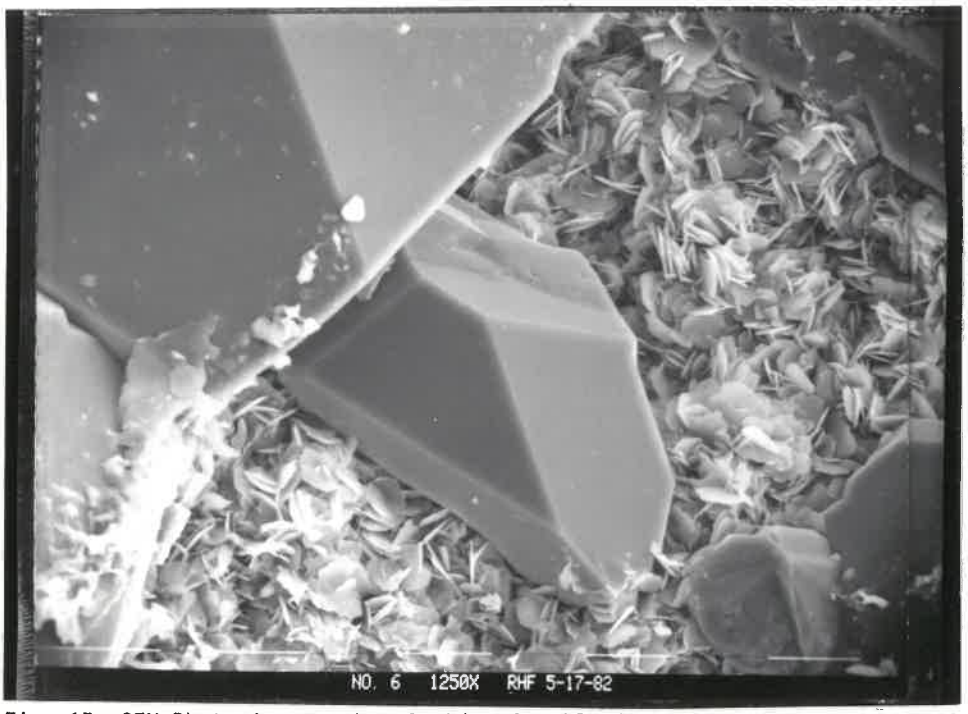

Fig. 17 SEM Photomicrograph - Authigenic chlorite overgrown by authigenic quartz - lithofacies C. White bars = 10 microns.

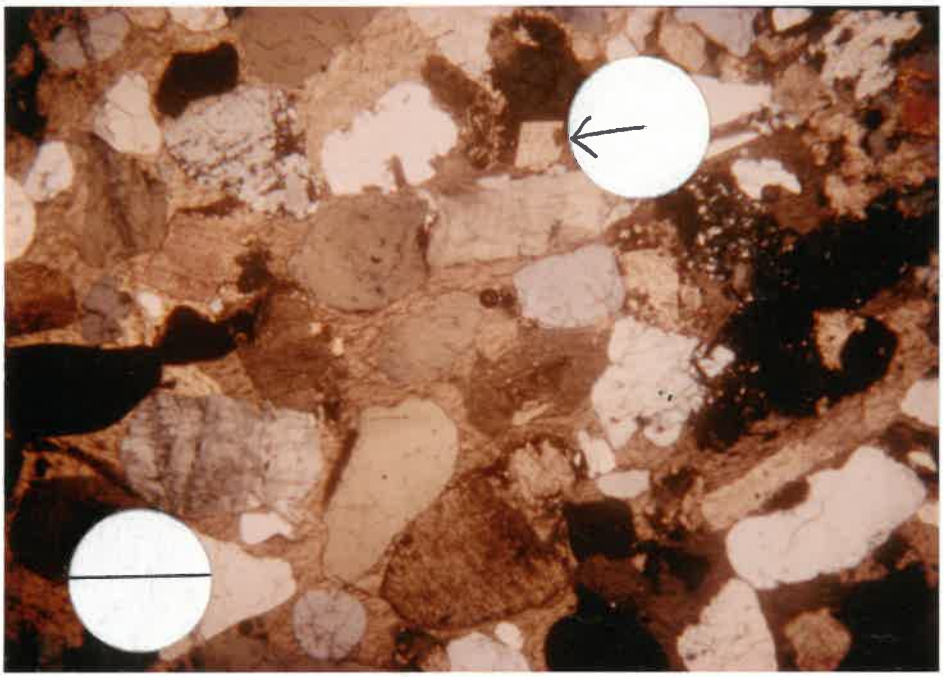

Fig. 18 Poikilotopic ferroan calcite cement - lithofacies A. Note ferroan dolomite replacement (arrow). Bar = 0.7mm. XN.

Poikilotopic cementation may involve one large crystal or several smaller ones. Crystal mosaics are also present. Relatively coarse-grained subequant, interlocking crystals is one type of mosaic (Fig. 19). Bladed crystals are present developed on skeletal grains (Fig. 20). This morphology may merge with smaller equant crystals in the center of the pore. Ferroan calcite cement is an early authigenic mineral, pre-dated only by minor quartz overgrowths.

Calcite

As revealed by staining, non-ferroan calcite (stained pink) is present in lithofacies E in core 1P (Fig. 21). Calcite cement ranges in abundance from 2.0 to 34.8 percent of the rock. The distribution of this poikilotopic cement is patchy in that it is associated with scattered skeletal grains and commonly with burrows. The paragenic relation of calcite is similar to that of ferroan calcite.

Ferroan Dolomite-Ankerite

Ferroan dolomite-ankerite (21.0 to 34.4 mole percent magnesium carbonate, 13.7 to 22.6 mole percent iron carbonate) is another authigenic mineral that can be found in all sandstone lithofacies, although it is most notable in lithofacies A (1P), B, and C (Fig. 22). The abundances range from 13.2 to 21.2 percent, 1.8 to 32.0 percent, and 1.5 to 28.5 percent, respectively. It is recognized by its rhombic crystal form and by a turquoise color when stained (Dickson, 1965). The distinction between dolomite and ankerite is made at a molar iron to magnesium ratio of one, above which the mineral is termed ankerite (Evamy, 1969). In that the molar calcium to mangesium plus iron ratio is greater than one, the dolomite-ankerite in these sandstones is not stoichiometric (Appendix B). Non-stoichiometric dolomite is thought to be most

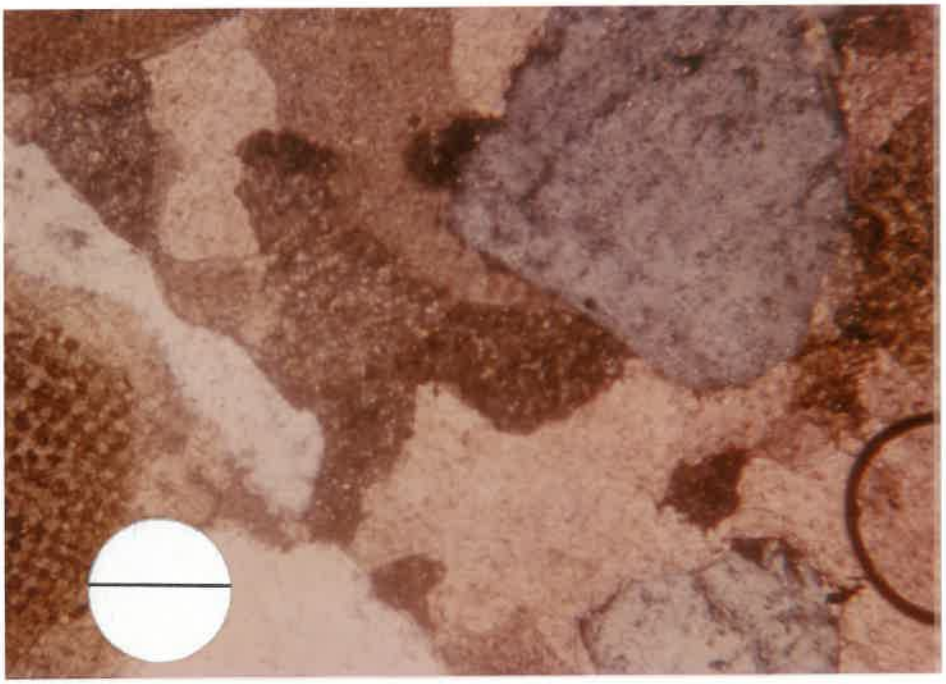

Fig. 19 Pore-filling mosaic of ferroan calcite cement - lithofacies A. Note pelmatozoans at left and top left. Bar = 0.2mm. XN.

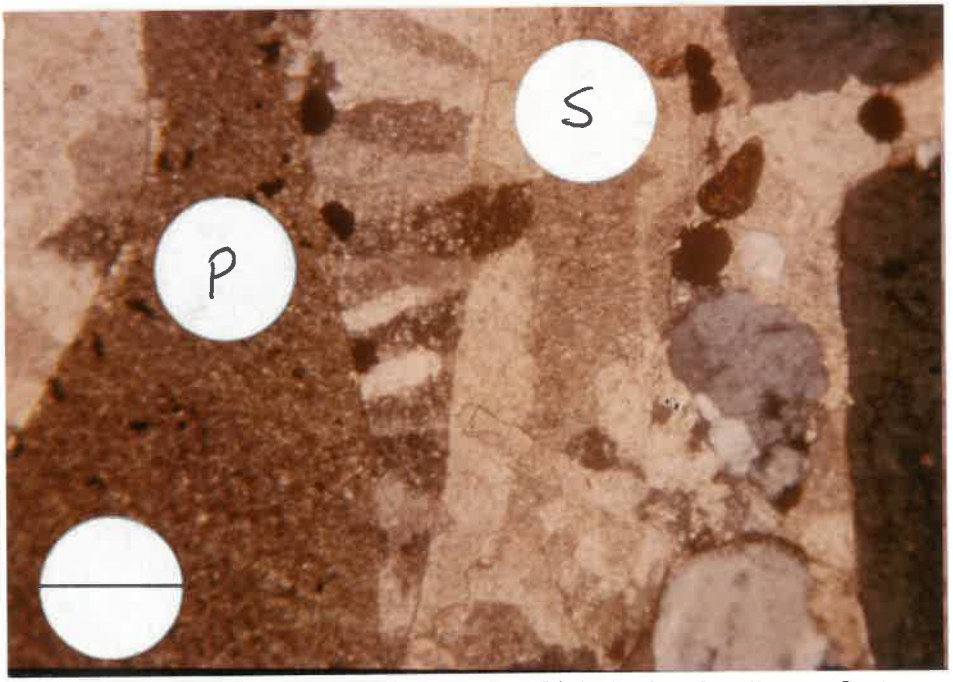

Fig. 20 Bladed ferroan calcite cement - lithofacies A. Note pelmatozoan grain (P) and spar fill of dissolved fossil fragment (S). Bar = 0.2mm. XN.

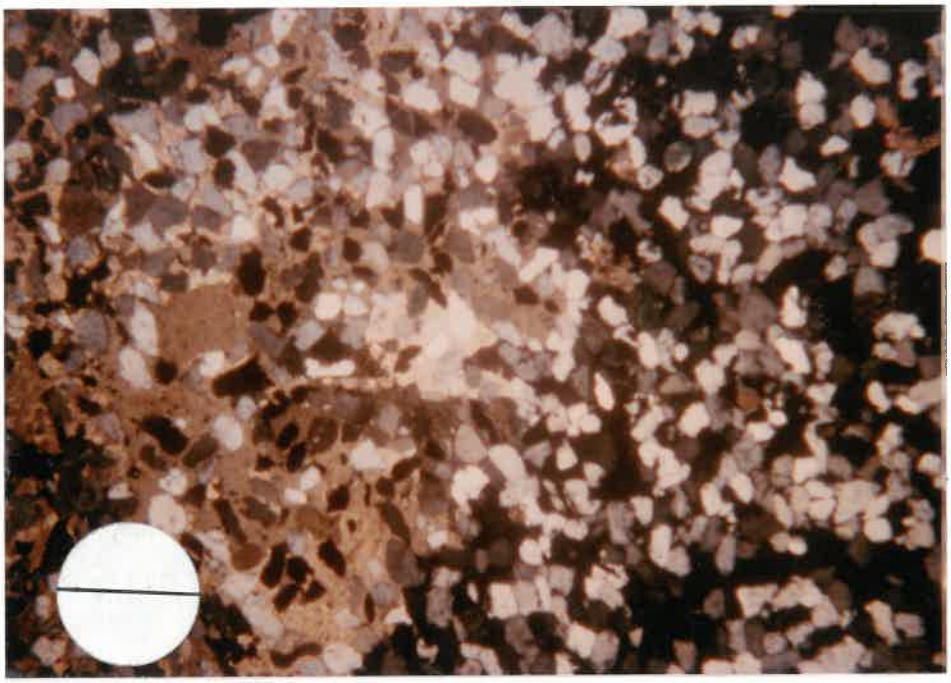

Fig. 21 Patchy poikilotopic calcite cement - lithofacies E (core 1P).
Bar = 0.7mm. XN.

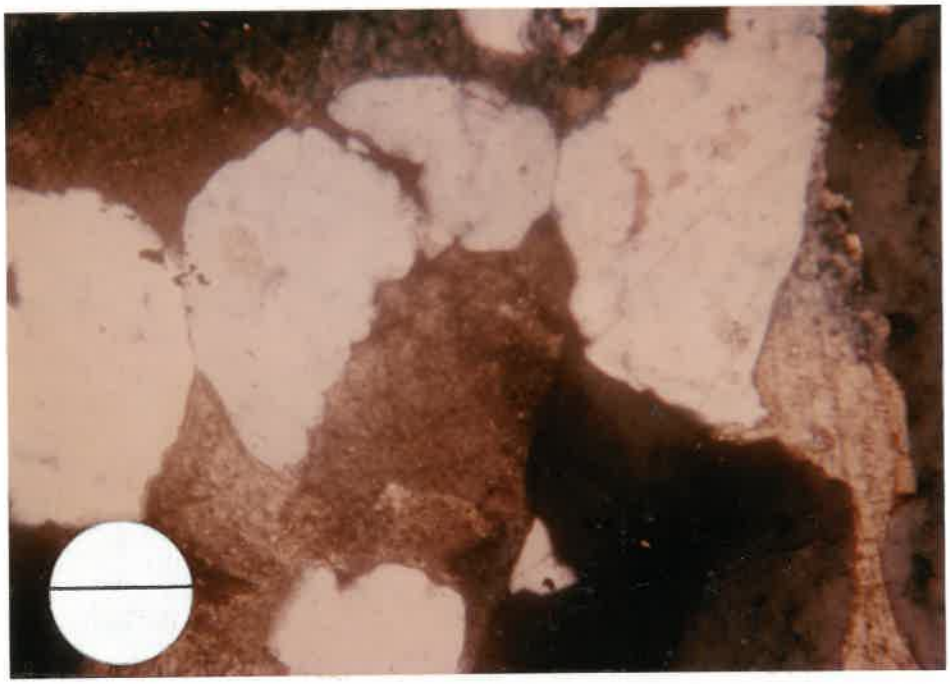

Fig. 22 Ferroan dolomite-ankerite cement - lithofacies B.
Bar = 0.2mm. XN.

common in modern rocks, but is known in ancient rocks ranging to the Cambrian Period (Blatt, et al., 1980, p. 510).

Much of this dolomite-ankerite has the curved crystal faces and cleavage, and the sweeping extinction of saddle (baroque) dolomite (Radke and Mathis, 1980). This type of dolomite has been found as a replacement and a cement, and in association with hydrocarbons, mineralization, and sulfate-bearing carbonates (Radke and Mathis, 1980).

In Kearny Formation sandstones ferroan dolomite-ankerite most commonly occurs as coarse-silt to very coarse sand-sized subhedral to euhedral crystals, which are isolated or grouped in clusters. Almost always it is a late stage replacement mineral, although commonly crystals extend into pore spaces and act to cement grains. Clay minerals in the form of glauconite, shale clasts, and matrix are preferentially replaced by ferroan dolomite-ankerite. Feldspar, quartz, and pelmatozoan grains, however, are included among replaced (and etched) grains. In core 1P (lithofacies A) ferroan dolomite is present as syntaxial-poikilotopic cement (8.0 to 17.5 percent) as well as a replacement of skeletal grains.

Chlorite

Authigenic chlorite is present in all sandstone lithofacies except A and muddy units such as lithofacies E in core 5LA and lithofacies D in 1LG. It is particularly abundant in lithofacies C and in the bioturbated sandstone of core 1P, where it ranges from 2.1 to 11.8 percent of the rock (Figs. 17, 23). Chlorite is recognized by its light green color, low birefringence, and platelet structure in SEM (Wilson and Pittman, 1977). Chlorite is also identified in this study by X-ray diffraction. An authigenic origin is interpreted on the basis of a number

criteria listed by Wilson and Pittman (1977).The most reliable of these criteria include: pore-linings that are missing at grain contacts, chlorite covering authigenic quartz, and the radial alignment of individual plates on grains (Fig. 24).

Chlorite is present as a patchy grain-coating to pore-lining, to pore-filling clay (Fig. 23). Grain coatings are the earliest cement, generally preceding, but also post-dating quartz overgrowths. The radial alignment of chlorite plates is best developed on glauconite (chloritic) pellets (Fig. 24). The relationship between authigenic quartz and chlorite is further discussed in the section on diagenetic history.

Kaolinite

Kaolinite is another authigenic clay that is notable in Kearny Formation sandstones, particularly the upper sandstones. It is most significant in lithofacies B, constituting 2.0 to 9.2 percent of the rock (Fig. 25). Kaolinite is identified in thin section by its booklet to vermicular texture and low birefringence, and in SEM by stacks of pseudohexagonal plates (Fig. 26) (Wilson and Pittman, 1977). X-ray diffraction also indicates the presence of kaolinite.

Kaolinite occurs most commonly as a replacement of K-feldspar and as associated pore-filling patches (Fig. 27). It also is present as isolated pore-fillings and as a filling of secondary pores developed in shale clasts, detrital matrix, chlorite, and ferroan dolomite-ankerite (Fig. 25). The well-developed texture and inter-crystalline porosity suggests an origin as a secondary pore-filling as opposed to direct replacement (Scholle, 1979, p. 157). Most kaolinite is believed to have formed late in the diagenetic history because it occurs in secondary pores resulting from dissolution of ferroan dolomite-ankerite.

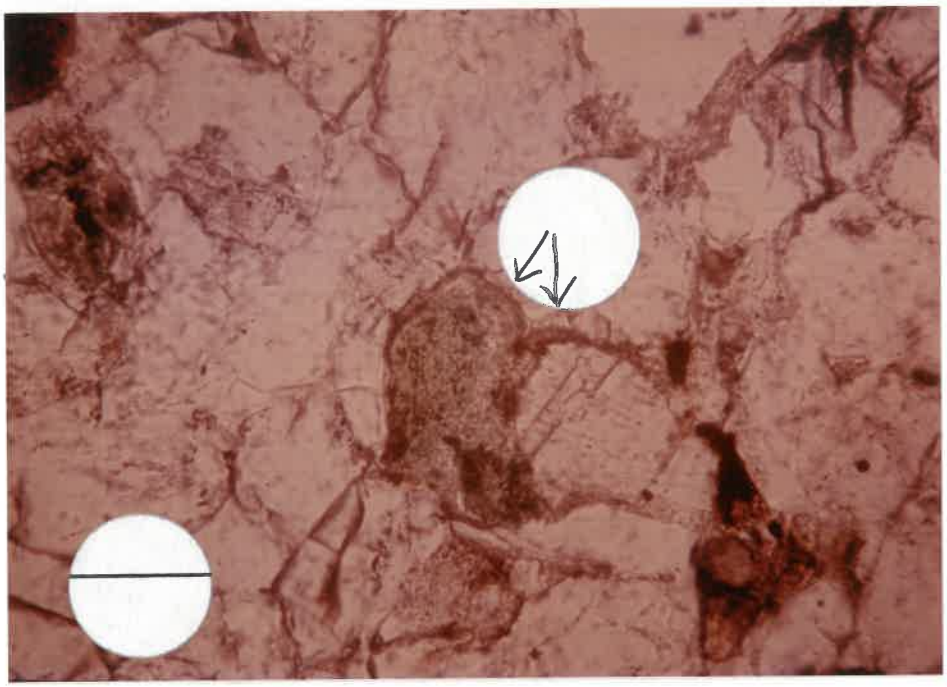

Fig. 23 Authigenic chlorite grain coatings on quartz and glauconite (arrows) - lithofacies D. Bar = 0.02mm. PL.

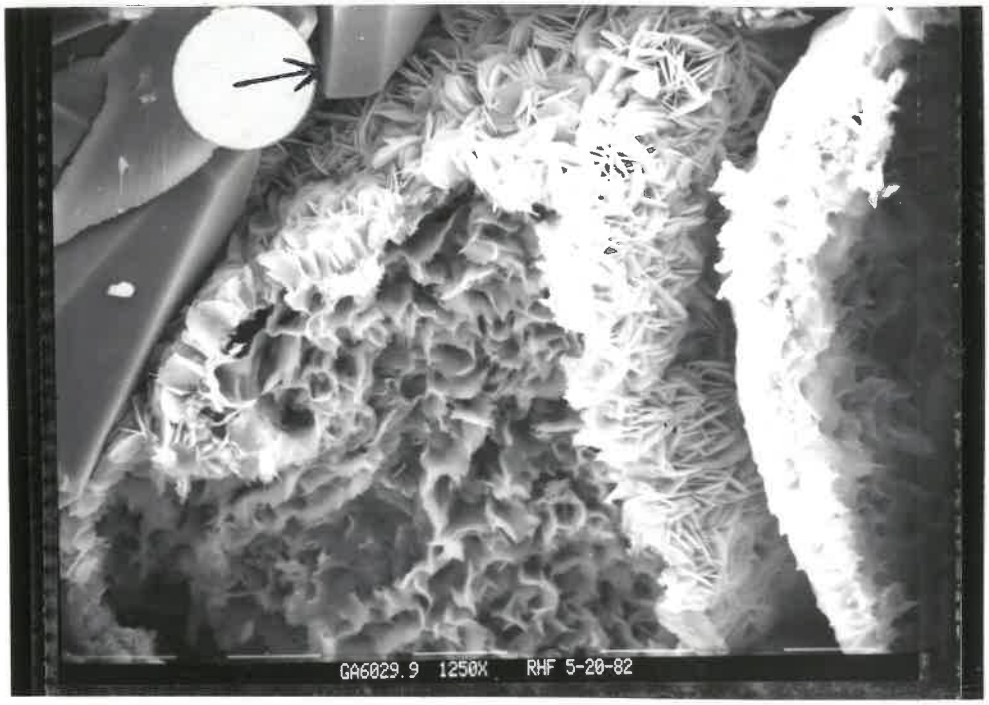

Fig. 24 SEM Photomicrograph - Authigenic chlorite coating on dissolved glauconite - lithofacies D. Note authigenic quartz (arrow). White bars = 10 microns.

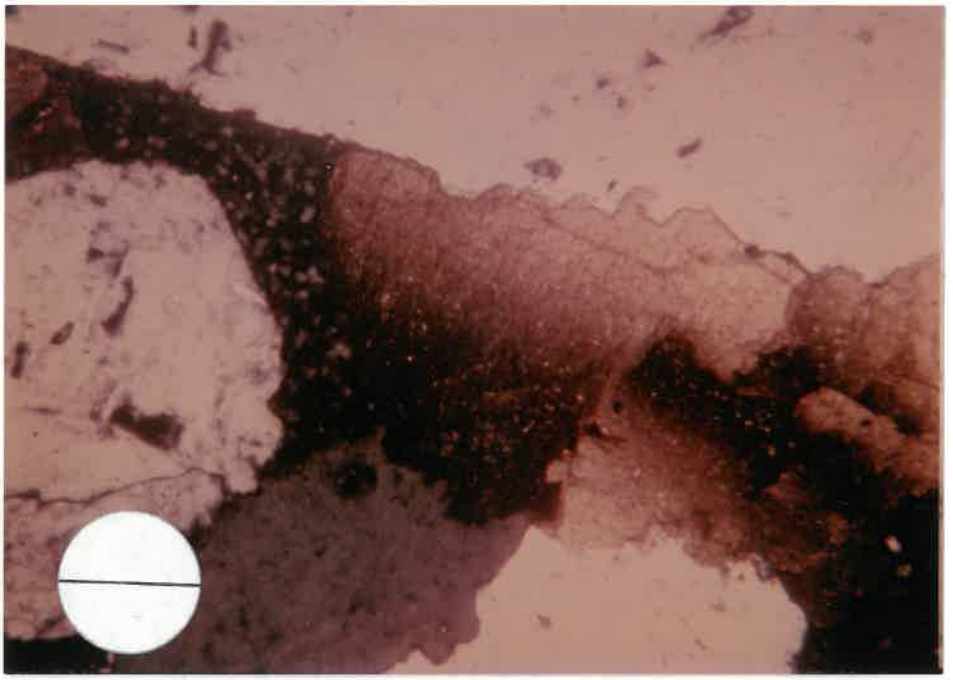

Fig. 25 Kaolinite-fill of dissolution pore in ferroan dolomite - lithofacies B. Bar = 0.2mm. XN.

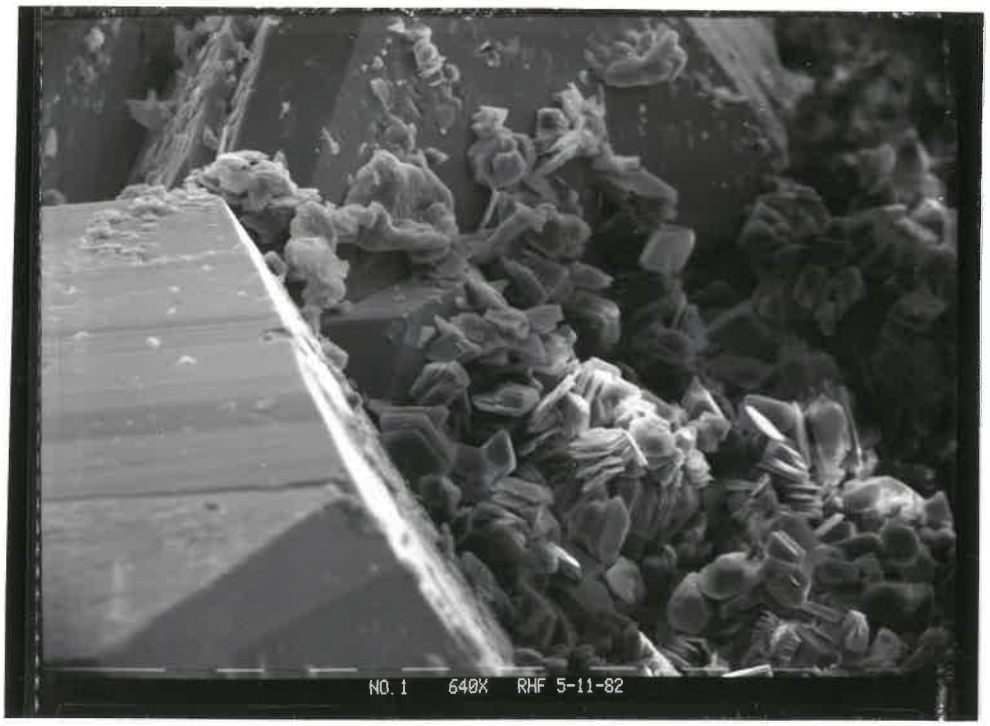

Fig. 26 SEM Photomicrograph - Authigenic kaolinite on quartz overgrowths - lithofacies B. White bars = 10 microns.

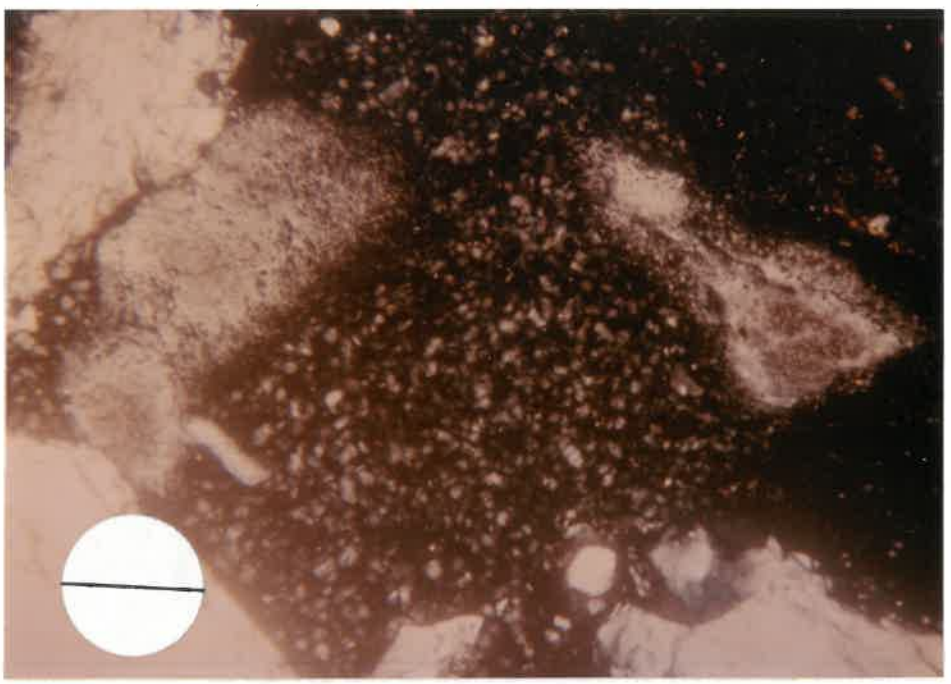

Fig. 27 Kaolinitization of K-feldspar - lithofacies B.
Bar = 0.2mm. XN.

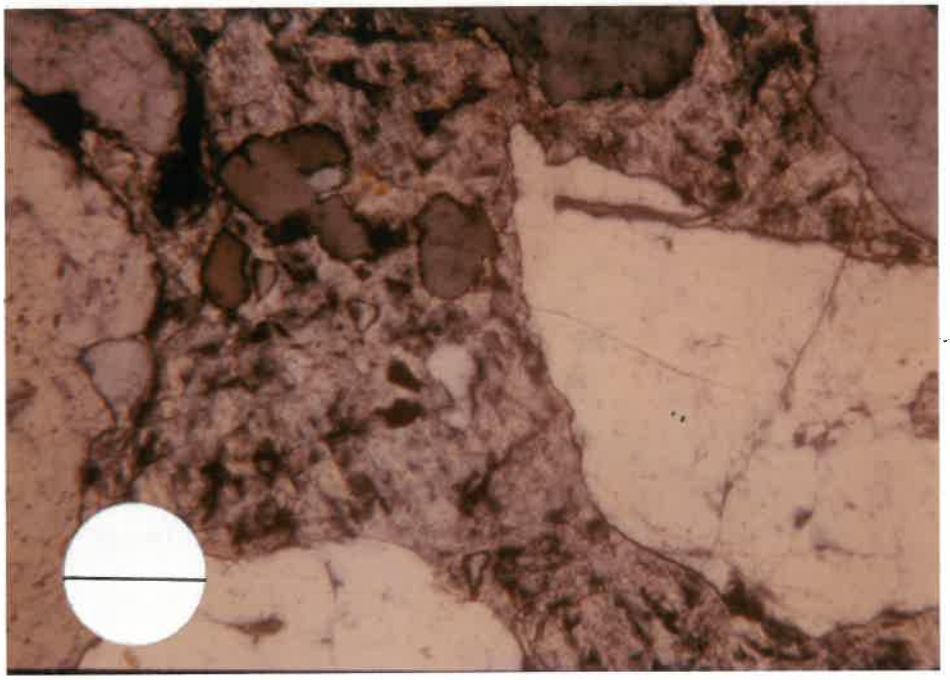

Fig. 28 Barite replacement and cement - lithofacies B.
Bar = 0.2mm. XN.

Additional Authigenic Minerals and Replacements

Cements

Relatively rare feldspar overgrowths show up as unaltered outer rims on detrital K-feldspar and plagioclase cores, some of which have been replaced by sericite.

Other less common or abundant cements include poikilotopic and replacement barite (Fig. 18). Barite, although not abundant, is present in lithofacies A (1P), B (5LA), C (1LG), and E (1P). The mineral barite has a birefringence similar to quartz but is distinguished by its higher refractive index, biaxial figure, orthorhombic crystal form, and two perfect cleavages (Scholle, 1979, p. 128).

An additional authigenic clay mineral observed in SEM is illite. Only a few lath-like crystals were noted and interpreted as illite (Wilson and Pittman, 1977). X-ray diffraction and SEM conducted by Cities Service Company on samples from core WD2 (lithofacies B) indicate minor amounts of mixed layer, illite-smectite clay are present (data from Core Labs report). Chlorite and kaolinite, however, are much more significant in this core as they are in all Kearny Formation sandstones studied.

Replacements and Alterations

A wide variety of replacements and alterations are present as diagenetic features in Kearny Formation sandstones. These are of relatively less importance to this study, so for the sake of brevity they are not discussed in the text. Table 3 is a summary of replacements and alterations.

TABLE 3

DIAGENETIC REPLACEMENT-ALTERATION FEATURES

Feature	Lithofacies
chert/quartz to calcite	A, D, E, F
phosphate to calcite	A
shell debris to calcite (solution fill)	A
glauconite to fine-grained calcite	A, E
shells (bryozoans) to fine-grained calcite	A, E
quartz to ferroan dolomite-ankerite	A, B, C, D
feldspar to ferroan dolomite-ankerite	A, B, C
clay/glauconite to ferroan dolomite-ankerite	A, B, C, D, E
shell debris to ferroan dolomite-ankerite	A, B
glauconite to fine-grained ferroan dolomite-ankerite	A, E
glauconite to chert/chalcedony	A
pelmatozoans to chert/chalcedony	A
clay clasts to barite	B
glauconite to chlorite	C, D, E
feldspar to chlorite	B, C, E
feldspar to kaolinite	A, B
shale clasts to kaolinite (solution fill)	B, C, D
feldspar to sericite	B, C
detrital clay/laminae to pyrite	A(1B), D(1B),E,F
detrital clay/laminae to hematite	B, D, E
chlorite to magnetite	D
detrital clays/quartz to siderite (Fig. 33)	D(ILG)
detrital clay/quartz to iron-free dolomite	F(WD2)
glauconite to phosphate	D

Other Diagenetic Features-Processes

Several other diagenetic features are present in Kearny Formation sandstones that indicate the occurrence of processes other than cementation. Included are the porosity reduction mechanisms bioturbation and compaction, and porosity enhancement by dissolution.

Bioturbation

Bioturbation of interbedded sands and muds takes place penecontemporaneously with deposition and is believed to usually result in porosity reduction (Jonas and McBride, 1977). Porosity loss results from a decrease in sorting and the introduction of clays into pore spaces in sand. The importance of bioturbation in reducing porosity applies to lithofacies D, E, and F. This is particularly true, obviously, where shale laminae and burrowing are most abundant.

Compaction

Compaction is a fundamental mechanism of porosity loss that takes place by several processes: grain slippage-rotation, deformation of ductile and brittle grains, and pressure solution (Jonas and McBride, 1977). Compaction begins as an early diagenetic process by the first mechanism unless it is arrested by early cementation. Pressure solution often is a relatively late process that takes place with continued burial. The effects of compaction are most readily identified in this study as deformed grains and pressure solution. Ductile grains are abundant throughout most of the sandstones as shale clasts and glauconite. Deformation and flowage of some of these grains reflects compaction (Figs. 29, 30). In

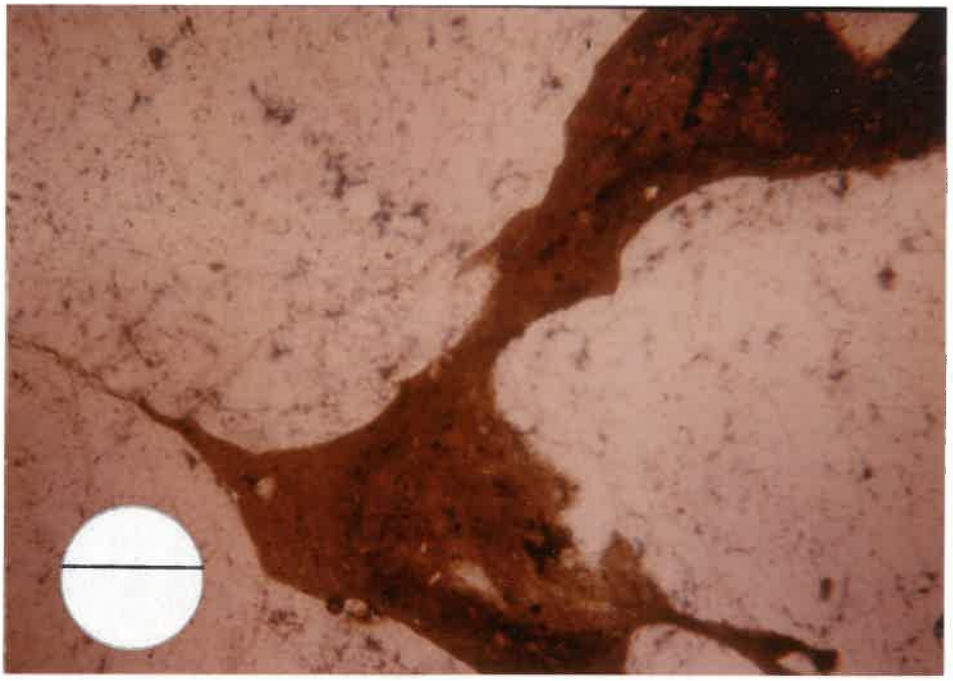

Fig. 29 Shale Clasts and compaction - lithofacies B.
Bar = 0.2mm. PL.

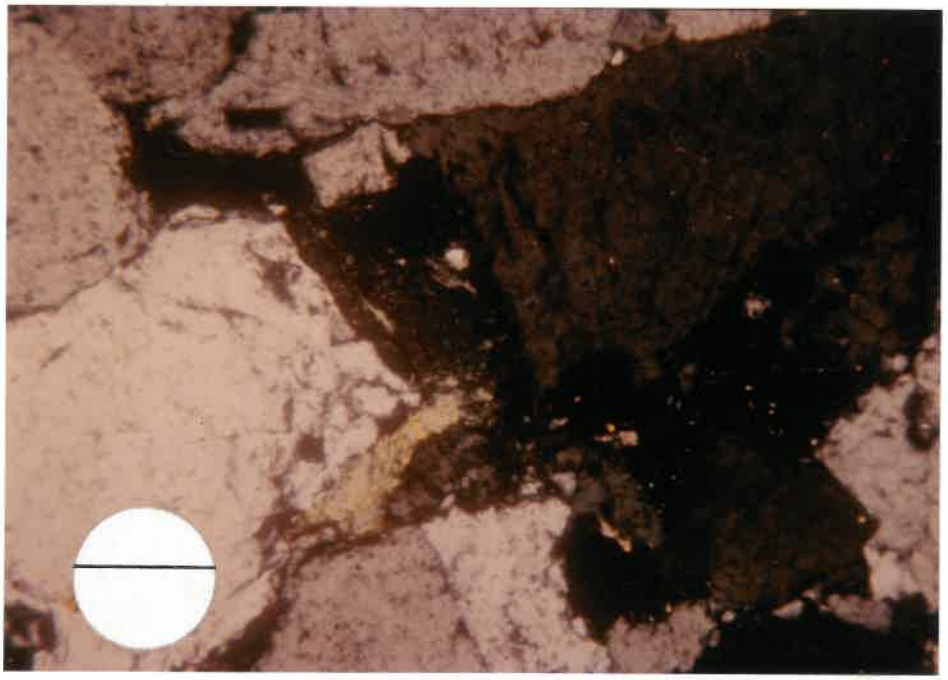

Fig. 30 Glauconite and compaction - lithofacies C.
Bar = 0.14mm. XN.

addition, brittle and elongate micas and organic phosphate have suffered deformation and breakage and have thus served as a mechanism of compaction.

Pressure solution has also taken place in Kearny Formation sandstones as evidenced by the presence of stylolites (Fig. 31). Stylolites are found in association with clay laminae, within ferroan calcite cement, and along cement-skeletal grain boundaries. Solution of quartz grains and carbonate has taken place in the formation of stylolites. Sutured grain contacts (microstylolites), however, are not an abundant feature. The total effect of compaction in reducing porosity is discussed in Chapter Seven.

Dissolution

Detrital clays, shale clasts, glauconite, feldspar, and ferroan dolomite-ankerite have all undergone some dissolution. Much of the resultant secondary porosity has been filled with authigenic kaolinite (Fig. 25). Secondary porosity developed by the late stage dissolution of feldspar and ferroan dolomite-ankerite replacements of feldspar is commonly preserved. In lithofacies B this makes a substantial contribution to the total porosity. Pore types are discussed further in the section on petrophysical properties.

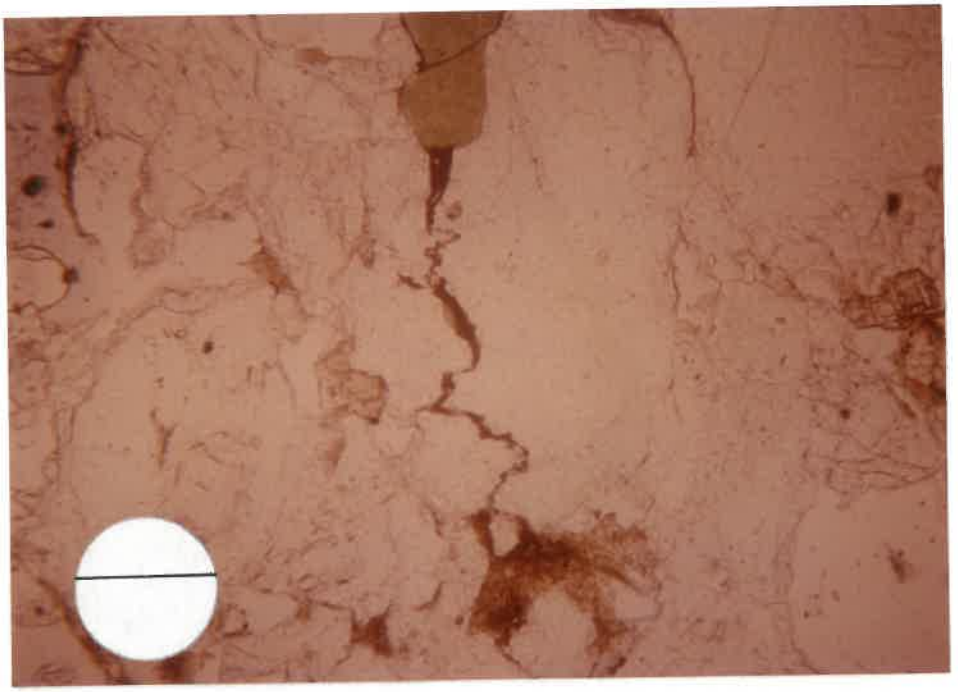

Fig. 31 Stylolite in lithofacies C.
Bar = 0.2mm. PL.

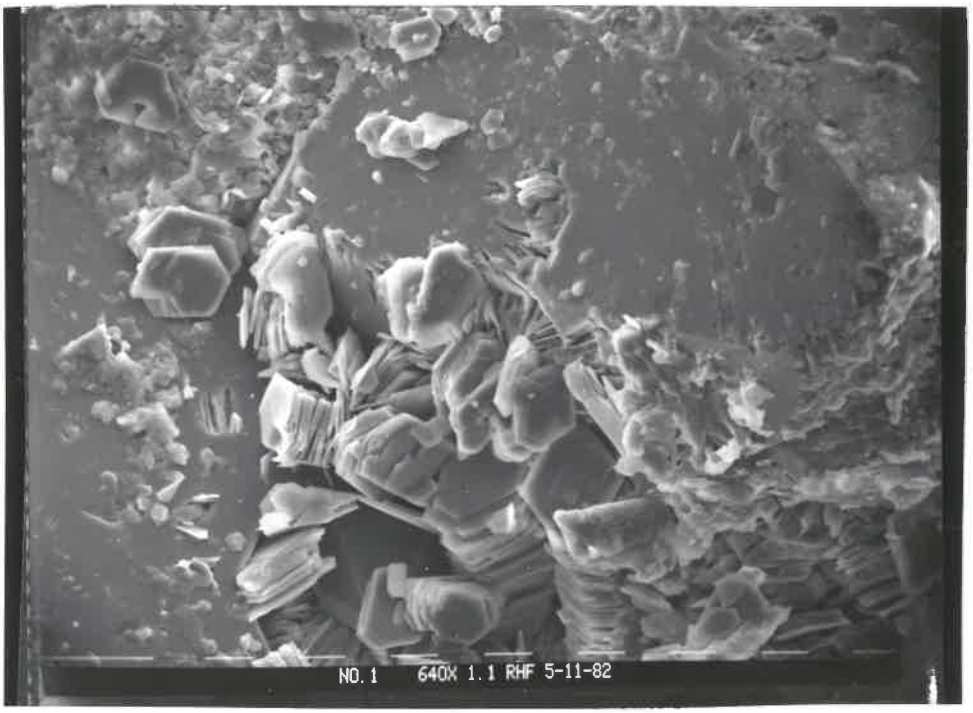

Fig. 32 SEM Photomicrograph - Authigenic kaolinite engulfed by quartz - lithofacies B. White bars = 10 microns.

CHAPTER V

DIAGENETIC HISTORY OF SELECTED KEARNY FORMATION SANDSTONES

Paragenetic Sequence

The diagenetic history of the sandstones studied is summarized by three general stages: 1) early diagenesis, 2) mainstage diagenesis, 3) late diagenesis. Early diagenesis as used here includes the formation of minerals prior to the first major pore-filling cement, quartz overgrowths. Included are reactions that take place penecontemporaneously with deposition and soon afterwards such as glauconitization, chloritization and the formation of pyrite. Most authigenic chlorite and some possibly kaolinite pre-dates quartz overgrowths. Mainstage diagenesis refers to the formation of the major pore-filling cements. Quartz cementation generally precedes pore-filling calcite, ferroan calcite and ferroan dolomite-ankerite. Grain replacements are also inferred to have taken place during this stage including that of shell fragments and filling of solution pores by sparry calcite, and glauconite by calcite. Late diagenesis includes the precipitation of ferroan dolomite-ankerite as a replacement mineral and cement, dissolution of dolomite and K-feldspar, and kaolinitization. It is difficulte to date the emplacement of oil because it was not observed in thin section. Because the presence of oil hinders further diagenesis it is likely that emplacement post-dates all other diagenesis (Longman, 1982, p. 117). Table 4, located at the end of this chapter, is a summary of the diagenetic stages.

Discussion

In early diagenesis reactions took place between the sediment and marine waters during deposition (halmyrolysis) and soon after deposition. Fecal pellets were altered to glauconite by growth of the mineral glauconite (glauconitic smectite) in pores within the pellets (Odin and Matter, 1981). Important in glauconitization is the establishment of a semi-confined micro-environment to which ions may transfer from sea water (Odin and Matter, 1981). Cloud (1955) summarized factors still believed important in glauconite formation including: slightly reducing conditions often associated with organic matter, marine salinity, slow sedimentation, and low levels of turbulence.

In lithofacies B (core WD2) it appears shale clasts and feldspars may have experienced chloritization. This possibility is suggested by the light green color (and brown) and low birefringence of many shale clasts and x-ray diffraction data (Cities Service Co.). Feldspars in this core appear also to have been replaced by a clay mineral along cleavage traces, which occured prior to dissolution. It seems likely that this clay is chlorite, and may have formed during early chloritization. The alteration of clays to chlorite (possibly also pertaining to fecal pellets), and growth of chlorite are fairly common processes of early marine diagenesis (Powers, 1957, Grim, 1968, p. 537, Folk, 1980, p. 94). It seems probable that some authigenic chlorite grain coatings characteristic of lithofacies C, D, and E originated during early diagenesis in the marine environment. An alternative or additional mechanism by which authigenic chlorite formed is by the alteration of glauconite under conditions of shallow burial (Fig. 12). Some glauconite observed partially exhibits an anamalous blue birefringence similar to chlorite. Chlorite coatings are also particularly well-developed in glauconite pellets. Dapples

(1967) believes the alteration of glauconite to chlorite is a common feature of low temperature phyllomorphic diagenesis. Authigenic chlorite in lithofacies B of core WD2 may have originated by the alteration chloritic shale clasts. Chlorite is most abundant in lithofacies C, D, and E, where glauconite is very abundant and where early carbonate cement is not widespread. This lithofacies association may be due to fact that chlorite originated by the alteration of glauconite. In addition, chlorite may have been dissolved where conditions were favorable for early calcite cementation (lithofacies A, portions of D, E).

Kaolinite that pre-dates quartz overgrowths (Fig. 32) in lithofacies B may represent early diagenesis in slightly acidic meteoric waters having a low concentration of potassium and magnesium (Jonas and McBride, 1977). Alumina and silica most likely came from the weathering of feldspar, which is abundant in this lithofacies. Alternatively, the feature in Figure 32 could also have resulted during late diagenesis, given that most alteration of feldspar seems to have occurred late.

Authigenic pyrite is present as a replacement of black clay laminae mainly in lithofacies D. This association is consistent with an early diagenetic origin in the marine environment under reducing conditions. Pyrite is believed to form by the reaction of H_2S, which is derived from bacterial sulfate reduction, with fine-grained iron minerals (Berner et al., 1979). Intermediate sufides (Fe_3S_4, FeS_{1-x}) form first, from which pyrite forms over a period of years by the general reaction (Berner et al., 1979):

$$Fe_3S_4 + 2\ H_2S = 3\ FeS_2 + 4\ H^+ + 4\ e^-$$

Sideritization is a process that may take place during early diagenesis or upon deep burial (Jonas and McBride, 1977, p. 80). Fine silt-to fine sand-sized

spherules and rhombs of siderite are present as a replacement, particularly of detrital clays, in lithofacies D in core 1LG (Fig. 33). Because siderite does not replace authigenic kaolinite, it probably formed prior to the kaolinite. In that the crystals of siderite are in part coarser than microcrystalline, and also replace quartz grains, sideritization possibly took place during deep burial rather than during early diagenesis (Jonas and McBride, 1977, p. 80). Given the unavailability of calcium and magnesium ions, siderite can form from reduced iron and bicarbonate generated during decarboxylation in associated shales (Curtis, 1978).

Mainstage diagenesis began with the precipitation of quartz overgrowths, which are extensive in all sandstones except in lithofacies A and in lithofacies D in core 1LG. Where poikilotopic calcite or ferroan calcite are present, quartz cementation was superceded relatively early as can be seen by the uncompacted nature of the grains (Figs. 18, 21). In lithofacies D (1LG) quartz overgrowths are small, perhaps because interstitial clays inhibited fluid migration. Thus, with some exceptions quartz overgrowths are ubiquitous features of mainstage diagenesis. Given that pore fluids are supersaturated with silica, the major problem in explaining overgrowth formation is accounting for the migration of sufficient pore volumes through the rock (Blatt, 1979). Blatt suggests this problem is resolved in many instances of early quartz cementation by invoking a model of vertically descending meteoric waters (1979, p. 148). Others believe that much quartz cementation occurs at depth greater than ground water flow, and therefore the above model would be inadequate (Jonas and McBride, 1977, p. 71).

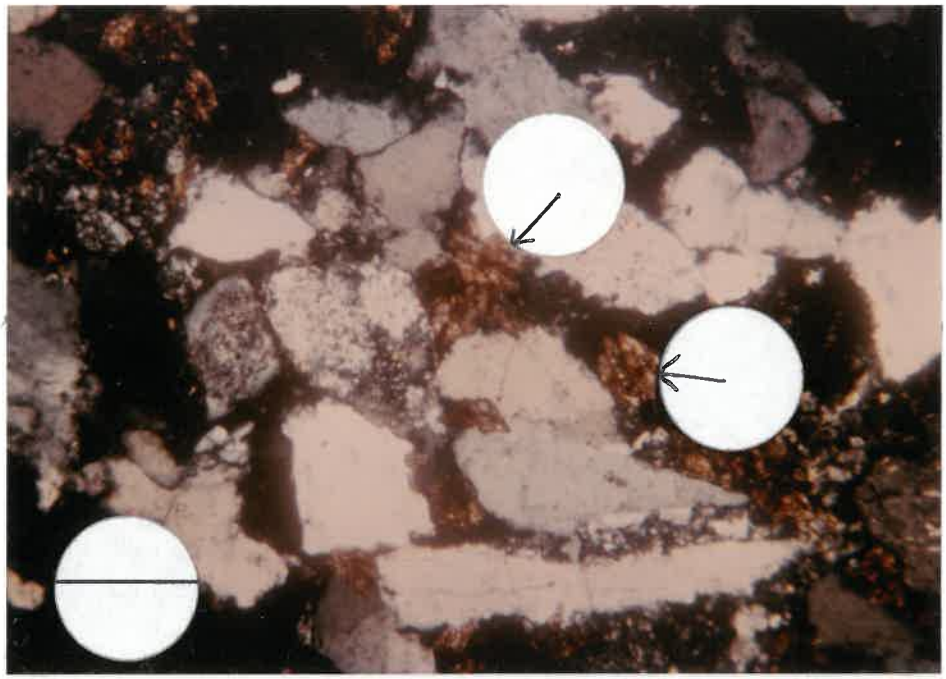

Fig. 33 Siderite replacement (arrows) - lithofacies D. (core 1LG). Bar = 0.2mm. XN.

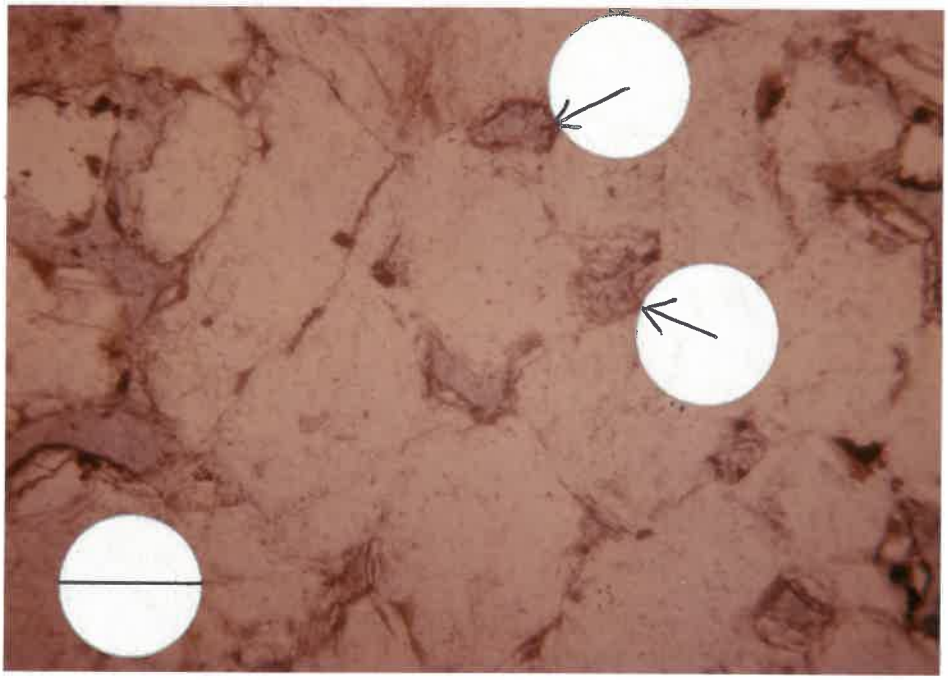

Fig. 34 Preserved primary intergranular porosity (arrows) - upper part of lithofacies C. Bar = 0.8mm. PL.

Factors that increase silica solubility and would thereby hinder precipitation include pH values above 9 and elevated temperatures (Jonas and McBride, 1977, p. 68). At pH values of about 9 silica tends to dissolve and be replaced by calcite. In the sandstones observed in this study early calcite (as well as dolomite, Fig. 22) commonly etches quartz and feldspars. At depth elevated temperature is a factor that would prevent the formation of authigenic quartz. Based on this it may be that quartz precipitates when rising compactional waters cool and the solubility of quartz decreases (Jonas and McBride, 1977, p. 68). Authigenic grain coatings, such as chlorite have also been shown to prevent nucleation of overgrowths (Lumsden and Pittman, 1968). As a whole authigenic chlorite has not been effective in inhibiting quartz cementation in the Kearny Formation sandstones studied. Apparently such grain coatings were discontinuous and quartz was able to nucleate and overgrow chlorite (Fig. 17).

A number of sources of silica have been suggested with the most important considered to include: dissolution (stylolitization) of quartz associated with high alkalinity or temperature, clay mineral diagenesis, and carbonate replacement of quartz and other silicates (Jonas and McBride, 1977, p. 72). Dissolution may account for some authigenic silica in lithofacies C (5LA), where stylolitization was facilitated by clay laminae. Another possible source of silica in marine Kearny Formation sandstones is the glauconite to chlorite transformation (Perez, 1978). Kaolinitization of feldspar may have provided silica for the formation of authigenic quartz. Much kaolinitization is believed to have occurred late in diagenesis. Therefore the Feature in Figure 32 may represent minor late stage silica cementation as opposed to early kaolinite.

Calcite and ferroan calcite cementation occurred early in the diagenetic history in lithofacies A and in parts D, E, and F. Quartz overgrowths pre-date these cements but are minor. Calcite and ferroan calcite occur in association with skeletal detritus, which is a likely source for much of the material for calcite cementation. Textures present including isopachous bladed and syntaxial overgrowths on echinoderms, are characteristic of those formed in the freshwater phreatic zone (Longman, 1981, p. 100). Ferroan and non-ferroan carbonates can precipitate below the water table (Evamy, 1969, p. 791).

Microprobe analysis of some samples of ferroan calcite cement reveals the following compositional ranges in mole percent: $CaCO_3$ 94.0 to 97.9, $MgCO_3$ 0.6 to 2.5, $FeCO_3$ 0.4 to 2.3, and $MnCO_3$ 0.3 (approximately 0.17 wt. percent Mn^{++}) to 2.2. Strontium carbonate content is so low as to be difficult to detect, but it is well below 0.05 mole percent. The significant component is $MnCO_3$, with a range of abundance suggestive of precipitation from meteoric waters (Meyers, 1974, 1978). Because of low concentrations and complexing in marine and subsurface brines, manganese contents sufficient to cause luminescence cannot be derived from these fluids (Churnet et al., 1982, Meyers, 1974). The lower limit of Mn^{++} in luminescent carbonates is on the order of 1,000 ppm (0.1 wt. percent, 0.18 mole percent) or even less (Pierson, 1981). Therefore, the abundances of $MnCO_3$ in the samples analysized is well within the range of a meteoric source.

Possibly the formation of calcite cements (and replacements) occurred during influx of meteoric waters associated with the development of an unconformity, such as occurs between the Morrowan-Atokan and Atokan-

Desmoinesian Stages. Blatt (1979) summarizes the results of several workers that imply early calcite cementation is often related to unconformities.

Ferroan dolomite-ankerite is a late stage replacement and pore-filling cement that is present in all lithofacies in differing abundances. It is most abundant in lithofacies A, B, and C. In A it occurs as a pore-filling cement where calcite is absent. Quartz overgrowths are better developed in these samples, possibly reflecting that dolomite formed late relative to calcite, and therefore quartz precipitation occurred for a longer period of time. In lithofacies B and C ferroan dolomite-ankerite is irregularly distributed with the exception of some concentration in the lower portions of the lithofacies.

Ferroan dolomite-ankerite is quite common as a late stage cement and replacement in sandstones and limestones. It often forms from saline waters at depth and elevated temperatures (Land and Dutton, 1978, Boles and Franks, 1979, Moore and Druckman, 1981). Radke and Mathis (1980) suggest that baroque dolomite may be indicative of 60 to 150^{o}C. Oxygen isotope data have been used to support elevated temperature conditions. Delta O^{18} values (relative to PDB) on the order of -7 to -8 are typically reported, which may reflect temperatures well over 100^{0}C (Milliken et al., 1981, p. 1404). This apparently assumes fractionation from saline water because subsurface water analysis usually presented indicates a brine composition. Delta O^{18} values obtained from ferroan dolomite-ankerite in the Kearny Formation relative to PDB are -6.04, -6.23, and -6.93 (Appendix B). This could indicate high temperatures of formation, which would have probably resulted from a high heat flow. The maximum depth of burial of the Kearny is uncertain, but it is unlikely it was a deep as 4,000 m (corresponding to approximately 120^{o}C) (Milliken et al.,

1981, p. 1404). Currently, the Kearny lies at a depth of about 1350 to 1900 m in the study area. On the other hand, these negative delta O^{18} values could be reflective of meteoric water in which case they would not be useful as temperature indicators (Pittman et al., 1982, p. 1592-1593).

Materials can be derived from clay mineral diagenesis, decarboxylation, and dissolution of skeletal detritus and carbonate cements, which take place in associated shales or in the sandstones themselves (Curtis, 1978). Ferroan dolomite in impermeable limestones often occurs in close association with clays, which are believed to contribute ions from the smectitie-illite transformation (McHargue and Price, 1982). Carbon isotope data is used to indicate source material for bicarbonate. Delta C^{13} values (relative to PDB) from marine derived carbon tend to be around zero. The influence of organic carbon, which is derived during late stage diagenesis from decarboxylation, tends to result in negative delta C^{13} values. Values on the order of -3 to -4 are typically reported for ferroan dolomite, and are interpreted to indicate an organic source (McHargue and Price, 1982, p. 883). Similar values were obtained from samples from the Kearny Formation: corresponding to the above oxygen values are delta C^{13} = -4.98, -0.97, and -4.56. Because of the close association of ferroan dolomite with clay minerals, the presence of ferroan dolomite replacement in impermeable lithofacies, and the delta C^{13} data, the interpretation of McHarge and Price (1982) seems applicable to the Kearny Formation. Thus materials were derived from internal sources: cations largely from clay minerals and organic matter and bicarbonate in part from organic material. Core 1P may be an exception to this in that ferroan dolomite is predominant as a pore-filling

cement suggesting precipitation from moving pore fluids and possibly external sources.

Microprobe analysis of ferroan dolomite cement indicate a very high $MnCO_2$ content (1.2 to 4.1 mole percent). Strontium carbonate is less than 0.05 mole percent. For some of the reasons discussed above, for ferroan calcite this high manganese content raises the question of a meteoric influence. A meteoric origin is contrary to the standard model for late stage ferroan dolomite-ankerite, which has precipitation taking place at depth below the influence of fresh water at high termperature. Dolomite from fresh water is an unusual notion, although mixing zone dolomites have been reported (Land, 1973). With the exception of pore-filling ferroan dolomite-ankerite in core 1P, the mode of occurrence seems inconsistent with precipitation from migrating meteoric (or mixed) waters. If this were the case there would probably be more pore-filling dolomite and less of a predominant association with clays. Also under such conditions ferroan dolomite replacement might not be expected in early cemented and therefore impermeable areas (lithofacies A). Thus it is difficult to explain the high $MnCO_3$ content of ferroan-dolomite in Kearny Formation sandstones. A speculation is that somehow a meteoric imprint was preserved from an earlier meteoric influence, which was sufficient to contribute manganese. Alternatively, this may be an indication that high manganese content is not strictly a fresh water indicator.

Kaolinitization and dissolution of carbonates and feldspar took place subsequent to cementation by ferroan dolomite-ankerite. This sequence is inferred from the following: (1) the source of authigenic kaolinite is the dissolution and alteration of potassium feldspar, (2) ferroan dolomite is not found

in secondary pores within feldspar, (3) kaolinite fills voids created by dissolution of dolomite.

Dissolution of ferroan dolomite-ankerite and K-feldspar created secondary porosity, especially in lithofacies B. Carbonates and feldspars dissolve under acidic conditions, such as can develop at depth in response to CO_2 or H_2S released during thermal maturation of organic matter (Schmidt and McDonald, 1979).

The conditions under which kaolinite forms and is stable are well-known and have been outlined by Keller (1964). One such condition is a low pH that is often linked to organic maturation. This is consistent with the above mentioned conditions suggested for dissolution. Other important factors include a high Alisi ratio and low concentrations or an absence of calcium, sodium, potassium, magnesium, and iron. Potassium feldspar represents a highly probable in situ source of aluminum and silicon. The form the aluminum is in is probably more important than concentration. In order for kaolinite to form, aluminum must be present as $Al(OH)_3$ (A. W. Walton, personal communication). Kaolinitization of feldspars is common in these sandstones, particularly lithofacies B (Fig. 27). Patches of authigenic kaolinite often occur in the vicinity of altered feldspars, as well as in secondary porosity in dolomite-ankerite.

Diagenesis in Kearny sandstones in southwest Kansas is similar in many ways to diagenesis in other Morrowan Stage sandstones. Lower Kearny lithofacies A corresponds to Adam's (1964) Type B sandstone as a lithofacies and diagenetic facies. This sandstone is "glauconitic" (chloritic), fossiliferous, poorly-sorted and cemented with poikilotopic calcite or dolomite. One significant difference between Type B and lithofacies A is that commercial

quality gas reservoirs occur in Type B as a result of dissolution of carbonate cement. Dissolution in lithofacies A has a minor effect on glauconite and feldspar but is otherwise not evident. Types of authigenic minerals and major diagenetic events are similar in upper Kearny sandstones (lithofacies B) and the upper Morrowan sandstones studied by Kasino and Davies (1979). They also found chlorite, kaolinite, and late stage ankerite as authigenic minerals in upper Morrowan sandstones. Their sequence of diagenetic events, however, is more complicated. It includes an early stage of calcite and silica cementation, dissolution of unstable grains and cement followed by silica and clay cementation. This was followed by ankerite as well as calcite cementation and then partial dissolution of these late cements. Dissolution was very important as in lithofacies B, although much involved carbonate cement as well as feldspars.

TABLE 4

SUMMARY OF MAJOR DIAGENETIC FEATURES

Diagenetic Feature	Occurrence	Relative Time of Formation	Source Materials
Glauconite	Abundant in all lithofacies except B and some F	Syndepositional	Sea water, substrate experiencing glauconitization, underlying sediments.
Chlorite	Abundant particularly in lithofacies C, D, some of E and F. Also present in lithofacies B.	Early, most pre-quartz overgrowths	Seawater, clays in the sediment, glauconite.
Quartz	Ubiquitous with the exception of lithofacies A. Best development in lithofacies E and F.	Mainstage, probably began pre-compaction and may have continued over a long period of time.	Possibly some early from meteoric waters. From clay mineral diagenesis at depth. Minor amount from pressure solution.
Calcite	Lithofacies E (Core 1P)	Mainstage, pre-compaction	Largely internal: skeletal detritus.

TABLE 4

SUMMARY OF MAJOR DIAGENETIC FEATURES (continued)

Diagenetic Feature	Occurrence	Relative Time of Formation	Source Materials
Ferroan Calcite	Particularly characteristic of lithofacies A. Also occurs in C, D, and some F.	Mainstage, pre-compaction	Largely internal: skeletal detritus. Iron from unstable iron compounds and clay.
Ferroan Dolomite-Ankerite	Widespread, more abundant in some of lithofacies A and in lithofacies B, C.	Late-stage	Largely internal: cations from clays, CO_2 in part from decarboxylation. Possibly also earlier carbonate.
Kaolinite	Particularly abundant and characteristic of lithofacies B.	Late-stage, most post ferroan dolomite-ankerite	Predominantly internal: K-feldspar
Dissolution	Widespread, but most notable is dissolution of ferroan dolomite, feldspar in lithofacies B.	Late-stage, post ferroan dolomite-ankerite	Acid pore fluids developed by input of CO_2 from decarboxylation.

CHAPTER VI

PETROPHYSICAL PROPERTIES

Methods

Petrophysical properties determined in this study include porosity, permeability, and pore-size distribution. This work was conducted in the Tertiary Oil Recovery Project laboratories at the University of Kansas, using methods similar to those in other TORP research (Woody, 1983). Raw data for pore-size distribution calculations were obtained from samples of the Kearny Formation by Core Laboratories in Tulsa, Oklahoma. Mercury porosimetry data taken by Core Labs, Tulsa, Oklahoma, were used to calculate pore-size distribution..

Samples used in the determination of petrophysical properties were cylindrical plugs 1.9 cm in diameter and 1.4 to 3.5 cm long. These were cut under 38 parts per thousand NaCl brine from the cores adjacent to locations of thin section samples. Plugs were cut perpendicular to the long axis of the core (horizontal), and no attempt was made to orient them relative to cross-bedding. This brine was used throughout the testing in an effort to maintain conditions close to what they are in the Kearny Formation currently, and to stabilize clay minerals. A value of 38 parts per thousand was calculated from data on the formation water produced from the Kearny obtained from the Kansas Geological Survey.

Four measurements of the length and six of the diameter were made on each of the 91 plugs on which porosity and permeability were determined. From the average of these measurements, the bulk volume of each plug was determined. Plugs from oil-producing zones were extracted with toluene for 12

hours to remove any residual oil. The plugs were all then dried in an oven at 75°C overnight, and stored in a dessicator.

Effective porosity, which is the ratio of interconnected void space to the bulk volume, for each dried plug was determined by standard liquid saturation (Amyx, et. al., 1960, p. 43-52). The dry plugs were first weighed using an analytical balance. The plugs were then placed in a flask and evacuated for 12 to 14 hours, after which time NaCl brine was admitted into the flask to achieve saturation. The saturated plugs were weighed and stored in brine until the completion of the permeability runs. Effective porosity was calculated from the saturation data as is outlined in Appendix C.

Brine permeabilities were determined on the plugs using a Ruska liquid permeameter (Amyx, et al., 1960). Three runs of a known volume of brine were conducted under a known pressure. The times for each run were averaged and permeability was calculated as outlined in Appendix C.

Samples submitted to Core Laboratories for mercury injection were leached of salt using warm methanol in a centrifugal extractor and dried to a constant weight at 210° F (99°C.). Mercury injection was run on each sample at incremental pressures from 3.0 to 2000 psia (0.2 to 140.6 kilograms/cm^2). Volume changes of mercury were measured on a vernier scale. This procedure for mercury injection is similar to that employed with the mercury porosimeter of the Tertiary Oil Recovery Project. Appendix C also contains a summary of calculations of pore-size distribution. Petrophysical data are compiled in Appendix B. Statistics of these data are compiled in Table 5 at the end of this chapter.

Porosity

Pore types present in the sandstones studied include preserved primary intergranular pores between framework grains; secondary intergranular pores resulting from dissolution of carbonate cement and shrinkage of glauconite; secondary intragranular pores resulting from dissolution of feldspar, clay clasts, and glauconite; and microporosity (intercrystalline) within masses of clay. Fracture porosity does not occur with the exception of rare pores within fractured micas. Lack of fractures reflects the fact that these sandstones have not been deeply buried or subjected to major tectonic stress. Intergranular porosity occcurs primarily as pore space preserved between quartz grains cemented by overgrowths (Figs. 34, 35). The recognition of secondary porosity has been outlined by Schmidt and McDonald (1979). Secondary dissolution porosity can be found in all lithofacies but the type and relative amounts differ. Feldspar dissolution is predominant in lithofacies B (Fig. 36). This reflects both the abundance of feldspar and the diagenetic history. Dissolution of carbonate includes that of fossils and cement, particularly ferroan dolomite-ankerite (Fig. 37). Dissolution, particularly of carbonate cements, is also of considerable importance in other upper Morrowan sandstones (Kasino and Davies, 1979). Some ferroan dolomite cement that replaced feldspar was later dissolved. Kaolinite fills some of the porosity created by dissolution of dolomite (Fig. 24). Dissolution of clay clasts is inferred from the presence of authigenic kaolinite, presumably filling secondary pores within the clasts. Well-formed kaolinite suggests later-infilling as opposed to alteration (Scholle, 1979, p. 157). Secondary porosity is also associated with glauconite and includes both dissolution and shrinkage (Figs. 23, 38).

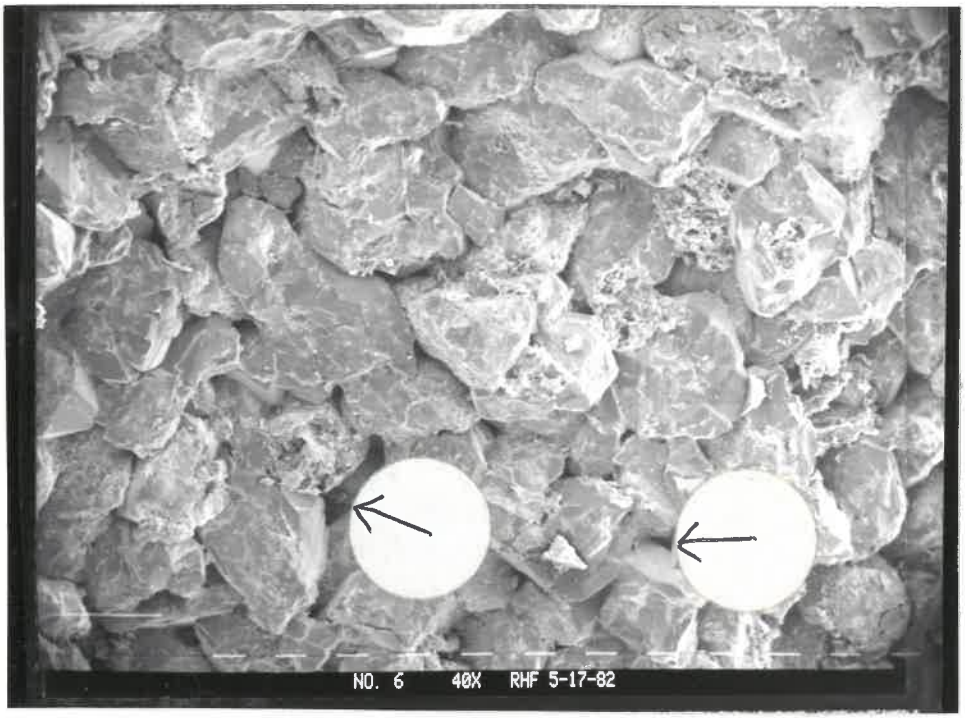

Fig. 35 SEM Photomicrograph - quartz overgrowth cement and preserved intergranular porosity (arrows) - lithofacies C. Note dissolved glauconite. White bars = 100 microns.

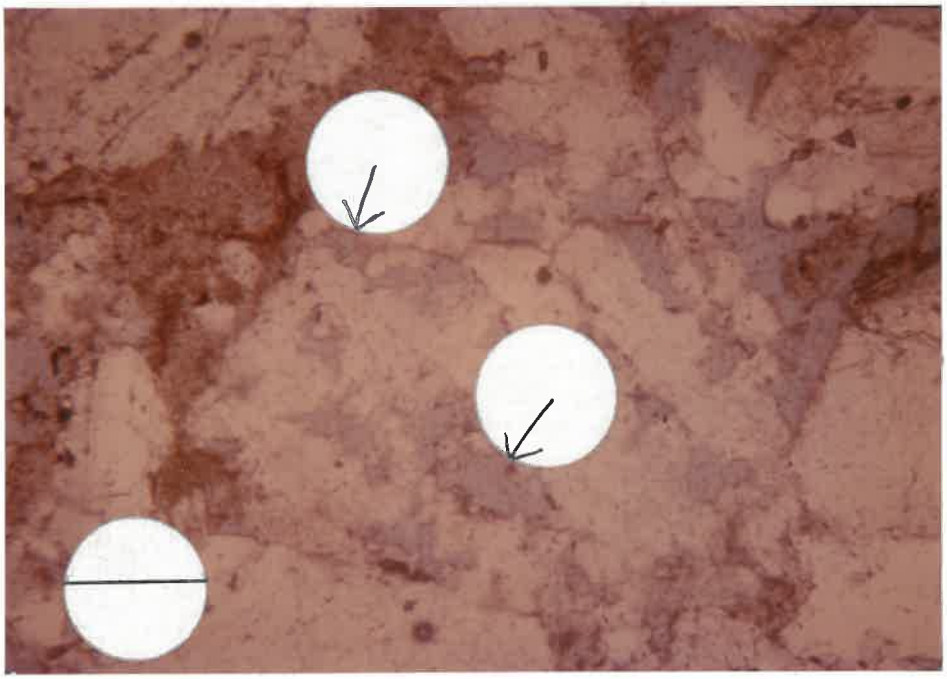

Fig. 36 Dissolution of K-feldspar (arrows) - lithofacies B. Bar = 0.2mm. PL.

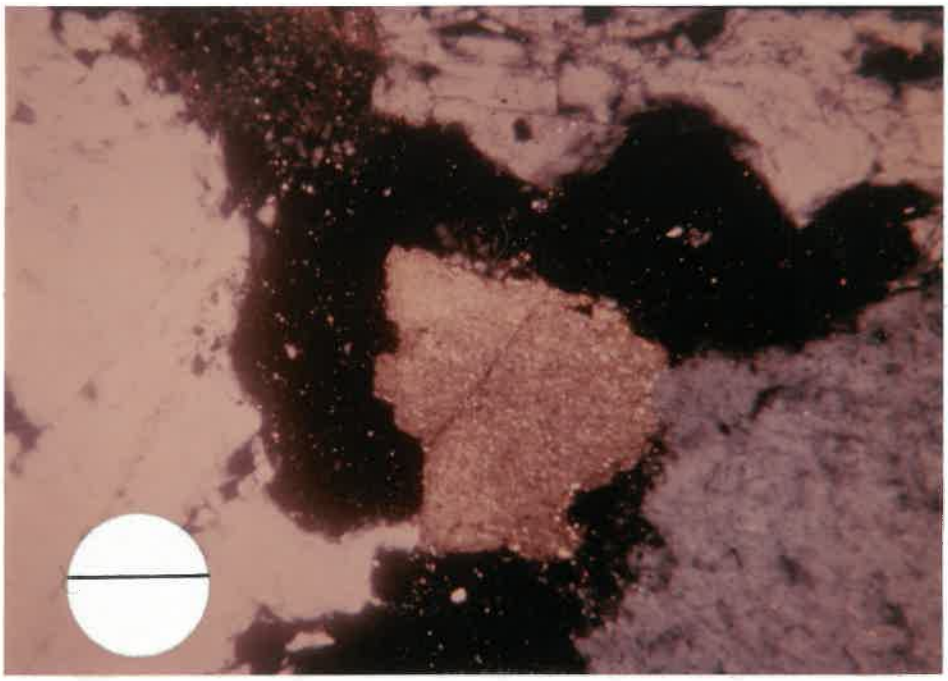

Fig. 37 Dissolution of ferroan dolomite - lithofacies B. Note ragged edges on dolomite. Bar = 0.2mm. XN.

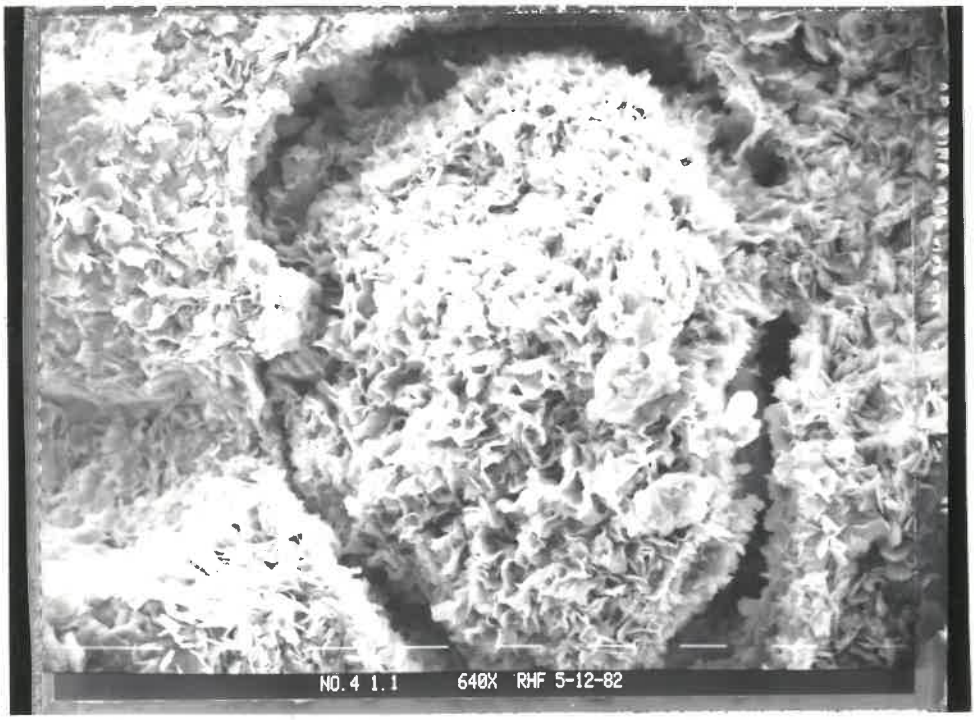

Fig. 38 SEM Photomicrograph - shrinkage of glauconite. White bars = 10 microns.

Microporosity is defined as pores with pore-aperture radius less than 0.5 microns (Pittman, 1979). Such porosity occurs among clay minerals, in pore-throats, and between grains and overgrowths. In Kearny Formation sandstones microporosity would be associated with detrital clays, authigenic kaolinite, chlorite, and also in between authegenic quartz and chlorite.

The amount of total effective porosity as determined by liquid saturation ranges from essentially 0 to 21 percent (Fig. 39). This figure is a plot of porosity and permeability by lithofacies. It can be seen that higher amounts of porosity are associated mainly with lithofacies B, C, and D. This corresponds in part with cores from oil producing intervals in the Kearny Formation.

During point counting porosity types were tallied as intergranular, secondary, and microporosity. Patches of clay were counted as microporosity. Much microporosity is missed during point-counting and therefore total porosity from point-count is usually less than that derived from petrophysical analysis (Pittman, personal communication). The difference is assumed to represent microporosity. In some cases in this study total porosity from point-count exceeded the value from liquid saturation. When this occurred the relative amounts of porosity types were taken as counted. An approximation of the relative proportions of pore types that make up the total porosity can thus be derived (Pittman, 1979). Such data from selected samples of high porosity lithofacies are plotted on a triangular diagram (Fig. 40). This serves as an attempt to characterize reservoir quality Kearny sandstones in terms of their geological (diagenetic) and petrophysical properties. From figure 40 it appears that lithofacies C and D tend to be somewhat more dominated by intergranular porosity than lithofacies B. These are lower Kearny sandstones in which quartz

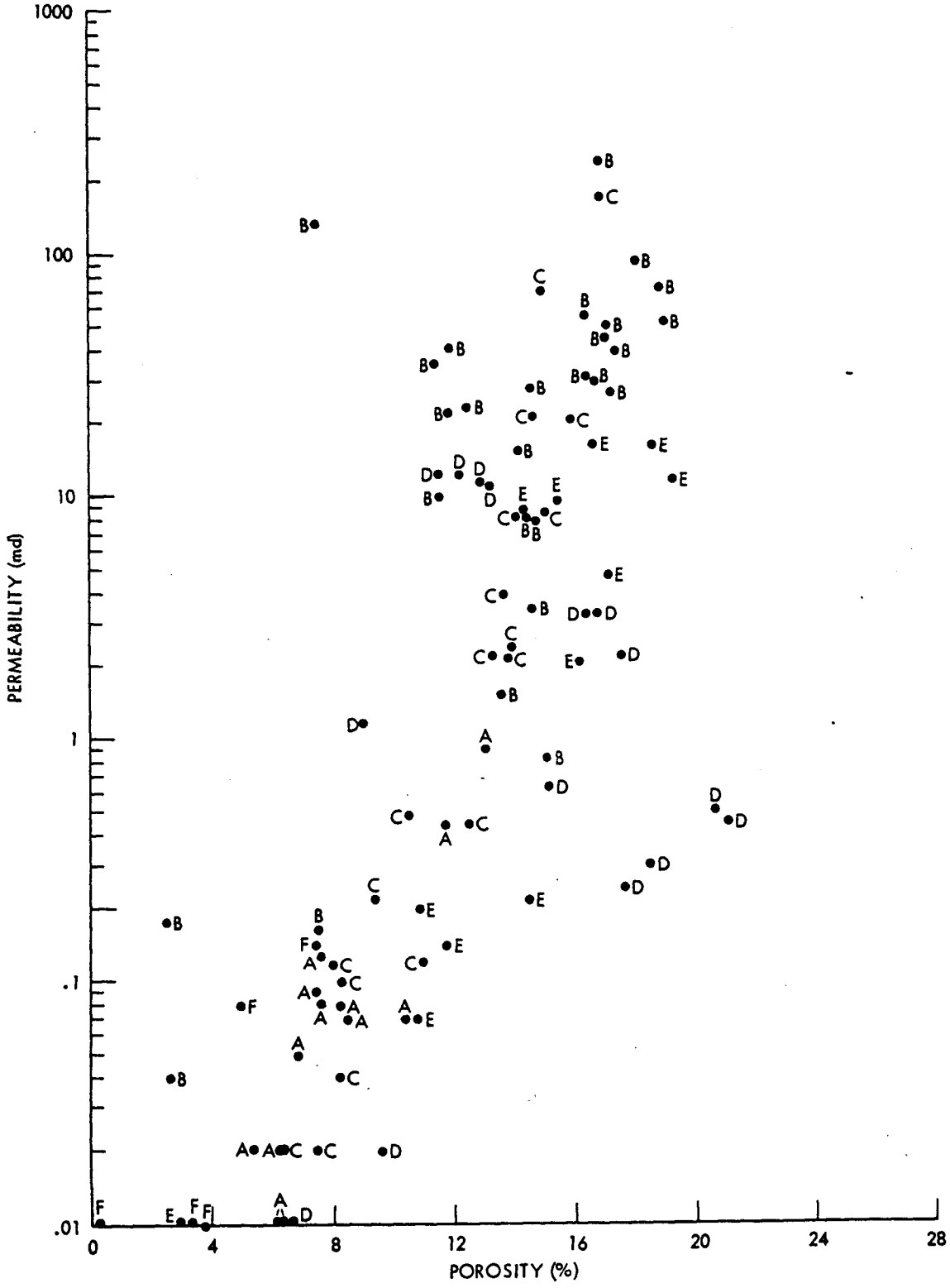

FIG. 39

Permeability versus porosity by lithofacies.

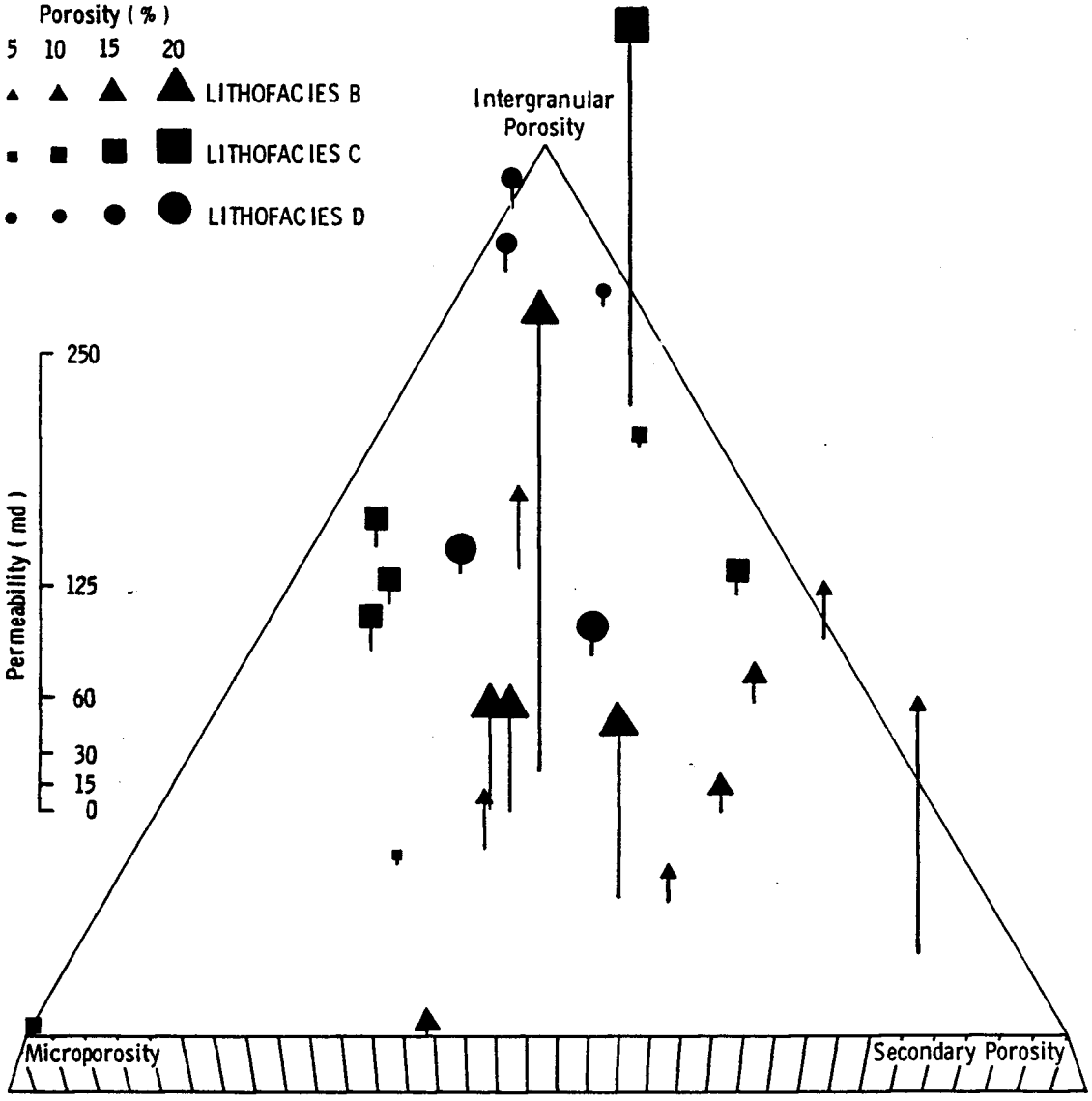

Fig. 40
Distribution of pore types in some samples from lithofacies B, C, and D. Length of stem in this lollipop diagram is proportional to permeability, size of top gives porosity.

overgrowths and chlorite are the predominant diagenetic minerals. Micropores occur in association with chlorite and between overgrowths. In contrast, upper Kearny Formation sandstones (lithofacies B) contain significant secondary and microporosity, five of the ten samples from this lithofacies have over half of their pores of secondary origin. This corresponds in part, to detrital potassium feldspar content. Feldspar has undergone dissolution and is also a likely source for kaolinite, which contains microporosity.

Permeability

Permeability to brine ranges from essentially 0 to 248 millidarcies (Fig. 39). The higher values, as with porosity, occur mainly in lithofacies B, C, and D (in core 1B). In general, permeability increases with porosity following an approximately linear trend. The overall correlation between porosity and permeability is 0.74, and ranges from 0.17 to 0.95 (Table 5). The correlation is poorest for lithofacies D, reflecting the textural differences between samples from different cores. In core 1LG lithofacies D has high porosity but low permeability and is distinct from other samples of lithofacies D. This can be explained by abundant clay matrix and high microporosity. Correlation is highest for lithofacies C, which is dominated by preserved intergranular porosity and therefore is expected to follow a linear trend. This is consistent with the generalization that log permeability is proportional to the first power of porosity (Pettijohn et al., 1973, p. 96). The regression coeficients of porosity and permeability for each lithofacies were tested for their significance (Sokjal and Rohlf, 1969, p. 424). The results indicate that none of the coefficients are significant based on the number of data points and their scatter (Appendix C). It

is therefore not pssible to conduct an analysis of covariance to determine the similarity of the different populations (lithofacies).

In figure 40 it is apparent that with exceptions, somewhat higher permeabilities are related to greater intergranular porosity. Lithofacies B shows a scatter of points in the lower-half of the figure. These permeability values are relatively high, reflecting the interconnected pore system provided by the preserved intergranular porosity. Data points of lithofacies B (Fig. 39) in part follow a direct relationship, which may also be an indication that secondary pores are interconnected (Kasino and Davies, 1979, p. 189).

Porosity and permeability values that depart strongly from the general trend of points are affected by additional factors such as clay content, patchy carbonate cementation, and effective pore radii.

Pore-Size Distribution

A small number of samples (19) was used in the determination of pore size distribution by mercury injection. Pore-size distribution is an additional petrophysical property used to characterize reservoirs; it indicates what percentage of pore throats occur at various radii (Amyx et al., 1960, p. 167). The purpose in doing this was to measure effective pore-radii and the breakthrough radius (Pittman, 1979).

Approximate breakthrough pore radii are included in Appendix B. It appears that between and within lithofacies higher permeabilities are generally associated with relatively coarser breakthrough pore aperture radii. The correlation coefficient between breakthrough size and permeability is 0.90. Some, but not all of the higher permeabilities are also correlated with higher

porosities. Therefore, both porosity and effective pore radii correlate with permeability as follows: relatively higher porosity and coarser pore apertrues are associated with higher permeabilities. It can also be seen from these data that the lowest permeabilities are associated with small pore apertures and high porosities (high microporosity).

Mercury injection curves are compiled in Appendix B. Samples from lithofacies B are difficult to interpret as to breakthrough, but they indicate generally very coarse pore apertures but a wide range of sizes. Some curves from lithofacies C (core 5LA) and D (core 1B) are from oil-producing intervals in the lower Kearny, and they indicate relatively coarse breakthroughs and well-sorted pore apertures (Pittman, 1979). Coarser, better-sorted (i.e. smaller size range) pore radii have generally been found to correlate with higher permeabilities (Pittman, 1979, Gaida et al., 1973).

TABLE 5

STATISTICS OF PETROPHYSICAL DATA

	Porosity %			Permeability (md)				
	Range	Mean	Standard Deviation	Range	Mean	Standard Deviation	Correlation Coefficient	Regression Slope
Lithofacies A	5.4 to 13.0	8.1	2.3	0.01 to 0.91	0.214	0.33	0.73	0.21
Lithofacies B	2.5 to 18.9	13.7	4.4	0.04 to 248.40	40.33	52.32	0.70	0.15
Lithofacies C	6.4 to 16.8	12.0	3.2	0.02 to 176.40	16.82	42.14	0.95	0.35
Lithofacies D	6.6 to 21.0	14.5	4.3	0.01 to 12.60	4.00	5.08	0.17	3.84
Lithofacies E	2.9 to 19.2	14.0	4.5	0.01 to 16.60	5.83	6.42	0.89	0.22
Lithofacies F	0.2 to 7.4	3.9	2.6	0.00 to 0.14	0.04	0.06	0.79	22.36

Correlation Coefficients - x = Pore Size (Breakthrough)

y = Porosity, Permeability

Pore Size and porosity = 0.13

Pore Size and Permeability = 0.90

CHAPTER VII

RELATIONSHIPS AMONG GEOLOGICAL AND PETROPHYSICAL PROPERTIES

One of the main purposes of this investigation is to attempt to determine the associations among geological properties (processes) and petrophysical properties. Geological properties such as mineralogy, grain size, and cements, are the products of geological processes such as sediment transport and sorting in a given depositional environment, and post-depositional alteration (diagenesis). Diagenetic processes have been important in controlling petrophysical parameters. Pore-filling cements, particularly silica and carbonates, have reduced porosity and permeability significantly in certain lithofacies. Compaction has also played a part in porosity reduction. Dissolution has been important as a process of porosity enhancement. Where diagenesis is not acting as on overriding control, textural parameters are important in influencing petrophysical properties.

Diagenetic Controls

Authigenic Mineralogy

Pore-filling cements are a major factor associated with porosity and permeability reduction as would be expected. Many of the relatively low porosity and permeability values in Figure 39 correlate with compartively high percentages of cements. Table 6 is a summary of some samples that were point-counted, which shows a breakdown of pore-filling cements and petrophysical properties. Total cement is cross-plotted against porosity and permeability in figures 41 and 42. The overall correlation between total cement and porosity is -0.58.

TABLE 6

CEMENT ABUNDANCES AND PETROPHYSICAL PROPERTIES

Sample No.	Lithofacies	Silica (%)	Calcite (%)	Dolomite (%)	Barite (%)	Chlorite (%)	Kaolinite (%)	Total (%)	Porosity (%)	Permeability (md)
1B5747	A	8.0	—	5.8	—	—	1.5	15.3	10.4	0.07
1NA6064.5	A	0.8	34.8	—	—	—	—	35.6	7.4	0.91
1NA6092.5	A	3.5	31.2	—	—	—	—	34.7	6.9	0.05
1P5959	A	7.2	3.5	17.5	—	0.2	—	28.4	8.4	0.07
1P5975	A	10.8	6.8	8.0	0.8	—	—	26.4	7.6	0.08
26A6010.9	A	5.2	20.8	5.2	—	—	0.5	31.7	6.3	0.02
WD24484	B	1.5	—	—	—	—	5.0	6.5	15.0	0.83
WD24485.3	B	2.2	—	0.5	—	—	1.0	3.7	18.7	75.8
WD24490.3	B	1.0	—	2.5	—	—	3.5	7.0	14.4	8.22
WD24497.8	B	4.0	—	—	—	—	6.0	10.0	16.9	45.3
WD24497.9	B	2.0	—	—	—	—	3.5	5.5	14.6	7.85
WD24505	B	0.7	—	9.3	—	—	2.7	12.7	2.6	0.04

Table 6 continued

CEMENT ABUNDANCES AND PETROPHYSICAL PROPERTIES

Sample No.	Lithofacies	Silica (%)	Calcite (%)	Dolomite (%)	Barite (%)	Chlorite (%)	Kaolinite (%)	Total (%)	Porosity (%)	Permeability (md)
1JB5049.5	B	3.0	—	1.2	—	—	1.5	5.7	16.8	248.38
1JB5053.5	B	4.0	—	1.5	—	—	1.8	7.3	17.0	50.47
1JB5057.5	B	1.0	—	5.0	—	—	0.5	6.5	11.9	22.29
1JB5057.6	B	1.3	—	4.7	—	—	—	6.0	7.4	134.86
1JB5060.5	B	—	—	11.0	—	—	1.0	12.0	2.5	0.18
1LG5370	B	3.6	—	2.8	—	—	4.4	10.8	11.4	35.78
1LG5379	B	2.2	—	—	0.8	—	1.2	4.2	14.6	3.48
1LG5380	B	0.8	—	15.0	—	—	0.8	16.6	11.5	9.83
1LG5388.7	B	2.9	—	5.6	—	—	3.5	12.0	12.5	23.08
26A6053.7	C	12.2	0.5	2.2	—	1.2	—	16.1	15.0	8.62
26A6057	C	11.8	12.2	0.8	—	2.2	—	27.0	15.9	20.23
26A6061.5	C	10.8	—	16.0	—	0.2	—	27.0	7.5	0.02

Table 6 continued

CEMENT ABUNDANCES AND PETROPHYSICAL PROPERTIES

Sample No.	Lithofacies	Silica (%)	Calcite (%)	Dolomite (%)	Barite (%)	Chlorite (%)	Kaolinite (%)	Total (%)	Porosity (%)	Permeability (md)
5LA5619.5	C	14.8	—	—	—	1.2	—	16.0	16.8	176.42
5LA5631.5	C	6.2	—	8.2	—	1.0	0.2	15.6	13.2	2.24
5LA5635.3	C	5.5	—	5.8	—	0.8	0.2	12.3	13.9	2.40
5LA5640.2	C	2.8	—	3.8	—	1.0	0.5	8.1	11.0	0.12
1B5731.2	D	16.2	—	—	—	4.5	—	20.7	8.9	1.17
1B5739	D	17.5	—	—	—	2.5	—	20.0	11.5	12.59
1P5933	E	10.2	9.8	0.2	0.2	3.5	—	23.9	16.6	16.59
1P5948	E	4.5	35.2	—	—	—	—	39.7	2.9	0.01
1NA6057.3	F	12.2	6.5	—	—	3.2	—	21.9	4.7	0.08
1NA6101.8	F	12.0	22.2	—	—	—	—	34.2	3.3	0.00

overall correlations: Total % cement and Porosity (%) = -0.58

Total % cement and Permeability = -0.63

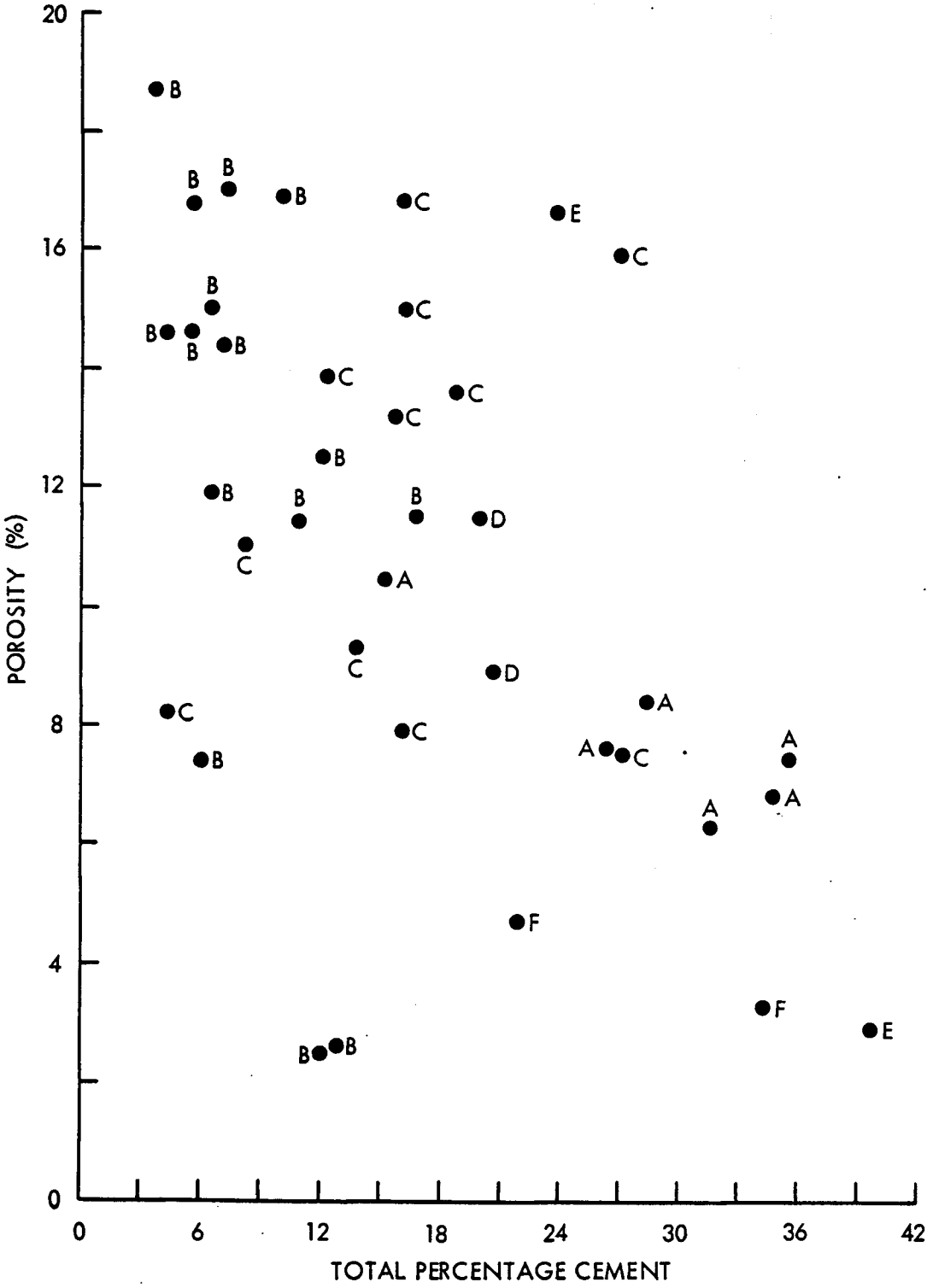

Fig.41
Porosity versus abundance of cement for samples from different lithofacies.

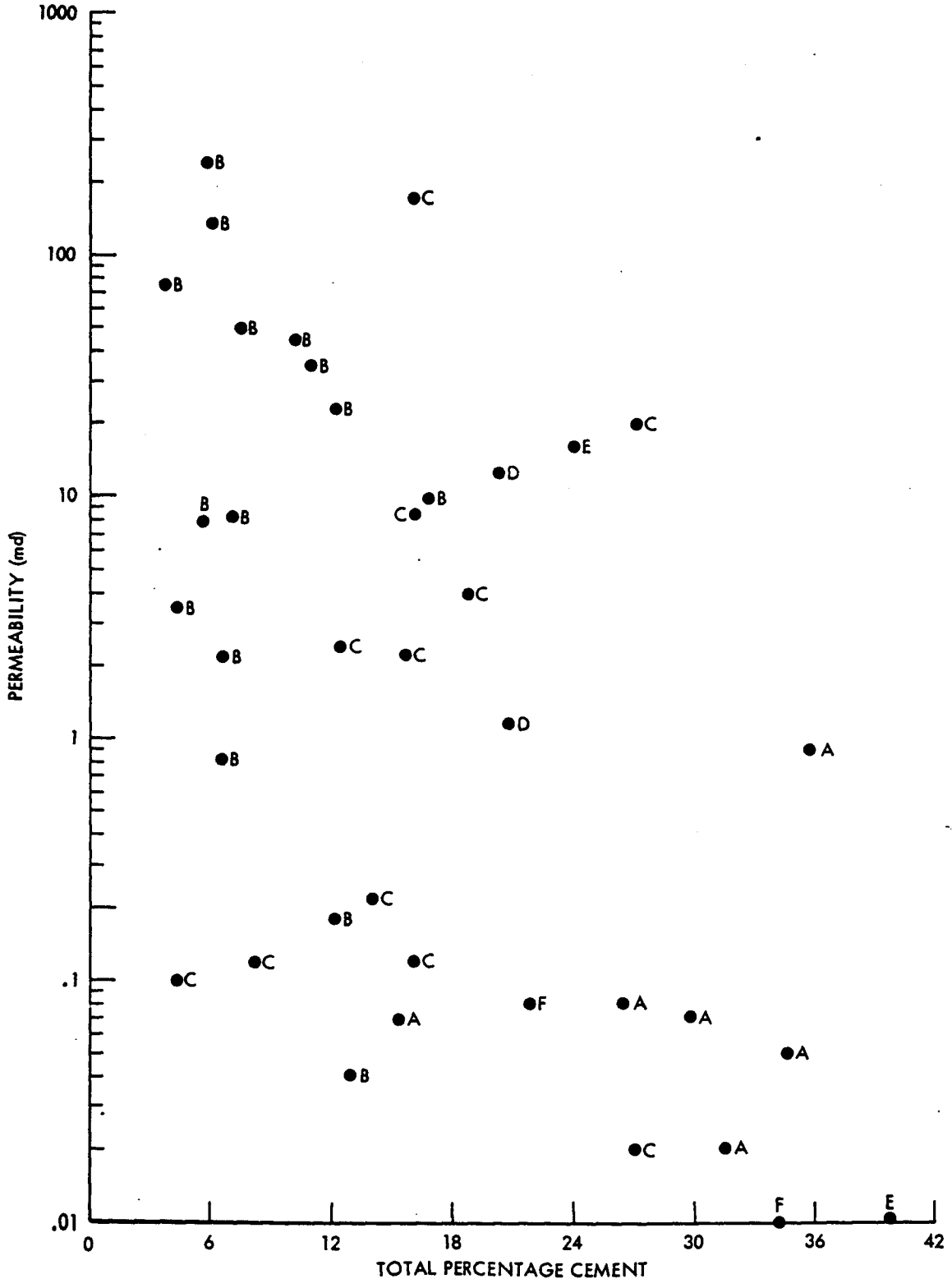

FIG. 42

Permeability versus abundance of cement for samples from different lithofacies.

This indicates there is some negative correlation but it is not a strong correlation. For lithofacies A alone the correlation is better (-0.88). The overall correlation between total cement and permeability (-0.63) is slightly stronger than between cement and prosoity. Although these correlation coefficients are not particularly strong, there does appear to be a trend of lower porosity and permeability with greater abundance of cement. Points that do not exhibit a strong control by cementation may in part be explained by other geological parameters, principally sorting. In some cases the percentage total cement can be misleading as to its influence on porosity and permeability. For example, petrographic study of samples JB5060.5 (core 1JB. depth - 5060.5 feet) and WD24505 suggest ferroan dolomite-ankerite is the principal factor responsible for reduction of porosity. The percentage of cement in these samples is comparatively low overall. Relative to other samples from these cores, however, JB5060.5 and WD4505 contain more than double the total cement.

Cementation has been most extensive in lithofacies A. As a consequence this lithofacies as a whole does not exhibit favorable porosity and permeability. In lithofacies F cementation and interlaminated to interbedded clays, as well as very-fine grain size are responsible for very low porosity and permeability. Cementation has also reduced porosity in lithofacies B, C, D, and E. In these sandstones, however, cements are less abundant and occur in a limited or patchy distribution, preserving primary porosity higher permeability. Patchy cements may not be effective in reducing permeability when the sandstone is coarse grained or very well-sorted, with consequent good porosity and large pore apertures.

In addition to the major silica and carbonate cements, authigenic chlorite and kaolinite have influenced petrophysical properties by adding microporosity. Chlorite grain coatings have not significantly acted to maintain porosity by hindering quartz cementation. Pittman (1979) has shown that argillaceous sandstones having predominantly microporosity also have low permeabilities, typically in the tenths of a millidarcy range. The effect chlorite and kaolinite have had on permeability is minimal, particularly in comparison to other pore-filling cements. Total microporosity as a whole, and with respect to samples containing abundant chlorite or kaolinite, is considerably less than that documented by Pittman. Petrographic and S.E.M. observations reveal that authigenic clays occur in patches, with primary and secondary pores remaining to a large degree free of thick clay-linings and fillings (Figs. 34, 36).

Compaction

Diagenetic features indicative of compaction were discussed previously. The sum effect of the various mechanisms of compaction on porosity reduction can be estimated by the following formula (Jonas and McBride, 1977, p. 42):

$$\phi \text{ loss by compaction} = \phi \text{ initial} - (\phi \text{ present} + \% \text{ cement})$$

where: ϕ initial = porosity at the time of deposition

ϕ present = present porosity from core plug or point-count analysis

% cement = total cement percentage from point-count.

This formula assumes compaction takes place prior to cementation. In the case of lithofacies A this is not strictly the case because stylolites were noted to have developed after cementation by ferroan calcite. Initial porosity must be assumed. Jonas and McBride suggest 45 percent for clean sands from point bars,

beaches, or dunes (Jonas and McBride, 1977, p. 42). Beard and Weyl (1973) showed that sorting has an effect on the porosity of artificially wet-packed unconsolidated sand. It may therefore be more accurate to use assumed initial porosities that are adjusted to sorting. In calculating estimated porosity loss by compaction for various clean samples, the initial porosities assumed were taken from Beard and Weyl (1973, p. 352) as adjusted to grain size and sorting. Table 7 contains the results of these calculations.

It appears that compaction has been most significant in lithofacies B and in core 5LA (lithofacies C), with the exception of the upper portion (5LA5619.5). Compaction was aided in lithofacies B by ductile shale clasts (Fig. 28). Shale clasts, matrix, and pressure solution facilitated compaction in lithofacies C (5LA) (Fig. 31).

Dissolution

The effects of dissolution as a diagenetic process of porosity formation can be seen in glauconite, ferroan dolomite-ankerite cement, and potassium feldspar predominantly. Dissolution is most notable in lithofacies B, involving feldspar and ferroan dolomite-ankerite cement. Secondary intragranular porosity in potassium feldspar is very well-exhibited in core WD2 (Fig. 36). Dissolution of the dolomite is best developed in core 1LG, although kaolinite fills some of the resultant pores (Fig. 24)

In lithofacies B, secondary dissolution porosity exceeds primary porosity and ranges from about 30 to 80 percent of the total porosity. This porosity probably represents at least in part, effective porosity, and therefore likely contributes to permeability. In other upper Morrowan sandstones dissolution is important in creating the total effective porosity (Kasino and Davies, 1979).

TABLE 7

POROSITY REDUCTION BY COMPACTION

Sample No.	L-Facies	Grain Size[1]	Sorting[2]	Pi(%)[3]	Cement(%)	Porosity(%)	Porosity Reduction(%)
1B5747	A	Lower Fine	mod. well	34.3	15.3	10.4	8.6
1NA6064.5	A	Upper Coarse	mod. well-well	35.2	35.6	7.4	0.0
1NA6092.5	A	Lower Coarse	mod. well	33.3	34.7	6.8	0.0
1P5959	A	Upper Coarse	mod. well	32.4	28.4	8.4	0.0
1P5975	A	Lower Coarse	mod. well	33.3	26.4	7.6	0.0
1P6010.9	A	Lower Coarse	mod. well	35.8	31.7	6.3	0.0
WD24484	B	Upper Medium	poor	31.5	6.5	15.0	10.0
WD24485.3	B	Lower Very Coarse	mod. well-well	38.0	3.7	18.7	15.6
WD24490.3	B	Upper Very corase	well	38.0	7.0	14.4	16.6
WD24497.8	B	Upper Medium	mod. well	34.2	10.0	16.9	7.3
WD24497.9	B	Upper Coarse	poor	27.1	5.5	14.6	7.0
WD224505	B	Lower Granule	well	38.0	12.7	2.6	22.7
1JB5049.5	B	Upper Coarse	well	38.0	5.7	16.8	15.5
1JB5053.5	B	Lower Caorse	well	38.4	7.3	17.0	14.1
1JB5057.5	B	Lower Very Coarse	well	38.0	6.5	11.9	19.6
1JB5057.6	B	Upper Very Corase	well	38.0	6.0	7.4	24.6
1JB5060.5	B	Very Coarse-Granule	well	38.0	12.0	2.5	23.5
1LG5370	B	Upper Coarse	well	38.0	10.8	11.4	15.5
1LG5380	B	Upper Coarse	mod. well	32.4	16.6	11.5	4.3
1LG5379	B	Upper Coarse	well	38.0	4.2	14.6	19.2
1LG5388.7	B	Upper Coarse	mod. well	32.4	12.0	12.5	7.9
2GA6053.7	C	Lower Coarse	mod. well	33.3	161	15.0	2.2
2GA6057	C	Lower Coarse	mod. well-well	35.8	27.0	15.9	0.0
2GA6061.5	C	Upper Medium	mod. well-well	36.2	27.0	7.5	1.7
5LA5619.5	C	Lower Medium	very well	41.5	16.0	16.8	8.7
5LA5626.5	C	Upper Fine	well	39.1	18.7	13.6	6.8

TABLE 7 (continued)

POROSITY REDUCTION BY COMPACTION

Sample No.	L-Facies	Grain Size[1]	Sorting[2]	Pi(%)[3]	Cement(%)	Porosity(%)	Porosity Reduction(%)
5LA5631.5	C	Lower Medium	very well	40.2	15.6	13.2	11.4
5LA5635.3	C	Upper Medium	med. well-well	38.5	12.3	13.9	12.3
5LA5640.2	C	Medium-Coarse	mod. well	33.8	8.1	11.0	14.7
5LA5648.2	C	Lower Coarse	well	38.4	16.1	7.9	14.4
5LA5641.3	C	Upper Coarse	mod. well-well	35.2	4.3	8.2	22.7
1B5731.2	D	Upper Fine	mod. well	35.6	20.7	8.9	6.0
1B5739	D	Upper Fine	well	40.2	20.0	11.5	8.7
1P5933	E	Lower Fine	very well	43.0	23.9	16.6	2.5
1P5948	E	Lower Fine	very well	43.0	39.7	2.9	0.4
1NA6057.3	F	Upper Very Fine	mod. well	35.6	21.9	4.7	9.0
1NA6101.8	F	Upper Very Fine	mod. well	35.6	34.2	3.3	0.0

[1]Most measurements based on visual estimates, some on actual measurements of long axis of grains.

[2]Sorting estimates based on visual comparaters - Beard and Weyl (1973).

[3]Pi is the assumed initial porosity. When sorting or grain size is borderline, values from different categories were averaged. For grain sizes of very coarse and above, no Pi values were given. The highest values given by Beard and Weyl was used in this instance. (Estimates from Beard and Weyl, 1973).

[4]Values of 0.0 reflect negative calculated values. As negative values are meaningless, they are taken to essentially reflect very little or no porosity reduction due to compaction.

Textural Controls

Grain Size

Mean grain size determinations were made on 19 thin sections from lithofacies B and C, from cores 1JB, WD2, and 5LA. Cementation does not appear to be an overriding control on petrophysical properties in these cores, and and therefore grain size was investigated as a possible controlling factor. Grain size is a textural property that controls permeability in such a manner that permeability generally increases with grain size, while porosity remains unchanged (Pettijohn et al., 1972, p. 525). Smaller grain size results in smaller pore throats and therefore lower permeability. In light of this the correlation between permeability and grain size for the 19 samples overall, and by lithofacies is poor (Fig. 43). Correlation coefficients are -0.10, (lithofacies D), -0.53 (lithofacies B), and -0.62 (lithofacies C). This indicates grain size is not the predominant control on permeability in these cores. A poor correlation between grain size and petrophysical properties in lithofacies B is similar to data obtained by Kasino and Davies (1979). They attributed this to the control of secondary porosity, which may also apply to lithofacies B. In lithofacies C for samples that have larger mean grain sizes, sorting is poorer, pore apertures are smaller, and microporosity is higher (below). These factors are responsible for controlling permeability. For some similar porosity samples from lithofacies of different grain sizes, permeability does appear to increase with grain size. These samples are plotted as triangles in Figure 43.

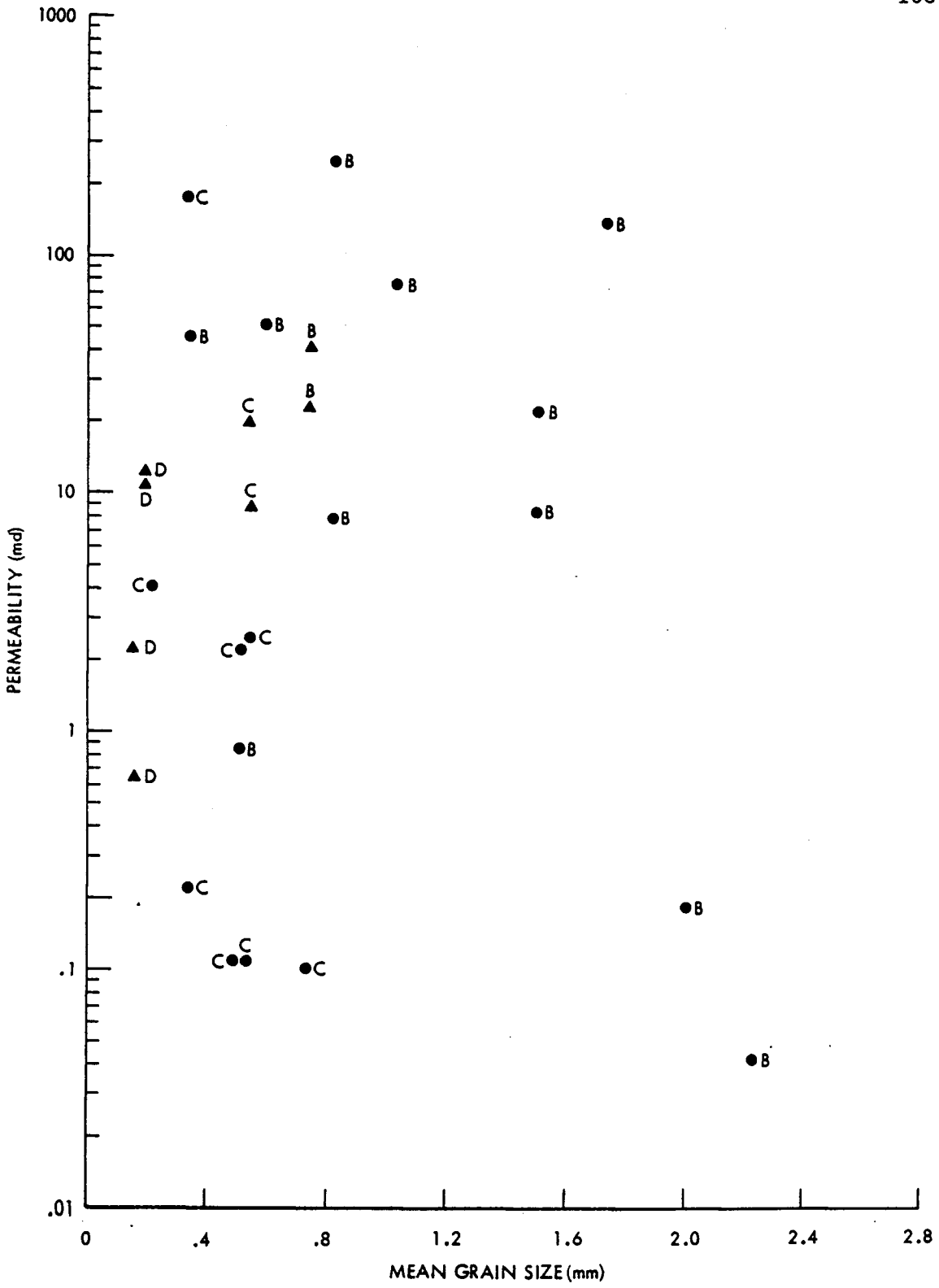

FIG. 43

Permeability versus grain size for some samples from different lithofacies. (▲ are estimated modal)

Other Textural Controls

Other textural characteristics that exert a control on petrophysical properties include sorting, packing (compaction) and the presence of interstitial clays (or microporosity). These factors are believed to be important in Kearny Formation sandstones in certain lithofacies. In general poorer sorting and tighter packing result in lower porosity and permeability (Pettijohn et al., 1972, p. 525). Lower permeability results from smaller pore apertures. Abundant microporosity is associated with low permeability (Pittman, 1979).

In core 5LA (lithofacies C) the upper portion of the interval tends to be better sorted, less compacted, and has relatively low microporosity, and these factors contribute to higher porosity and permeability (Tables 7 and 8). It is notable that sample 5LA5619.5 has a high percentage of intergranular porosity (71.1% of total porosity) and a very coarse breakthrough pore aperture size (17 microns). High percentages of primary intergranular porosity are usually associated with larger pore aperatures and high permeability, which are indicative of a good reservoir (Pittman, 1979). These geological parameters are likely to affect petrophysical properties in lithofacies B in a similar way, but the data obtained do not clearly support this.

The importance of abundant clays in reducing permeability is evident in lithofacies D (core 1LG) (not represented on triangular plot) and E (core 5LA). Abundant matrix clas resultant in a small breakthrough pore aperture size (0.9 microns) and high microporosity. Permeability is therefore low despite sometimes high porosities, due to clay adsorption (Table 5, 1LG5368.5).

In addition, the scale of sedimentary structures is a probable factor that contributes to permeability differences between rippled and laminated

TABLE 8

PORE TYPE DISTRIBUTION AND MEAN GRAIN SIZE

Sample No.	Lithofacies	Porosity(%)	Permeability(md)	Primary Porosity(%)	Secondary Porosity(%)	Microporosity(%)	Grain Size (mm)
WD24484	B	15.0	0.83	0.0	38.3	61.7	0.51
WD24485.3	B	18.7	75.38	17.4	48.1	34.5	1.04
WD24490.3	B	14.4	8.22	25.0	54.5	20.5	1.51
WD24497.8	B	16.9	45.29	25.5	32.0	42.5	0.37
WD24497.9	B	14.6	7.85	37.7	51.4	10.9	0.82
IJB5049.5	B	16.8	248.39	29.8	34.5	33.7	0.83
IJB5053.5	B	17.0	50.47	25.0	33.9	41.0	0.61
IJB5057.5	B	11.9	22.29	21.0	33.6	45.4	1.51
IJB5057.6	B	7.4	134.86	9.5	81.0	9.5	1.74
5LA5619.5	C	16.8	176.42	71.1	22.9	6.0	0.34
5LA5625.3	C	9.3	0.22	66.7	25.6	7.7	0.34
5LA5626.5	C	13.6	4.00	55.0	6.0	39.0	0.23
5LA5631.5	C	13.2	2.24	50.0	43.6	6.4	0.32
5LA5635.3	C	13.9	2.40	48.6	10.8	40.6	0.35
5LA5640.2	C	11.0	0.12	29.9	2.3	74.8	0.49
4LA5648.2	C	7.9	0.12	19.4	25.8	54.8	0.54
5LA5651.3	C	8.2	0.10	0.0	0.0	100.0	0.74

lithofacies D, and cross-bedded and structureless lithofacies C and B. Small scale structures have been shown to be important in reducing permeability (Marafa, 1980).

Table 9 is an attempt to summarize the effects of geological characteristics on petrophysical properties in the sandstone lithofacies investigated.

TABLE 9

SUMMARY OF GEOLOGIC CONTROLS AND PETROPHYSICAL PROPERTIES

Lithofacies	Geologic Controls	Petrophysical Properties
A	Primarily abundant pore-filling ferroan calcite. Pore-filling quartz and ferroan dolomite.	Overall low porosity and permeability.
B	Complex: involving grain size, sorting amount of micro-porosity, abundance of shale clasts and compaction, ferroan dolomite-ankerite cement.	Generally high porosity, permeability, coarse pore size distribution. Coarse grain size - coarse pore sizes. Poor sorting; greater microporosity, shale clasts, ferroan dolomite-ankerite - lower porosity and permeability.
	Dissolution of dolomite, feldspar	Porosity enhancement
C	Pore-filling quartz, ferroan calcite minor ferroan dolomite. Sorting, amount of microporosity, intergranular porosity, compaction important.	Wide range of porosity, permeability, pore size distribution. Cements - porosity, permeability reduction; not always important. High degree of sorting, high percentage intergranular porosity, relatively less compaction - coarse pore sizes and high permeability.

TABLE 9

SUMMARY OF GEOLOGIC CONTROLS AND PETROPHYSICAL PROPERTIES (continued)

Lithofacies	Geologic Controls	Petrophysical Properties
D	Variable: Pore-filling quartz, ferroan calcite. Grain size, ripple cross-lamination, abundance of microporosity associated with detrital clays and shale clasts. High percentage of intergranular porosity.	Porosity - moderate to high. Permeability - low to moderately high. Pore size distribution - fine to moderately coarse. Fine grain size, ripple lamination and microporosity - fine pore sizes, low permeability, sometimes high porosity. Intergranular porosity - moderately high permeability.
E (Clean)	Pore-filling quartz and patchy calcite. Abundant preserved intergranular porosity.	Low to moderately high porosity, permeability. Moderately coarse pore size distribution. Patchy calcite - low porosity and permeability. Lack of calcite, preserved intergranular porosity - higher porosity, permeability.

TABLE 9

SUMMARY OF GEOLOGIC CONTROLS AND PETROPHYSICAL PROPERTIES (continued)

Lithofacies	Geologic Controls	Petrophysical Properties
E (Muddy)	Poor-sorting, abundance of micro-porosity. Some pore-filling quartz, ferroan calcite	Low to moderately high porosity, low permeability. Fine pore size and abundance of microporosity - fine pore sizes and low permeability.
F	Variable: Pore-filling quartz and ferroan calcite, fine grain size. Interlaminated clays.	Low porosity and permeability.

CHAPTER VIII

IMPLICATIONS FOR ENHANCED RECOVERY IN THE KEARNY FORMATION

Concerning the cores used in this study oil production has come from lithofacies C (5LA) and D (1B) of the lower Kearny, and from lithofacies B in the upper part of the formation. These lithofacies also have the highest porosity and permeability, and coarsest pore sizes of all lithofacies. Favorable petrophysical properties also occur in the clean, bioturbated sandstone, lithofacies E in core 1P, but this interval was not productive. Thus, further considerations relative to enhanced recovery are focused on sandstone lithofacies B, C, D, and E.

It is important to understand the reservoir and its heterogeneities on a scale ranging from field size to the pore network itself, in order to simulate the reservoir and evaluate its enhanced recovery potential (Ebanks, 1977, Harris, 1975). This involves geology in rock, framework, and reservoir quality studies (Harris, 1975, p. 626). This thesis details geologic aspects and controls at the lower end of the scale, as opposed to reservoir geometry and thickness trends. Therefore, only the factors controlling fluid flow in the important cores studied and the associated authigenic minerals are discussed here, in terms of the implications for enhanced recovery.

Fluid Flow

In order to simulate flow, it is necessary to know which geologic parameters control trends of porosity and permeability within the reservoir. Since the cores used in this study differ as to depositional environment and

lithology, it is not possible to construct a general reservoir model based on the control offered by the eight cores. On the other hnd, the cores may be discussed individually as to how fluid flow might be controlled in a reservoir composed of a particular lithofacies. This presumes that the lithofacies described in this study maintain the same characteristics for some distance laterally. It should be pointed out, however, that core control of this study is inadequate to support that presumption. More cores are needed from the different lithofacies-reservoir types, as well as a closer spacing of cores.

In the lower Kearny, lithofacies C (2GA, 5LA), which probably represents offshore bars, higher porosity and permeability were found to occur in the upper half of the rock unit (Appendix A). Thus flow would be directed to this portion of the reservoir. In core 2GA grain size is slightly coarser in the upper portion of lithofacies, which is a possible factor for the coarse breakthrough pore apertures and the higher permeability. Total porosity is higher in the upper portion. In core 5LA sorting is better in the upper portion, microporosity is lower, primary porosity is higher, compaction is less significant, and breakthrough pore apertures are coarser. (Tables 7 and 8). These factors explain the higher permeability. Some low permeabilities do occur in the upper part of core 5LA. Permeability trends that might control fluid flow are not so pronounced in the other lower Kearny lithofacies studied. Good permeabilities occur throughout much of the producing sand in core 1B (lithofacies D), but reduction occurs in the upper 0.7 m that is related to a combination of geologic parameters. The bioturbated sandstone in 1P (lithofacies E) is characterized by patchy calcite cement throughout that reduces permeability in a similar patchy

distribution. Relatively high permeabilities do occur here, but the interval does not seem to be broken into separate flow units.

Upper Kearny reservoirs do not show a vertical trend of porosity and permeability within the main rock unit (lithofacies B). These sandstones were probably deposited in a deltaic environment, possibly in distributary channel fills. Although they are capped by impermeable interlaminated shale and sandstone (lithofacies F) and shale, a fining-up sequence is not well-developed through lithofacies B as is characteristic of point-bar sandstones (Reading, 1978, p. 33-34). In the point bar model because grain size and structure scale decrease upwards, greater porosities and permeabilities occur from the middle of the sand body downward (Ebanks, 1977, p. 102). Given such a model, fluid flow may be simulated to take into account the heterogeneity of permeability. In the case of lithofacies B, the geologic controls are complex, involving grain size, pore type-distribution of clays, and cementation. Average grain size ranges from medium sand to granule size, but does not seem to exert a predominant control on permeability (Fig. 43, Table 8), in fact, grain size and permeability seem inversely related. Higher total porosity is in part associated with higher permeability. In some cases abundant microporosity is a likely factor resulting in relatively lower permeability, although this is not applicable overall. These controls do not appear to follow a well-defined vertical trend and therefore permeability does not follow a pattern relative to the vertical position within lithofacies B. Reservoir simulation would seem to need a more complex, possibly statistical method to convey the distribution of permeability in this lithofacies. One factor, however, that appears characteristic in lithofacies B (1JB, WD2) is that the basal 0.3 m is completely cemented with ferroan dolomite-ankerite,

which substantially reduces porosity and permeability (Appendix A).

Rock-Fluid Interactions

A major area of concern in enhanced recovery is that of rock-fluid interactions. This was stressed at a recent workshop on the impact of geology in enhanced recovery (Peterson et al., 1982). It is here that the authigenic mineralogy that lines and fills pores comes into play in planning enhanced recovery projects. The consensus reached at the conference was that much more research is needed on rock-fluid interactions. It is clear, however, that certain authigenic minerals hinder the effectiveness of injected fluids, and as a result of interactions, lead to formation damage. Diagenetic clays have a high surface area and therefore tend to interact greatly with fluids, and present the problem of migration of fines into pore throats (Peterson et al., 1982, p. 14, Ebanks, 1977, p. 96). Carbonates, particularly iron-bearing carbonates, are of concern because of their reactivity with respect to carbon dioxide and acids (Peterson et al., 1982, p. 14). Both authigenic clays (chlorite, kaolinite) and carbonates (ferroan calcite, ferroan dolomite-ankerite) are present in the key lithofacies of the Kearny Formation discussed at the beginning of this chapter.

Chlorite is present in all these lithofacies but is more abundant in the lower Kearny, while kaolinite is much more abundant in lithofacies B of the upper Kearny. Chlorite is of additonal concern because it is a source of ferric ions that have a destructive effect on polymers and sulfonates (Peterson, et. al., 1982, p. 14). Iron that is liberated from chlorite, for example by acidization, can reprecipitate as ferric hydroxide ($Fe(OH)_3$), which is a material capable of blocking pore throats (Kasino and Davies, 1979, p. 192). Good design of EOR

projects requires steps to stabilize kaolinite and chlorite to prevent their migration, and to scavenge iron released from chlorite.

Of the authigenic carbonates, ferroan calcite is present in lithofacies C in core 2GA, and ferroan dolomite-ankerite occurs in all lithofacies, particularly B and C. These minerals are reactive and can liberate iron, resulting in the detrimental effects mentioned above. The carbonate minerals should be considered with regard to caustic processes (Peterson, et. al., 1982, p. 18).

Feldspar is a framework constituent that is abundant in lithofacies B. It has been suggested that feldspar can react with carbon dioxide (Peterson, et al., 1982, p. 14). Therefore this is an additional concern with respect to this particular recovery process should it be considered in the upper Kearny Formation.

CHAPTER IX

SUMMARY AND CONCLUSIONS

1. Six generalized sandstone lithofacies were recognized in this study:

Lithofacies A - medium to coarse-grained, poor to well-sorted, glauconitic, fossiliferous, cross-bedded sandstone. Lithofacies A probably represents deposition as a marine shelf sandbar.

Lithofacies B - medium to very coarse-grained, poor to well-sorted, lithic to feldspathic, cross-bedded sandstone. Lithofacies B represents deposition in marginal marine-deltaic environments, probably largely in distributary channels.

Lithofacies C - medium to coarse-grained, moderately well to very-well-sorted, glauconitic, cross-bedded sandstone. Lithofacies C was also probably deposited as a marine shelf sandbar.

Lithofacies D - very-fine to fine-grained, moderately well to well-sorted, glauconitic, rippled sandstone. Lithofacies D was deposited on a marine shelf as a sandbar (cross-bedded - core 1NA) and in interbar areas characterized by lower energy conditions. In core 1LG this lithofacies may represent tidal flat deposition.

Lithofacies E - glauconitic, bioturbated sandstone.

a) clean, fine-grained, and well to very well-sorted.

b) muddy, medium to coarse-grained, and poorly-sorted.

Lithofacies E was deposited on a marine shelf in an interbar area under relatively lower energy conditions. In such an environment bioturbation may be preserved due to lack of reworking of the sediments.

Lithofacies F - intercalated (to interlaminated, silt to fine-grained, glauconitic sandstone and black shale. Lithofacies F in core 1NA was probably deposited in a marine environment characterized by low but fluctuating energy conditions that produced interbedding of sand and shale. Where lithofacies F is associated with lithofacies B it probably represents overbank deposition.

2. Lower Kearny sandstones were deposited in a shallow marine environment under relatively high but variable energy conditions (lithofacies A, C) and lower, variable energy settings (lithofacies D, E, F). Sandstones of the upper Kearny (lithofacies B) were deposited in marginal marine-deltaic environments possibly as stream-mouth bars or distributary channel fills.

3. Petrographically the important reservoir sandstones fall into several categories (Folk, 1980):

   a) Poor to well-sorted, medium to very coarse sandstone: dolomite and quartz cemented submature to mature arkose to feldspathic litharenite (Lithofacies B).

   b) Moderately-well to very-well-sorted, medium to coarse sandstone: dolomite, calcite and quartz cemented submature to mature glauconitic subarkose (Lithofacies C).

   c) Moderately-well to well-sorted, very-fine to fine sandstone: calcite and quartz cemented submature to mature glauconitic quartzarenite (Lithofacies D).

4. Three major stages of diagenesis affected Kearny sandstones:

   a) Glauconite pellets and chlorite grain coatings formed during early

diagenesis. Pyrite replacements of detrital clays and possibly some kaolinite also formed early.

b) Mainstage diagenesis including pore-filling by quartz, calcite, ferroan calcite and ferroan dolomite. Some authegenic chlorite probably formed at this time as well as grain replacements including quartz by calcite, glauconite by calcite, and solution-fill of shell fragments by calcite.

c) Late diagenesis involved growth of ferroan dolomite-ankerite cement; dissolution of ferroan dolomite-ankerite, feldspars, and rock fragments; and kaolinitization.

5. Porosity and permeability ranges from 0-21% and 0 to 248 md, with highest values occurring in lithofacies B, C, and D.

6. Rocks with relatively high permeability are also highly porous and have coarse pore size distributions.

7. Diagenesis was somewhat different in each lithofacies. The results of diagenesis are most important in explaining facies to facies variations in porosity and permeability:

a) Pore-filling silica and carbonate cements as a factor of porosity and permeability reduction (particularly Lithofacies A).

b) Compaction and pressure solution that resulted in smaller effective pore radii and reduced porosity and permeability (Lithofacies B and C).

c) Dissolution of ferroan dolomite-ankerite and feldspar, which enhanced porosity, particularly in in Lithofacies B.

8. Grain size and sorting are additional factors that are of probable importance in controlling petrophysical properties. Permeability increases with grain size between lithofacies B, C, and D. Within lithofacies B and C for the samples measured there appears to be no relationship between grain size and permeability. To a certain degree permeability decreases with increasing grain size, which is a result of the influence of sorting, pore types, pore throat size, and cementation. In lithofacies C of core 5LA high permeability samples have the best sorting (well to very well sorted).

9. Authigenic chlorite, kaolinite and iron-rich carbonates pose potential problems for enhanced recovery concerning:

a) High surface area of clays and their potential to adsorp injected fluids.

b) Migration of fines (Kaolinite-lithofacies B).

c) Reactivity and the release of iron into pore systems.

10. In general the Kearny Formation sandstones studied are similar in lithology, diagenesis, and petrophysical properties to other Morrowan Stage sandstones in the Anadarko Basin of Oklahoma and Texas, and in the Hugoton Embayment of southeastern Colorado.

REFERENCES CITED

Adams, W.L., 1964, Diagenetic aspects of Lower Morrowan, Pennsylvanian, sandstones, northwestern Oklahoma: AAPG Bulletin, v. 48, p. 1568-1580.

Amyx, J.M.; Bass, D.M., Jr.; and Whiting, R.L., 1960, Petroleum Reservoir Engineering, Physical Properties. New York, McGraw-Hill, 610 p.

Arro, E., 1965, Morrowan sandstones in the subsurface of the Hough area, Texas County, Oklahoma: Shale Shaker, v. 16, n. 1, p. 2-16.

Avis, L.E., and Boothby, D.R., 1982, Promising Morrow sandstone discoveries in southeastern Colorado: Oil and Gas Journal, May 31, p. 163-170.

Bagnold, R.A., 1954, Experiments on gravity-free dispersion of large solid spheres in newtownian flow undershear: Royal Soc. Lond., Proc. ser.A 225, p. 49-63.

Bailey, E.H. and Stevens, R.E., 1960, Selective staining of K-feldspar and plagioclase on rock slabs and thin section: Am. Mineralogist, v. 45, p. 1020-1025.

Beard, D.C. and Weyl, P.K., 1973, Influence of texture on porosity and permeability of unconsolidated sand: AAPG Bulletin, v. 57, p. 349-369.

Berner, R.A.; Bladwin, T.; and Holdren, G.R., Jr., 1979, Authigenic iron sulfides as paleosalinity indicators: Jour. Sed. Pet., v. 49, n. 4, p. 1345-1350.

Blatt, H., 1979, Diagenetic processes in sandstones, in Scholle, P.A., and Schluger, P.R., eds., Aspects of Diagenesis: SEPM, Spec. Pub., n. 26, p. 349-369.

Blatt, H.; Middleton, G.; and Murray, R., 1980, Origin of Sedimentary Rocks: New Jersey, Prentice-Hall, 782 p.

Boles, J.R., and Franks, S.G., 1979, Clay diagenesis in Wilcox sandstones of southwest Texas: Implications of smectite diagenesis on sandstone cementation: Jour. Sed. Pet., v. 49, n. 1, p. 55-70.

Brenner, R.L., and Davies, D.K., 1974, Oxfordian sedimentation in western interior United States: AAPG Bulletin, v. 58, n. 3, p. 407-428.

Burst, J.F., 1958, 'Glauconite' pellets: their mineral nature and applications to stratigraphic interpretations: AAPG Bulletin, v. 42, n. 2, p. 310-327.

Busch, D.A., 1961, Prospecting for stratigraphic traps:, in Peterson, J.A., and Osmond, J.C., eds., Geometry of Sandstone Bodies: AAPG, p. 220 -232.

Churnet, H.G.; Misra, K.C.; and Walker, K.R., 1982, Deposition and dolomitization of Upper Knox carbonate sediments, Copper Ridge district, East Tennessee: Geol. Soc. Amer. Bull., v. 93, p. 76-86.

Cloud, P.E., Jr., 1955, Physical limits of glauconite formation: AAPG Bulletin v. 39, n. 4, p. 484-492.

Crone, A.J., 1974, Experimental studies of mechanically-infiltrated clay matrix in sand: Geol. Soc. Amer., Abstract with programs, vol. 6, no. 7, p. 701.

Curtis, C.D., 1978, Possible links between sandstone diagenesis and depth-related geochemical reactions occurring in enclosing mudstones: Jour. Geol. Soc. London, v. 435, p. 107-117.

Dapples, E.C., 1967, Diagenesis of sandstones, in Larsen, G. and Chilingar, G.V., eds., Diagenesis in Sediments: Developments in Sedimentology No. 8, New York, Elsevier, p. 91-126.

DeRaaf, J.F.M., Boersma, J.R., and Van Gelder, A., 1977, Wave-generated structures and sequences from a shallow marine succession, Lower Carboniferous, County Cork, Ireland: Sedimentology, v.24, p. 451-483.

Dickinson, W.R., 1970, Interpreting detrital modes of Graywacke and Arkose: Jour. Sed. Pet. v. 40, n. 2, p. 695-707.

Dickson, J.A.D., 1965, A modified staining technique for carbonates in thin section: Nature, February, p. 587.

Dodd, J.R. and Stanton, R.J., Jr., 1981, Paleoecology, Concepts and Applications: New York, John Wiley and Sons, 559 p.

Ebanks, W.J., Jr., 1975, Kansas oil for enhanced recovery: a resource appraisal: in Tertiary Oil Recovery Project Contribution 1, 31 p.

Ebanks, W.J., Jr., 1977, Geology in the enhanced recovery of oil: in Proceedings of the Second Tertiary Oil Recovery Conference - Tertiary Oil Recovery Project Contribution 3, p. 92-107.

Evamy, B.D., 1969, The precipitational environment and correlation of some calcite cements deduced from artificial staining: Jour. Sed. Pet., v. 39, n. 2, p. 787-821.

Folk, R.L., 1980, Petrology of Sedimentary Rocks: Hemphill Pub. Co., Austin, Texas.

Gaida, K.H., et al., 1973, Rasterelektronenmikroscopische untersuchunger des porenraumes von sandsteinen: Erdoel-Erdgas-Zeitschrift v. 9, n. 89, p. 336-343.

Grim, R.E., 1968, Clay Mineralogy. McGraw-Hill, New York.

Harris, D.G., 1975, The role of geology in reservoir simulation studies: Jour. Pet. Tech. (May), p. 625-632.

Jonas, E.C. and McBride, E.F.,1977, Diagenesis of Sandstone and Shale: Application to the Exploration for Hydrocarbons: Continuing Education Prog. Pub. No. 1 Dept. of Geol. Sci., Univ. of Texas, at Austin, 165 p.

Kasino, R.E. and Davies, D.K., 1979, Environments and diagenesis, Morrow sands, Cimarron County (Oklahoma), and significance to regional exploration, production, and well completion practices, in Hyne, N.J., ed., Pennsylvanian Sandstones of the Mid-Continent, N.J. Hyne: Tulsa Geol. Society, Tulsa, Oklahoma, p. 169-194.

Keller, W.D., 1970, Environmental aspects of clay minerals: Jour. Sed. Pet., v. 40, n. 3, p. 788-813.

Khaiwka, H.K., 1968, Geometry and depositional environments of Pennsylvanian reservoir sandstones, northwestern Oklahoma: Ph.D. Dissertation, University of Oklahoma, Norman.

Land, L.S. and Dutton, S.P., 1978, Cementation of a Pennsylvanian deltaic sandstone: isotopic data: Jour. Sed. Pet., v. 48, n. 4, p. 1167-1176.

Land, L.S., 1973, Contemporaneous dolomitization of middle Pleistocene reefs by meteoric water, north Jamaica: Bulletin Marine Science, v. 23, p. 64-92.

Longman, M.W., 1982, Carbonate Diagenesis as a Control on Stratigraphic Traps (with examples from the Williston Basin): AAPG Education Course Note Series. no. 21 (Tulsa), 159 p.

Marafa, H.Y., 1980, A Study of the Relationships Between Porosity, Permeability, Dispersion, Pore-Size Distribution and Sedimentary Structures for Two Sandstone Rocks: M.S. Thesis, University of Kansas, Lawrence.

McHargue, T.R., and Price, R.C., 1982, Dolomite from clay in argillaceous or shale-associated marine carbonates: Jour. Sed. Pet., v. 52, n. 3, p. 873-886.

McManus, D.A., 1959, Stratigraphy and Depositional History of the Kearny Formation (Lower Pennsylvanian) in Western Kansas: Ph.D. Dissertation, University of Kansas, Lawrence.

Merriam, D.F., 1955, Structural Development of the Hugoton Embayment (Kans.): in Moore, C.A., ed., 4th Subsurface Geology Symposium Procedures: p. 81-97.

Meyers, W.J., 1974, Carbonate cement stratigrapy of the lake valley formation. (Mississippian) Sacramento Mts., New Mexico: Jour. Sed. Pet., v. 44, n. 3, p. 837-861.

Meyers, W., 1978, Carbonate cements: their regional distribution and interpretation in Mississippian limestones of southwestern New Mexico: Sedimentology, v. 25, p. 371-400.

Milliken, K.L., Land, L.S., and Loucks, R.G., 1981, History of burial diagenesis determined from isotopic geochemistry, Frio Formation, Brazoria County, Texas: AAPG Bulletin, v. 65, n. 8, p. 1397-1413.

Moore, C.H., and Druckman, Y., 1981, Burial diagenesis and porosity evolution, Upper Jurassic Smackover, Arkansas and Louisiana: AAPG Bulletin, v. 65, n. 4, p. 597-628.

Odin, G.S., and Matter, A., 1981, Deglauconiarum origine: Sedimentology, v. 28, p. 611-641.

Paul, S.E., and Bahnmaier, E.L., 1981, 1980 Oil and Gas Production in Kansas -- Energy Resources Series 18: Kansas Geological Survey, University of Kansas, Lawrence.

Paul, S.E., and Bahnmaier, E.L., 1982, Enhanced Oil Recovery Operation in Kansas 1981 -- Energy Resources Series 21: Kansas Geological Survey, University of Kansas, Lawrence.

Perez, K.P., 1978, Diagenesis of the Shannon Sandstone, Southwestern Powder River Basin, Wyoming: Master's Thesis, University of Wyoming, Laramie.

Peterson, M.(ed.)., 1982, The Impact of Geologic Parameters on Enhanced Oil Recovery-Workshop Proceedings: Bartlesville Energy Technology Center, Oklahoma, U.S. Dept. of Energy, 42 p.

Pettijohn, F.J.; Potter, P.E.; and Siever, R., 1972, Sand and Sandstone: New York, Springer-Verlag, 618 p.

Pierson, B.J., 1981, The control of cathodolominescence in dolomite by iron and manganese: Sedimentology, v. 28, p. 600-610.

Pittman, E.D., 1979, Porosity, diagenesis, and productive capability of sandstone reservoirs, in Scholle, P.A. and Schluger, P.R., eds., Aspects of Diagenesis,: SEPM Spec. Pub. No. 26, p. 159-174.

Pittman, J.K., Fouch, T.D., and Goldhaber, M.B., 1982, Depositional setting and diagenetic evolution of some Tertiary unconventional reservoir rocks, Uinta Basin, Utah: AAPG Bulletin, v. 66, n. 10, p. 1581-1596.

Pittman, E.D., and Lumsden, D.N., 1968, Relationship between chlorite coatings on quartz grains and porosity, Spiro Sand, Oklahoma: Jour. Sed. Pet., Notes, v. 38, n. 2, p. 668-670.

Porrenga, D.H., 1967, Glauconite and chamosite as depth indicators in the marine environment: Marine Geology, v. 5, p. 495-501.

Potter, P.E.; Maynard, J.B.; and Pryor, W.A., 1980, Sedimentology of Shale - Study Guide and Reference Source: New York, Springer-Verlag, 306 p.

Powers, M.C., 1957, Adjustment of land derived clays to the marine environment: Jour. Sed. Pet., v. 27, n.4, p. 355-372.

Radke, B.M. and Mathis, R.L., 1980, On the formation and occurrence of saddle dolomite: Jour. Sed. Pet., v. 50, n. 4, p. 1149-1168.

Reading, H.G. (ed.), 1978, Sedimentary Environments and Facies: New York, Elsevier, 557 p.

Reineck, H.E., Singh, I.B., 1973, Depositional Sedimentary Environments: Springer-Verlag, New York, 439 p.

Ruby, C.H.; Horne, J.C.; and Reinhart, P.J., 1981, Cretaceous Rocks of Western N. American - A Guide to Terrigenous Clastic Rock Identification: Research Planning Institute, Inc., Columbia, S. Carolina, 100 p.

Schmidt, V. and McDonald, D.A., 1979, Texture and recognition of secondary porosity in sandstone: in Scholle, P.A. and Schluger, P.R., eds., Aspects of Diagenesis: SEPM Spec. Pub. No. 26, p. 209-225.

Schmidt, V. and McDonald, D.A., 1979, The role of secondary porosity in the course of sandstone diagenesis: in Scholle, P.A. and Schluger, P.R., eds., Aspects of Diagenesis: SEPM Spec. Pub. No. 26, p. 175-207.

Scholle, P.A., 1978, A color illustrated guide to carbonate rock constitutents, textures, cements, and porosities: AAPG Memoir No. 27, 241 p.

Scholle, P.A., 1979, A color illustrated guide to constitutents, textures, cements, and porosities of sandstones and associated rocks: AAPG Memoir No. 28, 201 p.

Sokal, R.R., and Rohlf, F.J., 1969, Biometry: San Francisco, W.H. Freeman and Company, 776 p.

Southard, J.B., 1975, Bed Configuration, in Depostional Envrionments as Interpreted from Primary Sedementary Structures and Stratification Sequences: SEPM Short Course No. 2, p. 5-44.

Spearing, D.R., 1975, Shallow marine sands, in Depositional Environments as Interpreted from Primary Sedimentary Structures and Stratification Sequences: SEPM, Short Course No. 2., p. 103-132.

Swanson, D.C., 1979, Deltaic deposits in the Pennsylvania Upper Morrow formation of the Anadarko Basin, in Hyne, N.J., ed., Pennsylvanian Sandstones of the Mid-Continent: Tulsa Geol. Soc., Tulsa, Oklahoma, p. 115-168.

Wilson, M.A. and Pittman, E.D., 1977, Authigenic clays in sandstones: recognition and influence on reservoir properties and paleoenvironmental analysis: Jour. Sed. Pet., v. 47, n. 1, p. 3-31.

Woody, M.D., 1984, Petrography, Diagenesis, and Petrophysics of Selected Cherokee Group (Desmoinesian Stage) Sandstones in Southeastern Kansas: M.S. Thesis, University of Kansas, Lawrence.

Zeller, D.E. (ed.), 1968, The stratigraphic succession in Kansas: Kansas State Geological Survey Bulletin 189, 81 p.

APPENDIX A

GRAPHICAL CORE DESCRIPTIONS

THIN SECTION SAMPLE LOCATIONS

Simplified core descriptions with locations of plugs and porosity-permeability values are included here. Thin section sample locations are shown by tick marks on the right side of the columns, and are also listed.

Letters to the right of the columns correspond to lithofacies. Contacts between units are indicated by solid, dashed, or wavy lines. Solid represents inferred abrupt contact, dashed is gradational, and wavy indicates erosional contact.

WILLIAMS D-2
C, SW, NW, SEC. 19, 33S, 42W
MORTON COUNTY, KS

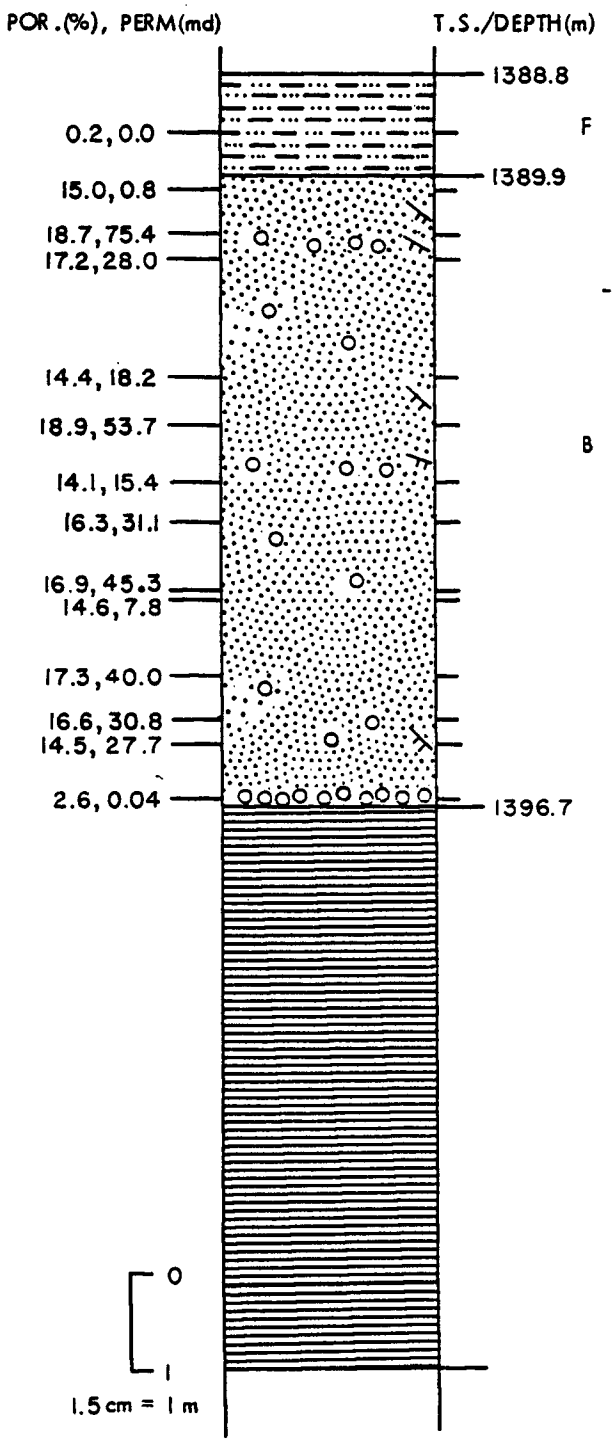

EXPLANATION

ROCK TYPES

Conglomeratic Cross-bedded Sandstone

Interlaminated Silt, Sand and Clay

Carbonaceous Shale

SEDIMENTARY FEATURES

Scoured Surface

1 JONES B
NW, NE, SEC. 9, 33S, 41W
MORTON COUNTY, KS.

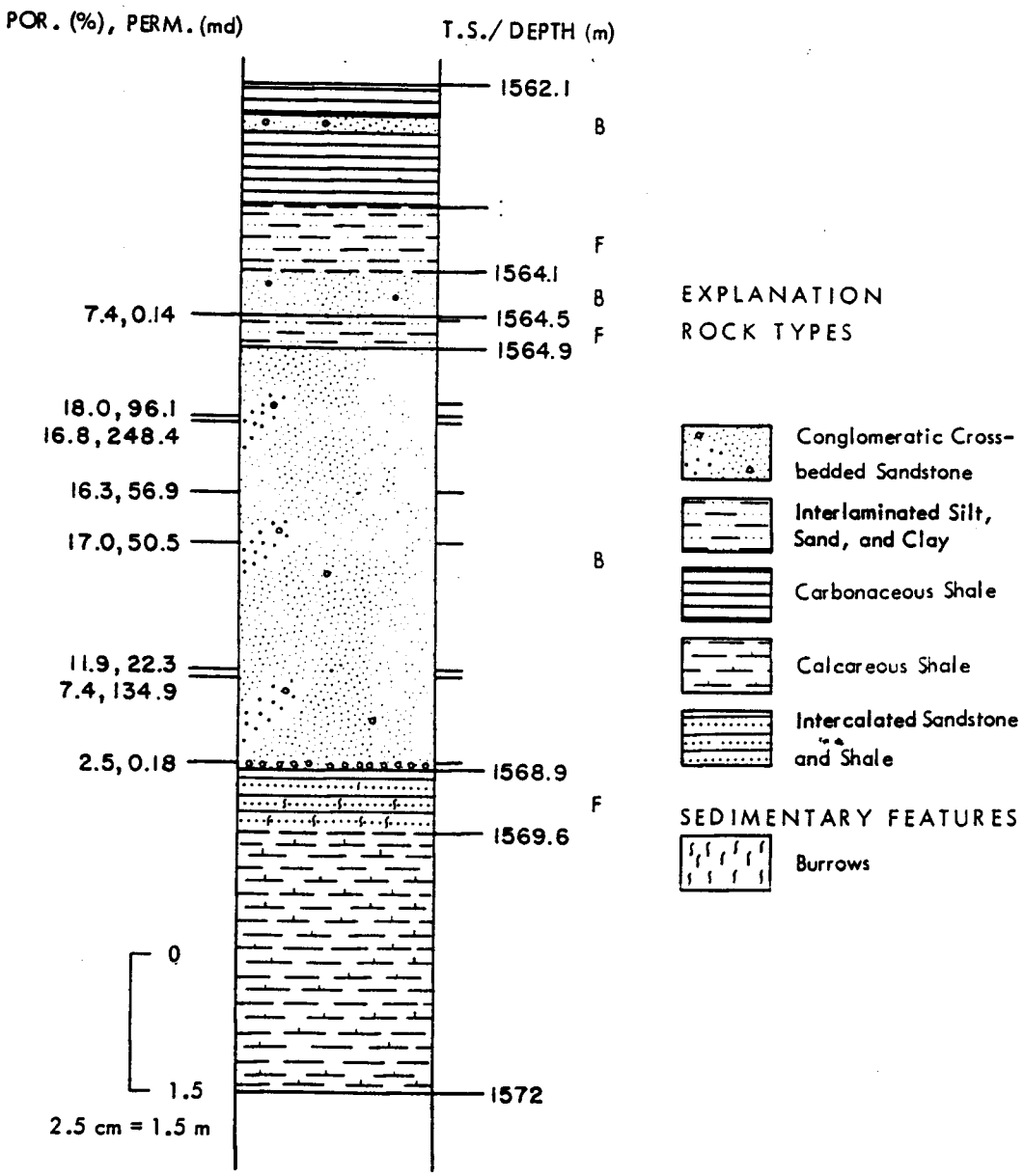

1 LOW G
C, SE, NW, SEC. 6, 33S, 40W
MORTON COUNTY, KS.

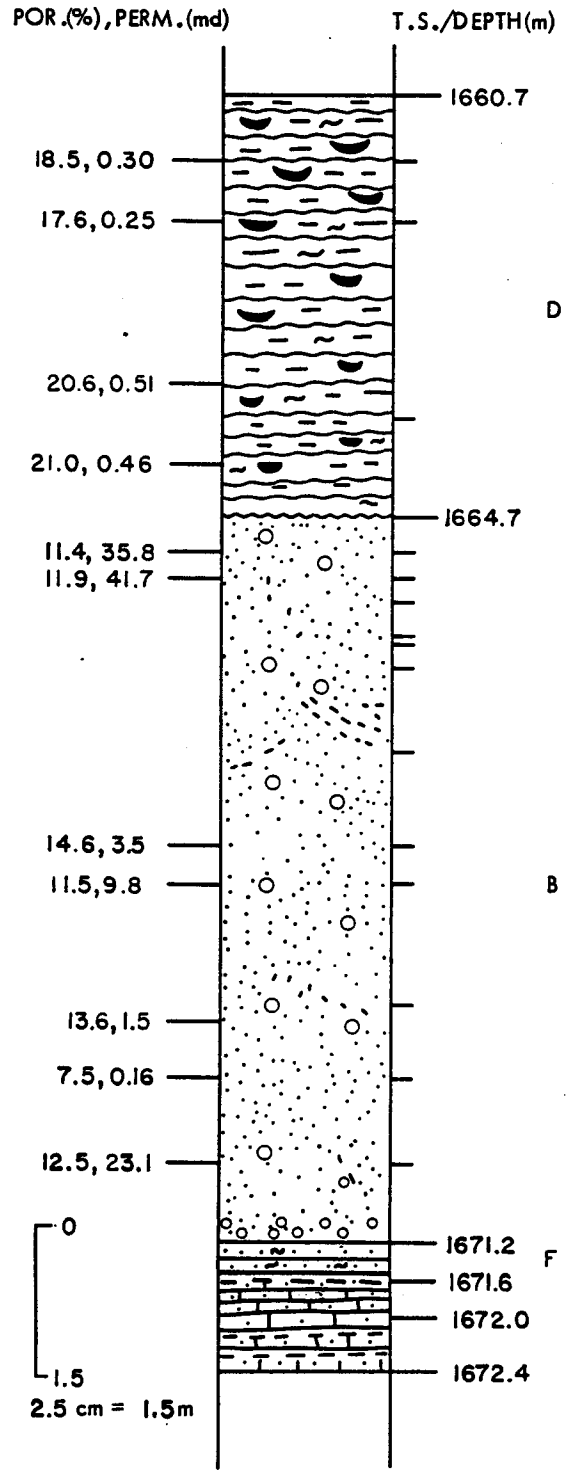

EXPLANATION

ROCK TYPES

- Muddy, Rippled Sandstone With Minor Flaser Bedding
- Conglomeratic Cross-bedded Sandstone
- Intercalated Sandstone and Shale
- Sandy Limestone
- Interbedded Sandy Limestone and Shale

SEDIMENTARY FEATURES

- Glauconite

5 LOW A
C, NE, SW, SEC. 8, 33S, 40W
MORTON COUNTY, KS.

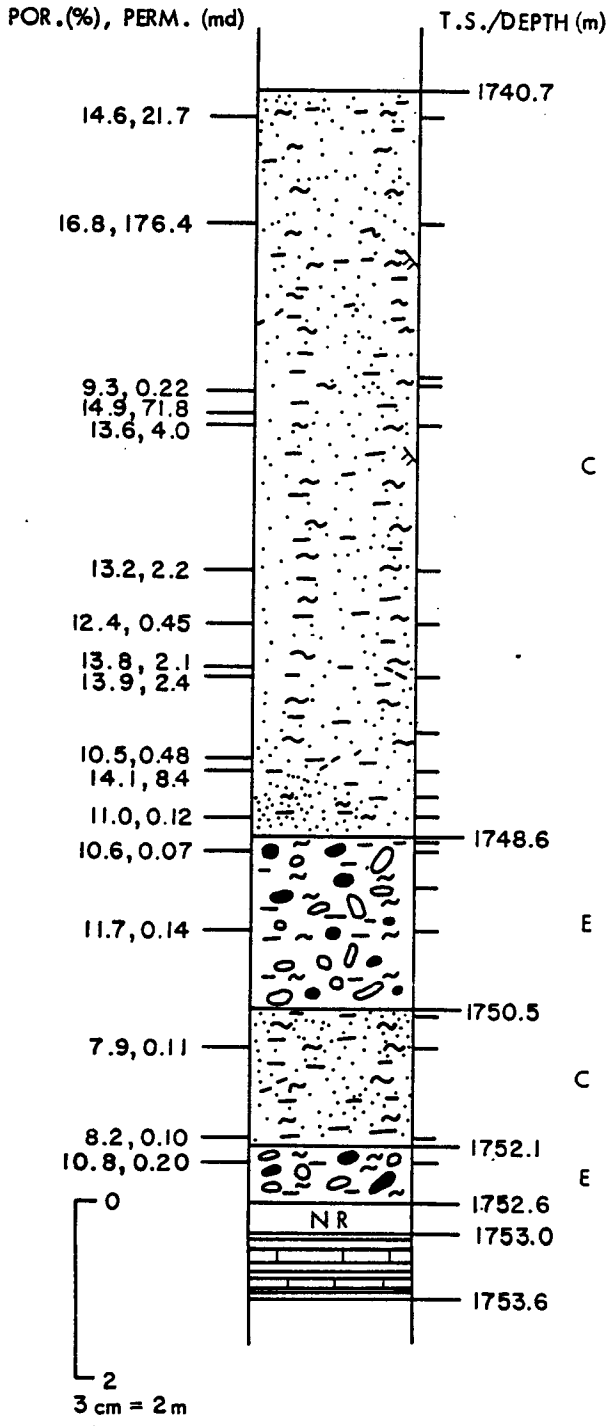

EXPLANATION

ROCK TYPE

- Glauconitic Cross-bedded Sandstone
- Muddy, Glauconitic Bioturbated Sandstone
- Intercalated Limestone and Green Shale

SEDIMENTARY FEATURES

- Clay Laminae
- Scour Surface

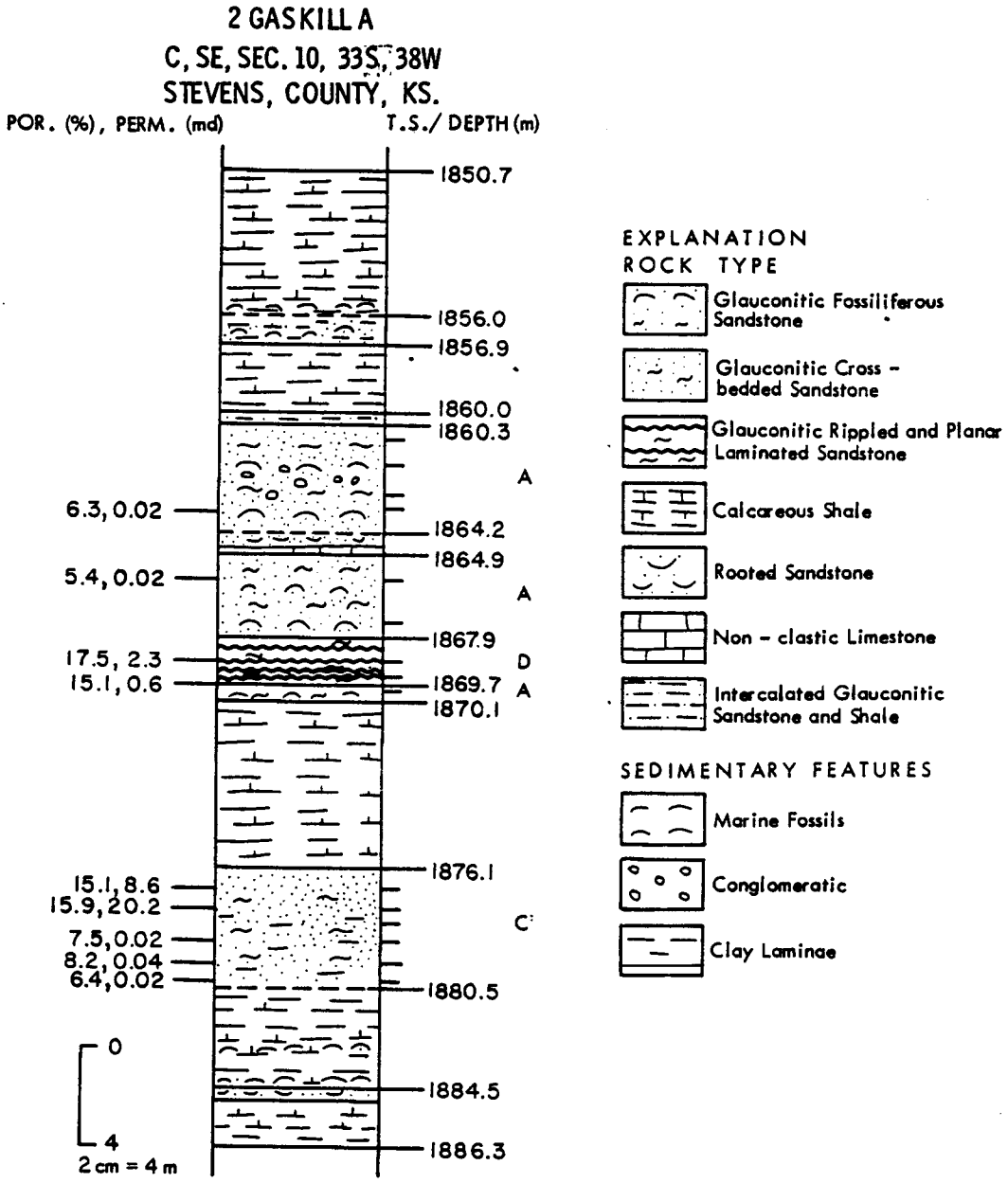
2 GASKILL A
C, SE, SEC. 10, 33S, 38W
STEVENS, COUNTY, KS.
POR. (%), PERM. (md)
T.S./ DEPTH (m)
1850.7
1856.0
1856.9
1860.0
1860.3
A
6.3, 0.02
1864.2
1864.9
5.4, 0.02
A
1867.9
17.5, 2.3
D
15.1, 0.6
1869.7
A
1870.1
1876.1
15.1, 8.6
15.9, 20.2
C
7.5, 0.02
8.2, 0.04
6.4, 0.02
1880.5
0
4
2 cm = 4 m
1884.5
1886.3
EXPLANATION
ROCK TYPE
Glauconitic Fossiliferous Sandstone
Glauconitic Cross - bedded Sandstone
Glauconitic Rippled and Planar Laminated Sandstone
Calcareous Shale
Rooted Sandstone
Non - clastic Limestone
Intercalated Glauconitic Sandstone and Shale
SEDIMENTARY FEATURES
Marine Fossils
Conglomeratic
Clay Laminae

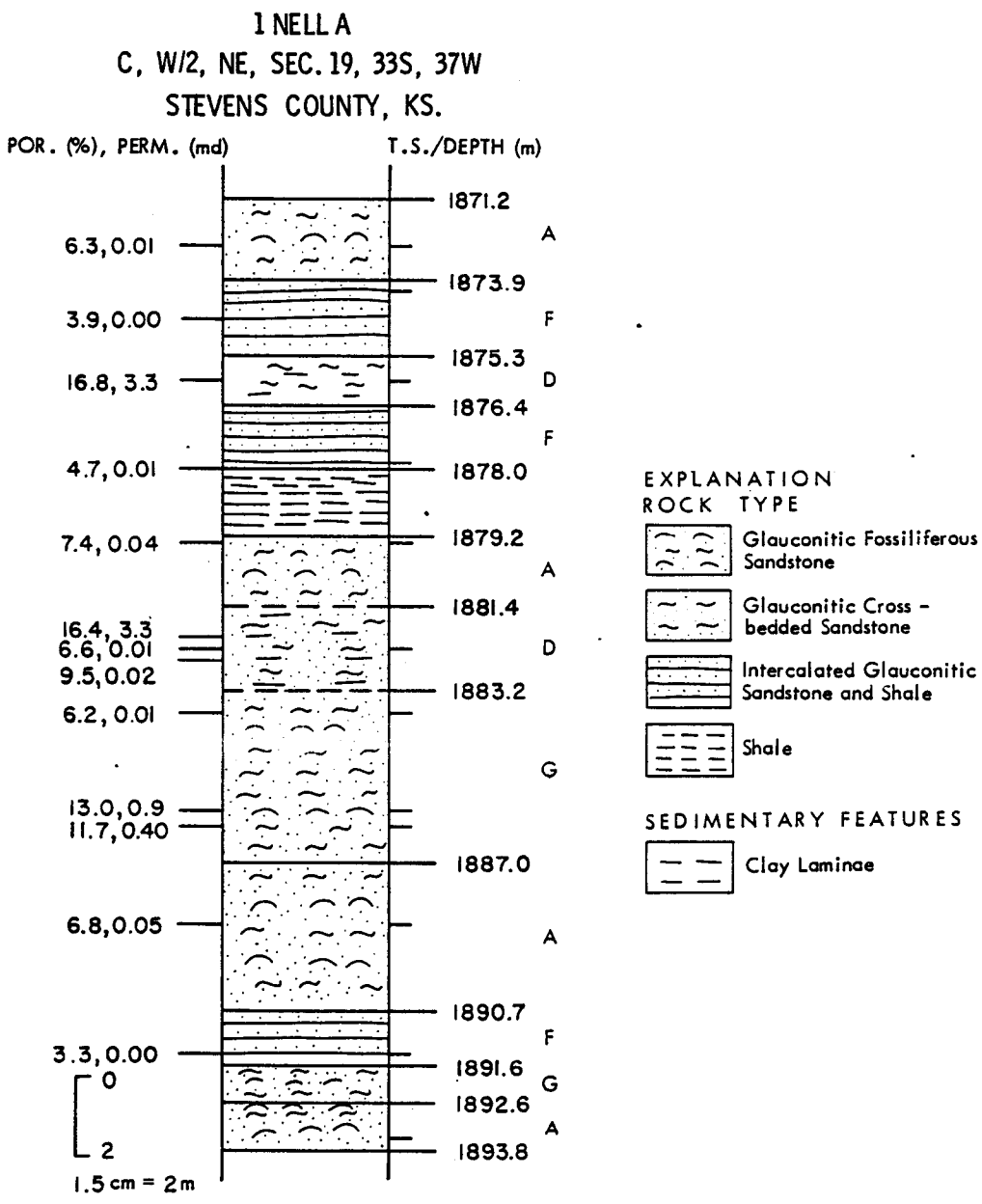
1 NELL A
C, W/2, NE, SEC. 19, 33S, 37W
STEVENS COUNTY, KS.
POR. (%), PERM. (md)
T.S./DEPTH (m)
1871.2
A
6.3, 0.01
1873.9
3.9, 0.00
F
1875.3
16.8, 3.3
D
1876.4
F
4.7, 0.01
1878.0
7.4, 0.04
1879.2
A
1881.4
16.4, 3.3
6.6, 0.01
D
9.5, 0.02
1883.2
6.2, 0.01
G
13.0, 0.9
11.7, 0.40
1887.0
6.8, 0.05
A
1890.7
F
3.3, 0.00
1891.6
G
0
1892.6
A
2
1893.8
1.5 cm = 2m
EXPLANATION
ROCK TYPE
Glauconitic Fossiliferous Sandstone
Glauconitic Cross - bedded Sandstone
Intercalated Glauconitic Sandstone and Shale
Shale
SEDIMENTARY FEATURES
Clay Laminae

1 PENNINGTON 32
C, SE, SEC. 16, 34S, 42W
SEWARD COUNTY, KS.

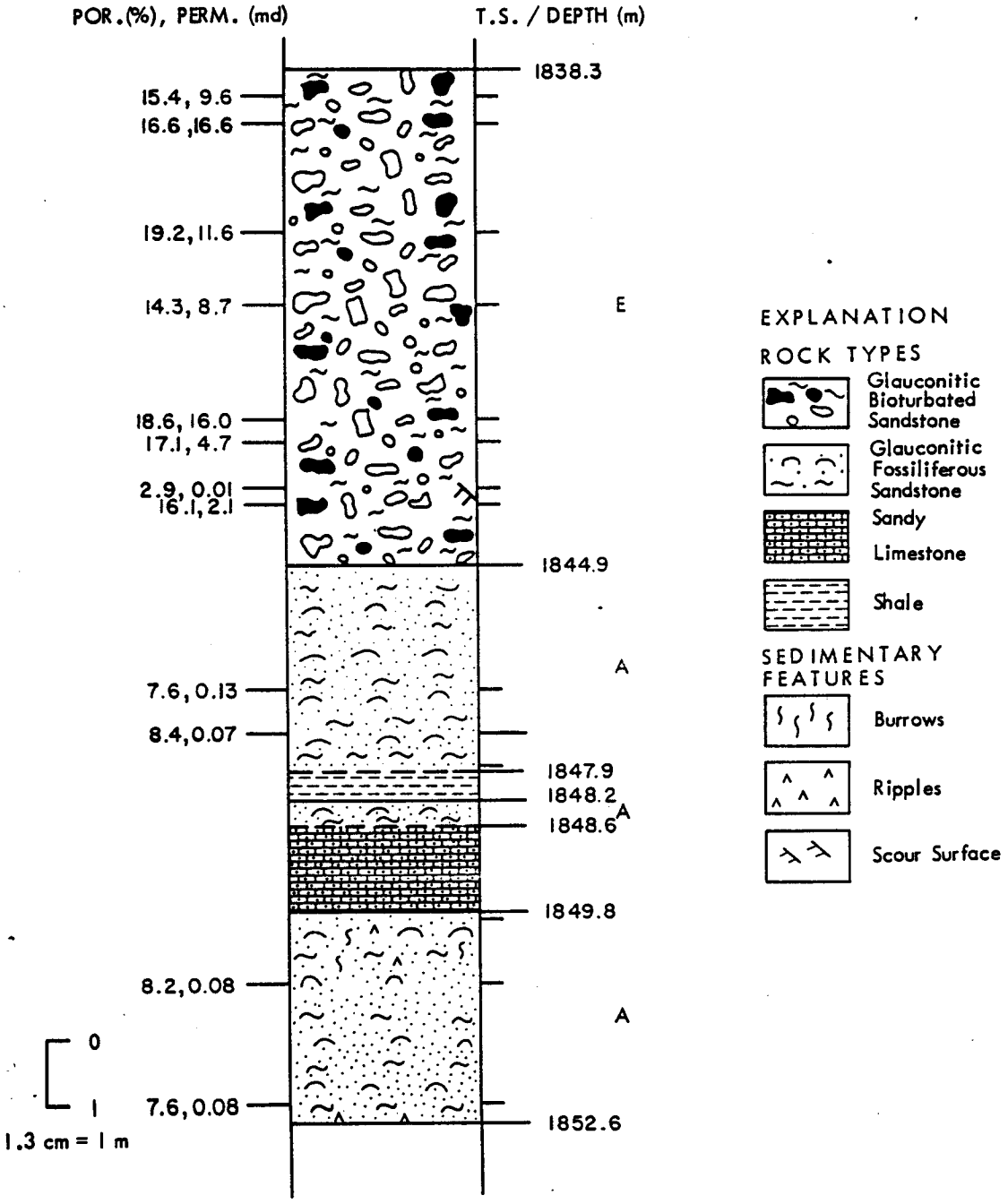

1 BOLAN
C, NW, SE, SEC. 6, 335, 29W
MEADE COUNTY, KS

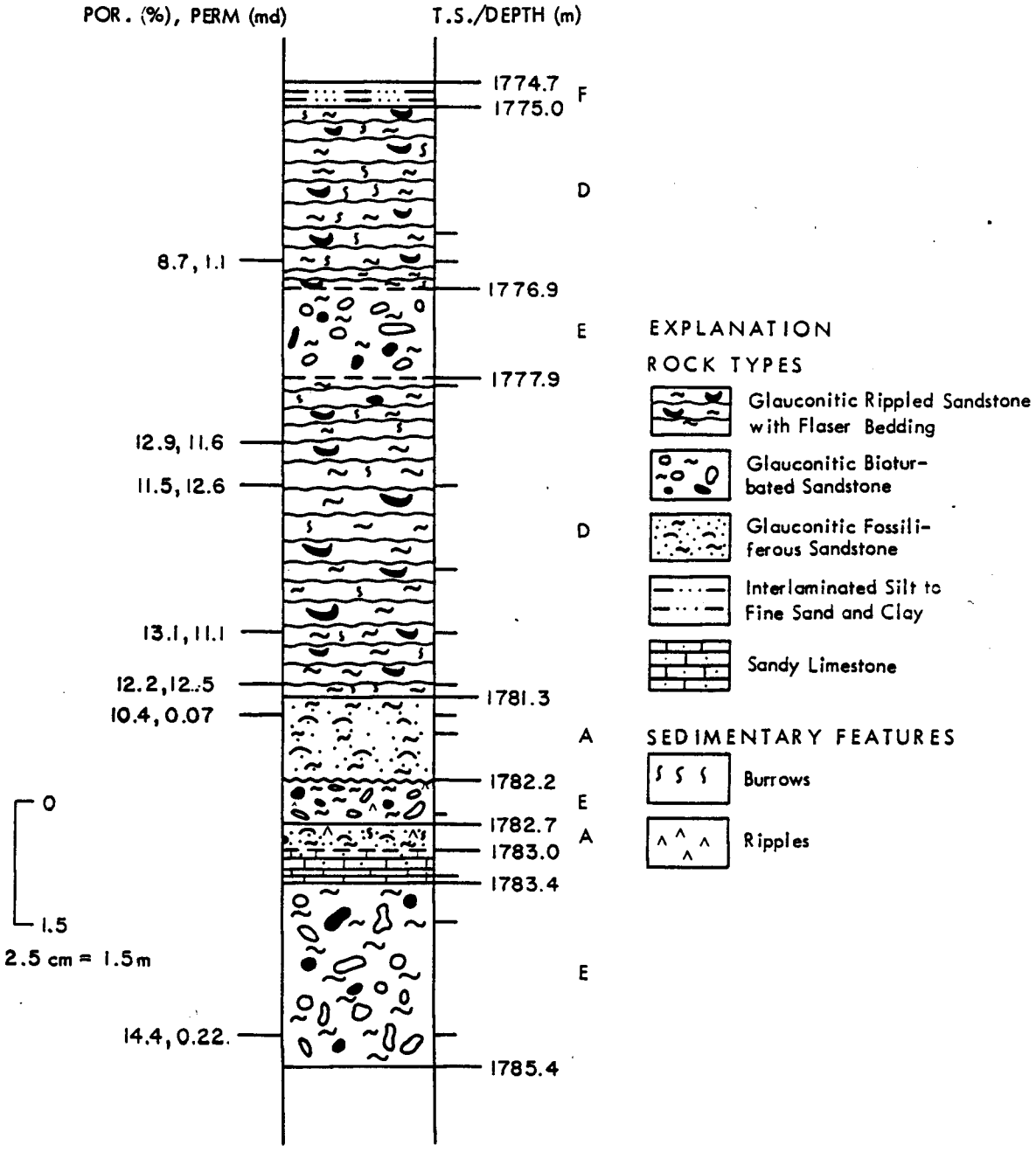

APPENDIX A

THIN SECTION SAMPLES

Sample No.	Lithofacies	Sample No.	Lithofacies
1B5747	A	2GA6003.2	A
1B5747.8	A	2GA6005.5	A
1B5752.7	A	2GA6010.9	A
1NA6040	A	2GA6019	A
1NA6064.5	A	2GA6024.2	A
1NA6076	A	2GA6031.9	A
1NA6083.6	A	WD24484	B
1NA6085	A	WD24485.3	B
1NA6092.5	A	WD24491.9	B
1NA6108	A	WD24493.8	B
1P5957	A	WD24495.3	B
1P5959	A	WD24497.8	B
1P5962	A	WD24497.9	B
1P5967	A	WD24500.9	B
1P5970	A	WD24502.2	B
1P5975	A	WD24503	B
1P5976	A	WD24505	B

Appendix A continued

THIN SECTION SAMPLES

Sample No.	Lithofacies	Sample No.	Lithofacies
1JB5040.7	B	1LG5388.7	B
1JB5048.9	B	2GA5988.2	C
1JB5049.4	B	2GA6009.7	C
1JB5049.5	B	2GA6053.7	C
1JB5051.9	B	2GA6057	C
1JB5053.5	B	2GA6059	C
1JB5057.5	B	2GA6061.5	C
1JB5057.6	B	2GA6063.5	C
1JB5060.5	B	2GA6065.7	C
1LG5370	B	5LA5615.8	C
1LG5370.7	B	5LA5619.5	C
1LG5371.5	B	5LA5625	C
1LG5372.5	B	5LA5625.3	C
1LG5372.7	B	5LA5626.5	C
1LG5373.5	B	5LA5631.5	C
1LG5376	B	5LA5633.5	C
1LG5379	B	5LA5635.3	C
1LG5380	B	5LA5637	C
1LG5383.7	B	5LA5638.5	C
1LG5386	B	5LA5639.3	C

Appendix A continued

THIN SECTION SAMPLES

Sample No.	Lithofacies	Sample No.	Lithofacies
5LA5640.2	C	1LG5366	D
5LA5647	C	1B5750.5	E
5LA5648.2	C	1B5754.3	E
5LA5651.3	C	1B5758.3	E
1B5726	D	1P5931	E
1B5730	D	1P5933	E
1B5731.2	D	1P5937	E
1B5735.5	D	1P5940	E
1B5739	D	1P5945	E
1B5742	D	1P5946	E
1B5744.2	D	1P5948	E
1B5746	D	1P5949	E
1NA6051.3	D	5LA5641	E
1NA6071.5	D	5LA5641.5	E
1NA6072.2	D	5LA5642.5	E
2GA6028.5	D	5LA5644	E
2GA6029.9	D	5LA5652	E
1LG5358	D	1NA6044	F
1LG5360	D	1NA6057.3	F

Appendix A continued

THIN SECTION SAMPLES

Sample No.	Lithofacies
1NA60101.8	F
WD24482	F
1JB5046.9	F

APPENDIX B

COMPILATION OF DATA

Isotope, microprobe analysis, and petrophysical data are tabulated here along with a compilation of pore size distribution curves. These curves were derived by mercury injection, with cumulative percent pore space saturated plotted against effective pore radius.

ISOTOPE DATA

This data was gathered by Cities Service Company, Tulsa, Oklahoma. Four samples were provided from cores used in this study.

Sample	Lithofacies	Cement	Isotopic Composition (relative to PDB)	
			delta ^{18}O	delta ^{13}C
5 Low A 5648.2'	C	Ferroan Dolomite-Ankerite	-6.93	-4.56
1 Jones B 5060.5'	B	Ferroan Dolomite-Ankerite	-6.23	-0.97
1 Low G 5386'	B	Ferroan Dolomite-Ankerite	-6.04	-4.98
1 Nell A 6064.5'	A	Ferroan Calcite and Skeletal Material	-8.46	-0.48

MICROPROBE DATA

Composition is normalized to 100 and reported in mole percent. Range is reported for the 2 sigma level of confidence. Strontium carbonate content borders on non-detectable and is in general less than 0.05 mole percent. Samples analyzed for strontium carbonate are indicated by an asterisk. This data was taken on an AMX 2 spectrometer microprobe at the Space Technology Center, University of Kansas.

MICROPROBE DATA

Ferroan Calcite

Sample	Lithofacies	$CaCO_3$(+0.2)	$MgCO_3$(+0.2)	$FeCO_3$(+0.2)	$MnCO_3$(+0.2)
2GA6010.9a*	A	97.8	0.9	0.7	0.6
2GA6010.9b*		97.7	0.6	1.0	0.7
2GA6010.9c		97.8	0.6	1.1	0.5
1NA6064.5a*	A	97.9	1.2	0.4	0.5
1NA6064.5b*		96.1	0.7	1.1	2.0
1NA6064.5d		96.3	0.7	1.2	1.7
1NA6064.5e		96.2	0.8	1.2	1.8
1NA6064.5f		96.0	0.6	1.2	2.2
1P5967a*	A	94.0	2.2	2.0	1.8
1P5967b*		95.4	2.0	2.3	0.3
1P5967c		95.2	2.5	1.9	0.4

MICROPROBE DATA continued

Ferroan Calcite

Sample	Lithofacies	$CaCO_3$(+0.2)	$MgCO_3$(+0.2)	$FeCO_3$(+0.2)	$MnCO_3$(+0.2)
1P5967d		95.4	2.2	2.0	0.4
1B5952.7a*	A	94.1	2.5	1.7	1.7
1B5952.7b		95.9	1.6	1.3	1.3
1B5952.7c		95.3	2.0	1.3	1.4

Ferroan Dolomite-Ankerite

Sample	Lithofacies	$CaCO_3$(+1.0)	$MgCO_3$(+0.5)	$FeCO_3$(+0.5)	$MnCO_3$(+0.2)
2GA6010.9d*	A	49.3	34.4	14.2	2.1
1NA6064.5c	A	62.2	21.0	13.7	3.1
1P59575a	A	56.1	22.3	17.8	3.6
1P5975b		55.4	23.9	16.6	4.1
1P5975c		55.1	23.8	16.3	3.7
1JB5060.5a*	B	54.1	30.3	14.5	1.2
1JB5060.5b		53.1	30.1	15.5	1.3
1LG5383.7a*	B	51.2	23.7	22.6	2.5
1LG5383.7b		53.6	24.1	20.2	2.1
1LG5383.7c		52.9	25.0	20.1	2.0

APPENDIX B

SUMMARY OF PETROPHYSICAL DATA

Sample No.	Lithofacies	Porosity (%)	Permeability (md)	Approximate Breakthrough (microns)
1B5747	A	10.4	0.07	
1NA6040	A	6.3	0.01	
1NA6064.5	A	7.4	0.09	
1NA6076	A	6.2	0.01	
1NA6083.6	A	13.0	0.90	4
1NA6085	A	11.7	0.44	
1NA6092.5	A	6.8	0.05	
1P5957	A	7.6	0.13	
1P5959	A	8.4	0.07	
1P5970	A	8.2	0.08	
1P5975	A	7.6	0.08	
26A6019	A	5.4	0.02	
26A6010.9	A	6.3	0.02	
WD24484	B	15.0	0.83	
WD24485.3	B	18.7	75.38	

Appendix B continued

SUMMARY OF PETROPHYSICAL DATA

Sample No.	Lithofacies	Porosity (%)	Permeability (md)	Approximate Breakthrough (microns)
WD24486.3	B	17.2	28.00	
WD24490.3	B	14.4	8.22	
WD24491.9	B	18.9	53.67	
WD24493.8	B	14.1	15.37	
WD24495.3	B	16.3	31.13	
WD24497.8	B	16.9	45.29	
WD24497.9	B	14.6	7.85	
WD24500.9	B	17.3	39.95	
WD24502.2	B	16.6	30.80	
WD24503	B	14.5	27.69	
WD24505	B	2.6	0.04	
1JB5049.4	B	18.0	96.10	
1JB5049.5	B	16.8	248.39	
1JB5051.9	B	16.3	56.86	
1JB5053.5	B	17.0	50.47	
1JB5057.5	B	11.9	22.29	
1JB5057.6	B	7.4	134.86	
1JB5060.5	B	2.5	0.18	

Appendix B continued

SUMMARY OF PETROPHYSICAL DATA

Sample No.	Lithofacies	Porosity (%)	Permeability (md)	Approximate Breakthrough (microns)
1LG5370	B	11.4	35.78	
1LG5370.7	B	11.9	41.68	?[1]
1LG5379	B	14.6	3.48	?
1LG5380	B	11.5	9.83	
1LG5384	B	13.6	1.54	
1LG5386	B	7.5	0.16	3
1LG5388.7	B	12.5	23.08	?
2GA6053.7	C	15.0	8.62	10
2GA6057	C	15.9	20.23	15
2GA6061.5	C	7.5	0.02	
2GA6063.5	C	8.2	0.04	
2GA6065.7	C	6.4	0.02	
5LA5615.8	C	14.6	21.70	
5LA5619.5	C	16.8	176.42	17
5LA5625.3	C	9.3	0.22	
5LA5626.3	C	14.9	71.83	
5LA5626.5	C	13.6	4.00	
5LA5631.5	C	13.2	2.24	

Appendix B continued

SUMMARY OF PETROPHYSICAL DATA

Sample No.	Lithofacies	Porosity (%)	Permeability (md)	Approximate Breakthrough (microns)
5LA5633.5	C	12.4	0.45	
5LA5635.1	C	13.8	2.14	5
5LA5635.3	C	13.9	2.40	
5LA5638.3	C	10.5	0.48	2
5LA5638.5	C	14.1	8.38	
5LA5640.2	C	11.0	0.11	
5LA5648.2	C	7.9	0.11	
5LA5651.3	C	8.2	0.10	
1B5731.2	D	8.9	1.17	5
1B5737.5	D	12.9	11.57	
1B5739	D	11.5	12.59	6
1B5744.2	D	13.1	11.09	
1B5745.7	D	12.2	12.52	
1NA6051.3	D	16.7	3.30	
1NA6071	D	16.4	3.30	
1NA6071.5	D	6.6	0.01	
1NA6072.2	D	9.5	0.02	
2GA6028.5	D	17.5	2.26	2.5

Appendix B continued

SUMMARY OF PETROPHYSICAL DATA

Sample No.	Lithofacies	Porosity (%)	Permeability (md)	Approximate Breakthrough (microns)
2GA6029.9	D	15.1	0.64	
1LG5358	D	18.5	0.29	
1LG5360	D	17.6	0.25	1
1LG65365.7	D	20.6	0.51	
1LG5368.5	D	21.0	0.46	0.9
1B5758.3	E	14.4	0.22	
1P5931	E	15.4	9.62	6.5
1P5933	E	16.6	16.59	
1P5937	E	19.2	11.64	
1P5940	E	14.2	8.70	
1P5945	E	18.6	16.03	6.5
1P5946	E	17.1	4.67	
1P5948	E	2.9	0.01	
1P5949	E	16.1	2.10	
5LA5641.5	E	10.6	0.07	
5LA5644	E	11.7	0.14	
5LA5652	E	10.8	0.20	0.8
1NA6045.2	F	3.9	0.00	

Appendix B continued

SUMMARY OF PETROPHYSICAL DATA

Sample No.	Lithofacies	Porosity (%)	Permeability (md)	Approximate Breakthrough (microns)
1NA6057.3	F	4.7	0.08	
1NA6101.8	F	3.3	0.00	
WD24482	F	0.2	0.00	
1JB5046.9	F	7.4	0.14	

[1]Question marks signify data was obtained but a breakthrough point is not apparent on the pore-size distribution curve (App.B).

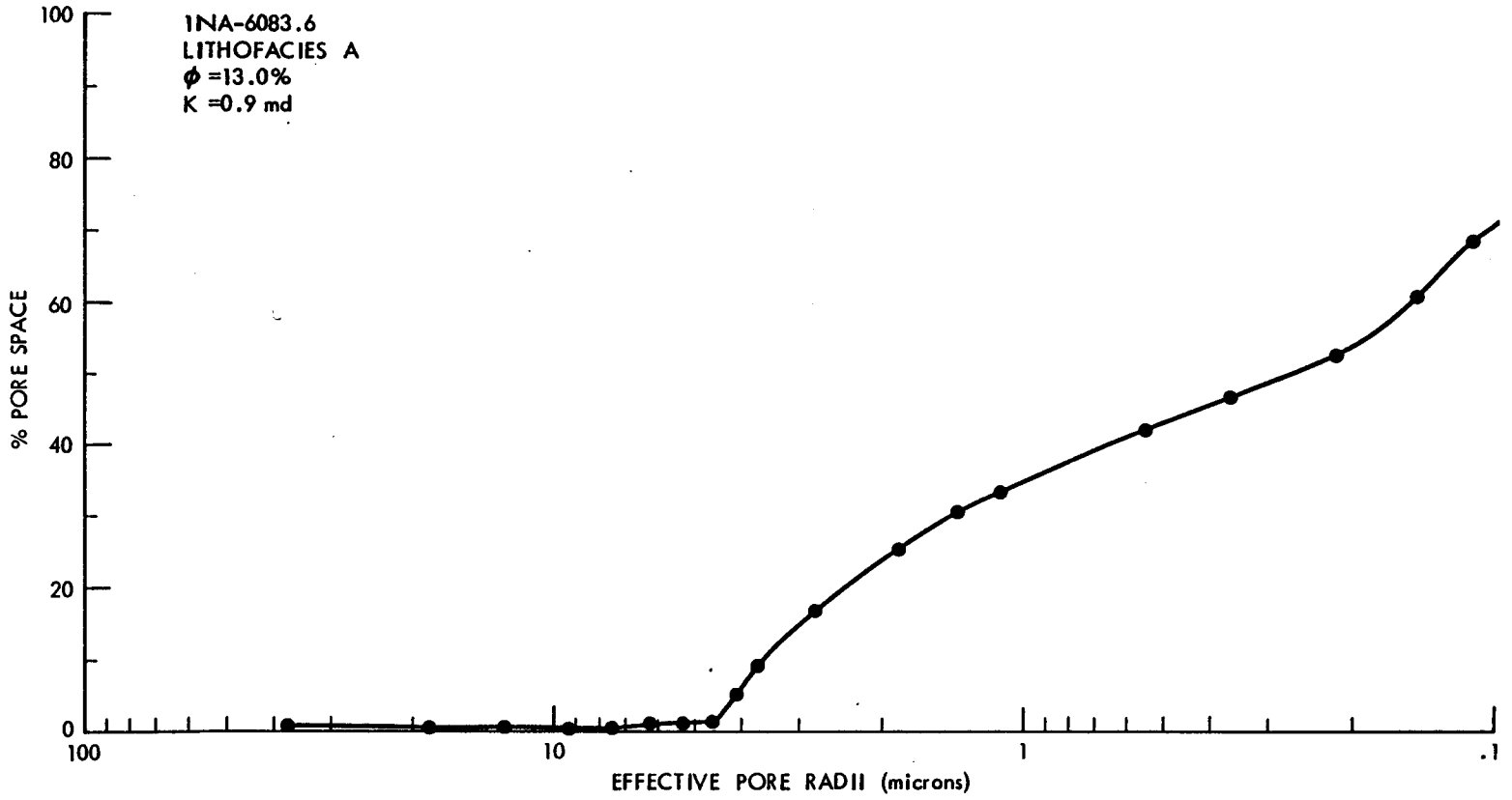
1NA-6083.6
LITHOFACIES A
ϕ =13.0%
K =0.9 md
100
80
60
40
20
0
% PORE SPACE
100
10
1
.1
EFFECTIVE PORE RADII (microns)

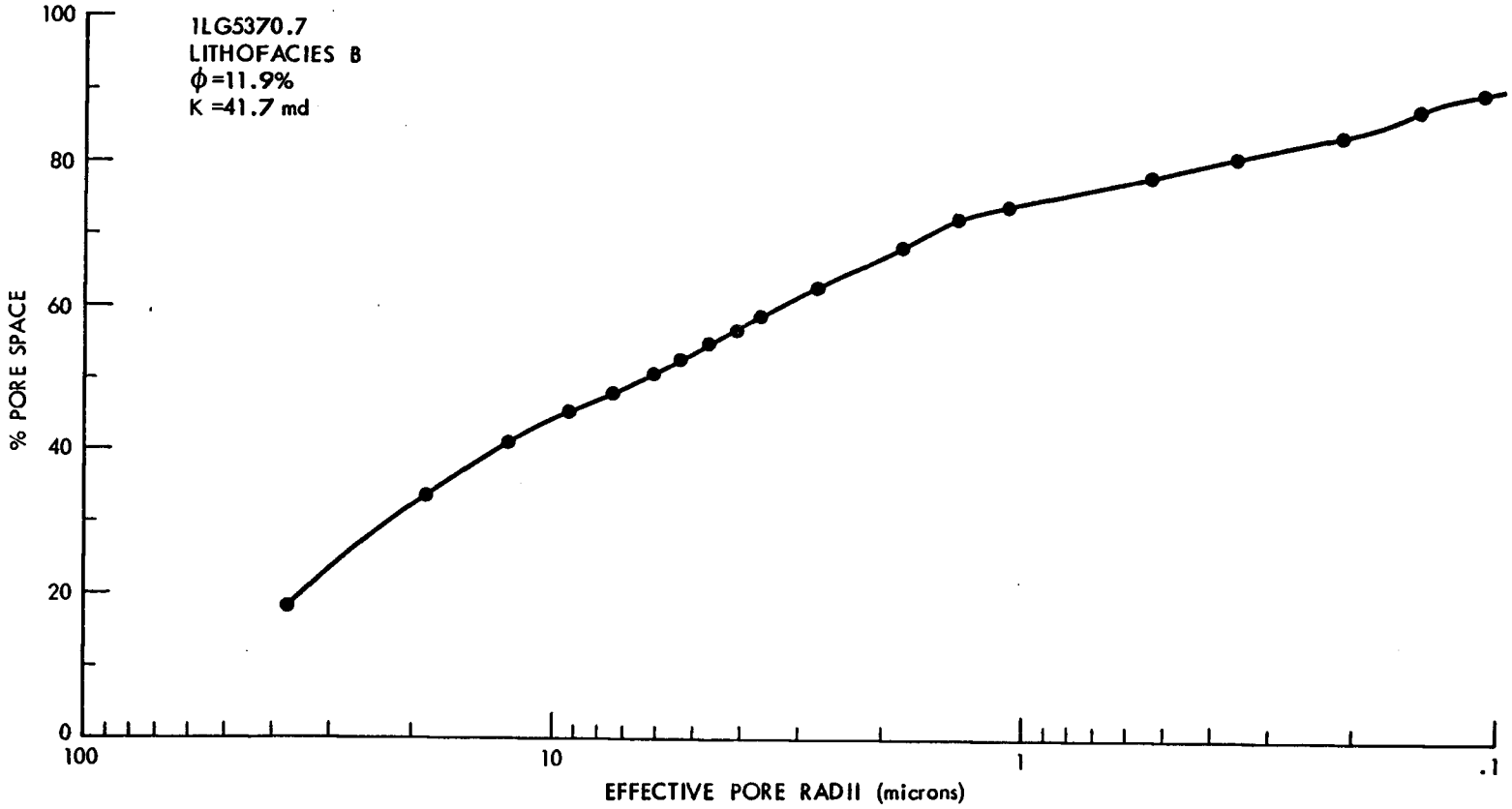
1LG5370.7
LITHOFACIES B
ϕ=11.9%
K =41.7 md
100
80
60
40
20
0
% PORE SPACE
100
10
1
.1
EFFECTIVE PORE RADII (microns)

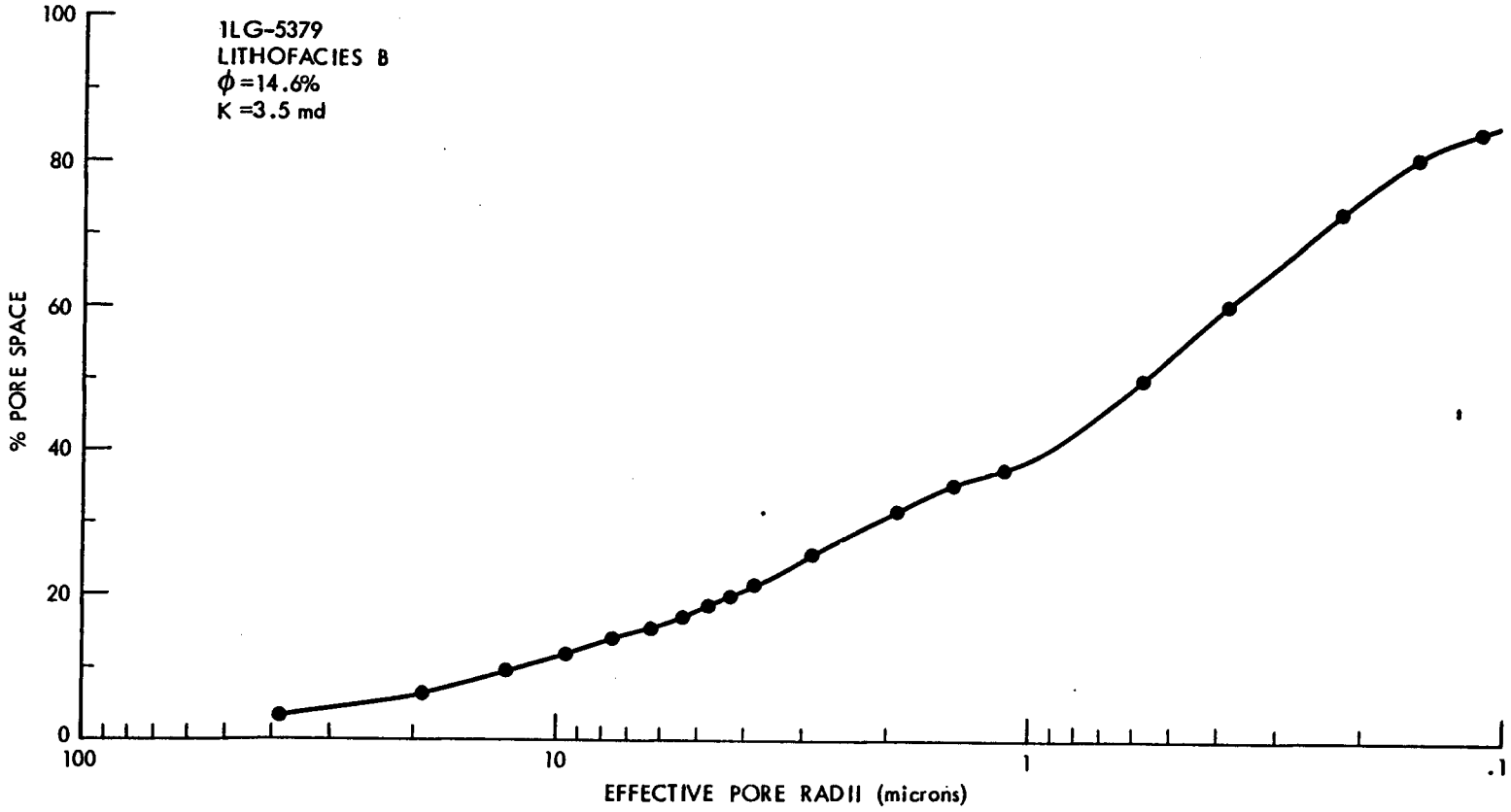
1LG-5379
LITHOFACIES B
ϕ=14.6%
K =3.5 md
100
80
60
40
20
0
% PORE SPACE
100
10
1
.1
EFFECTIVE PORE RADII (microns)

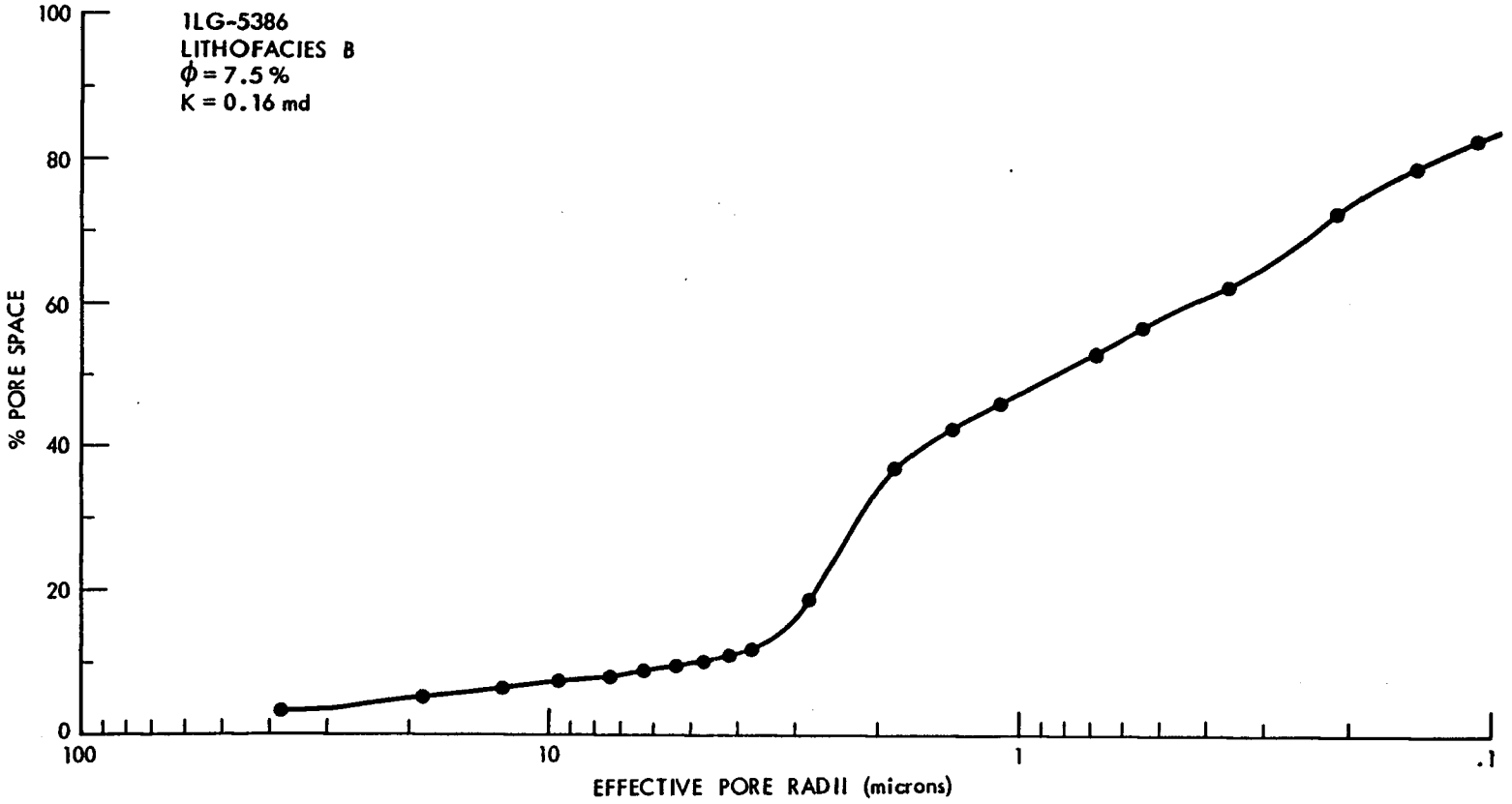
1LG-5386
LITHOFACIES B
ϕ = 7.5 %
K = 0.16 md
100
80
60
40
20
0
% PORE SPACE
100
10
1
.1
EFFECTIVE PORE RADII (microns)

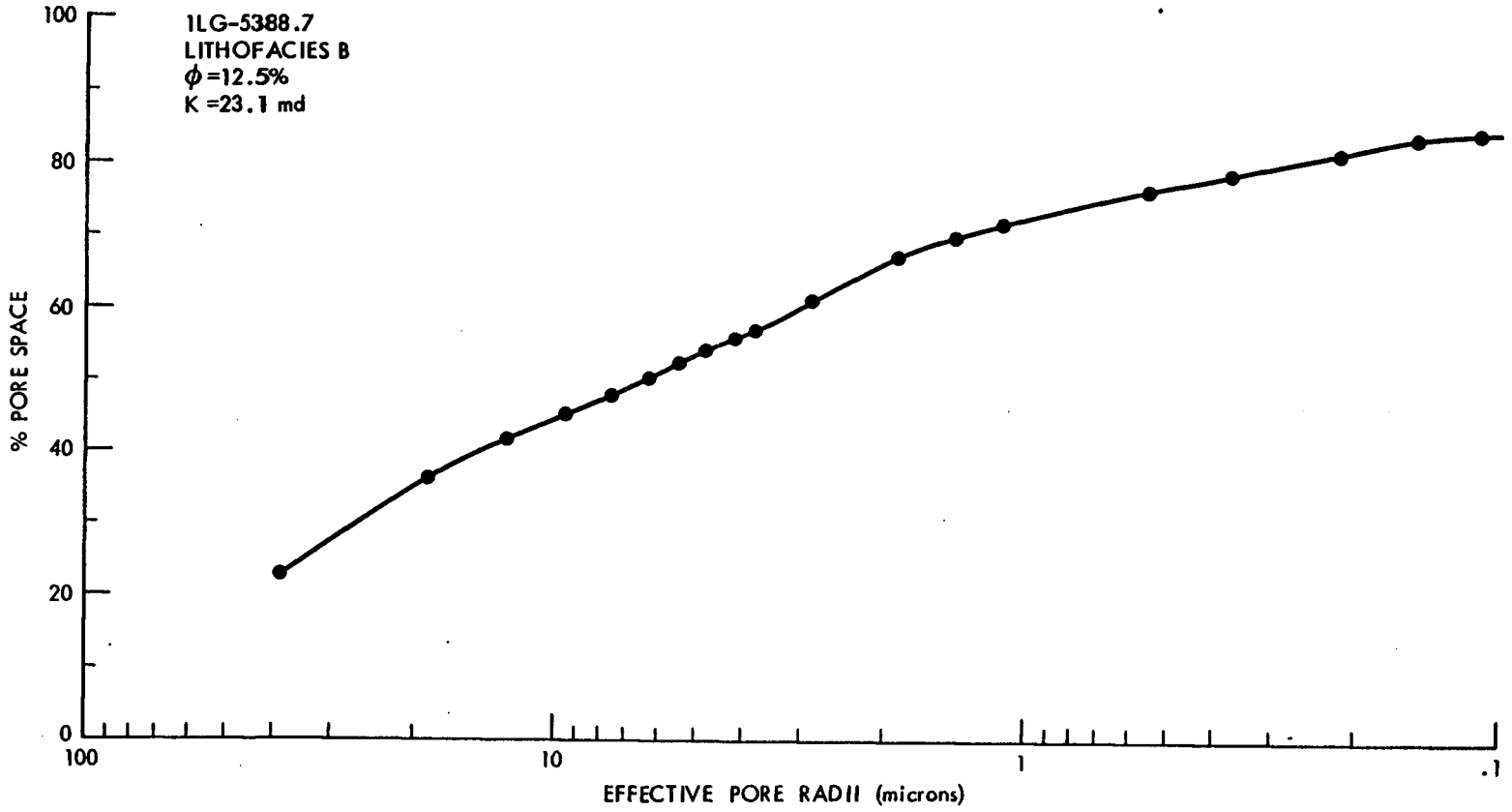
1LG-5388.7
LITHOFACIES B
ϕ=12.5%
K =23.1 md
100
80
60
40
20
0
% PORE SPACE
100
10
1
.1
EFFECTIVE PORE RADII (microns)

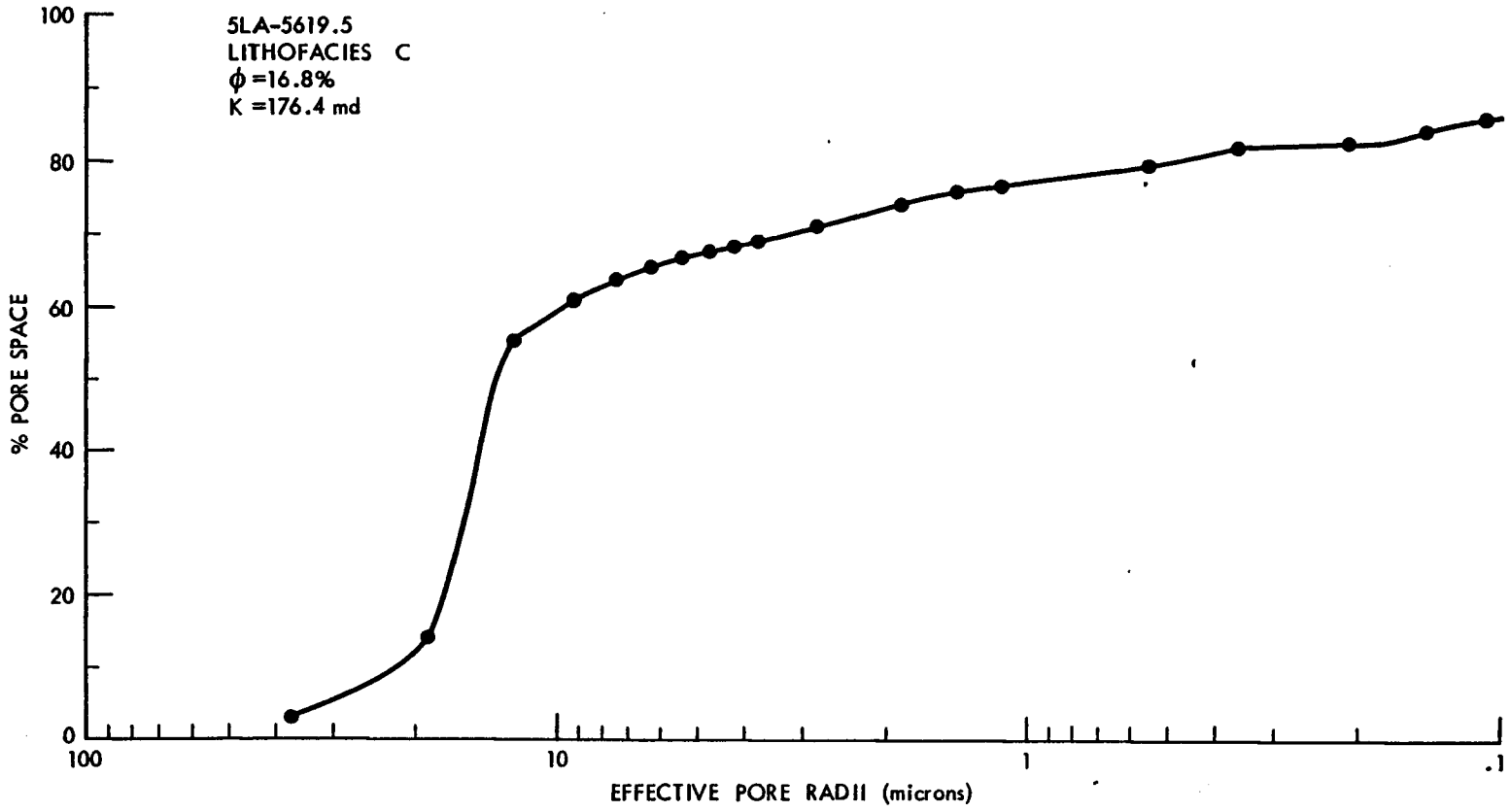
5LA-5619.5
LITHOFACIES C
ϕ =16.8%
K =176.4 md
100
80
60
40
20
0
% PORE SPACE
100
10
1
.1
EFFECTIVE PORE RADII (microns)

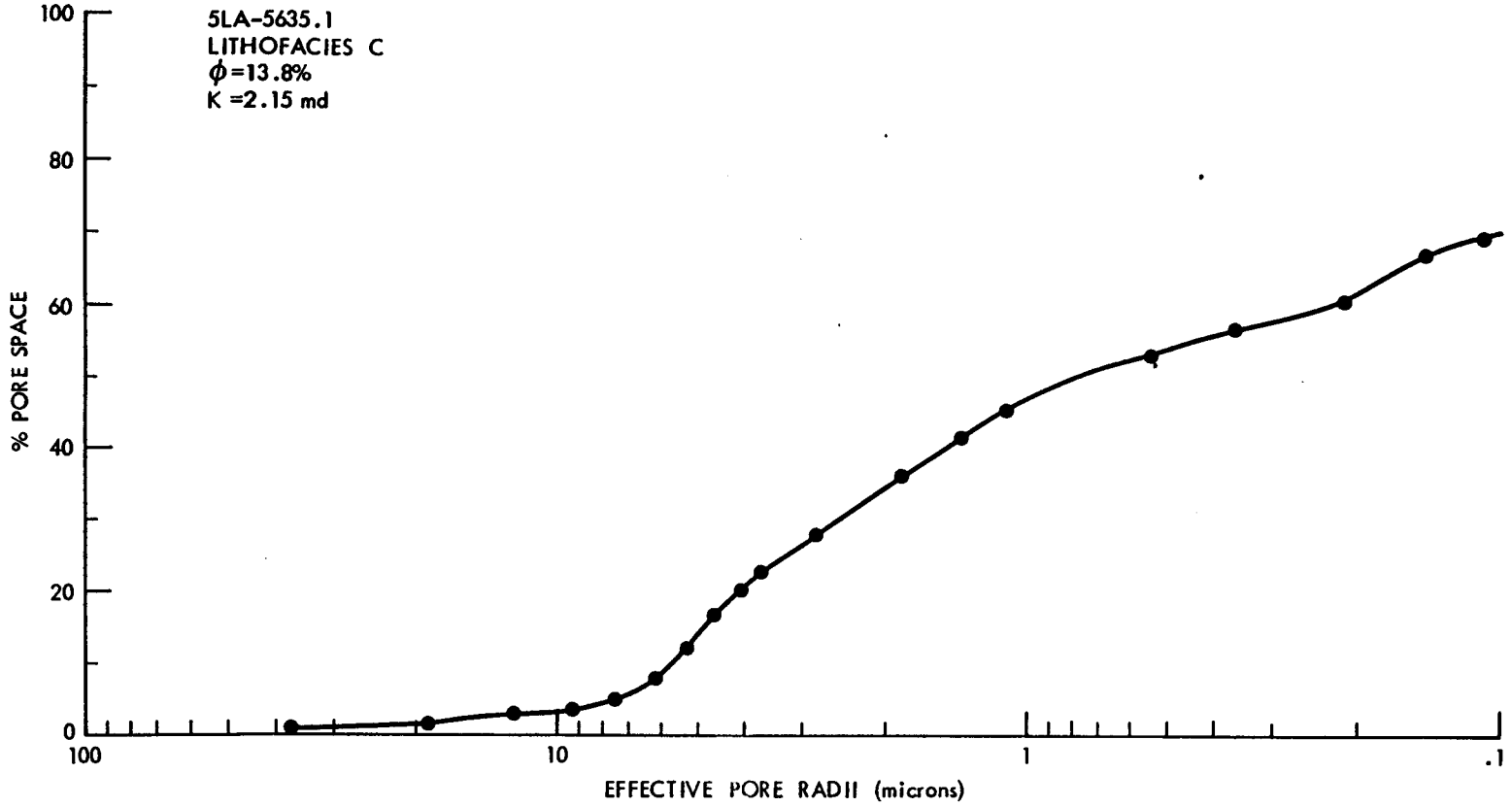
5LA-5635.1
LITHOFACIES C
ϕ=13.8%
K =2.15 md
100
80
60
40
20
0
% PORE SPACE
100
10
1
.1
EFFECTIVE PORE RADII (microns)

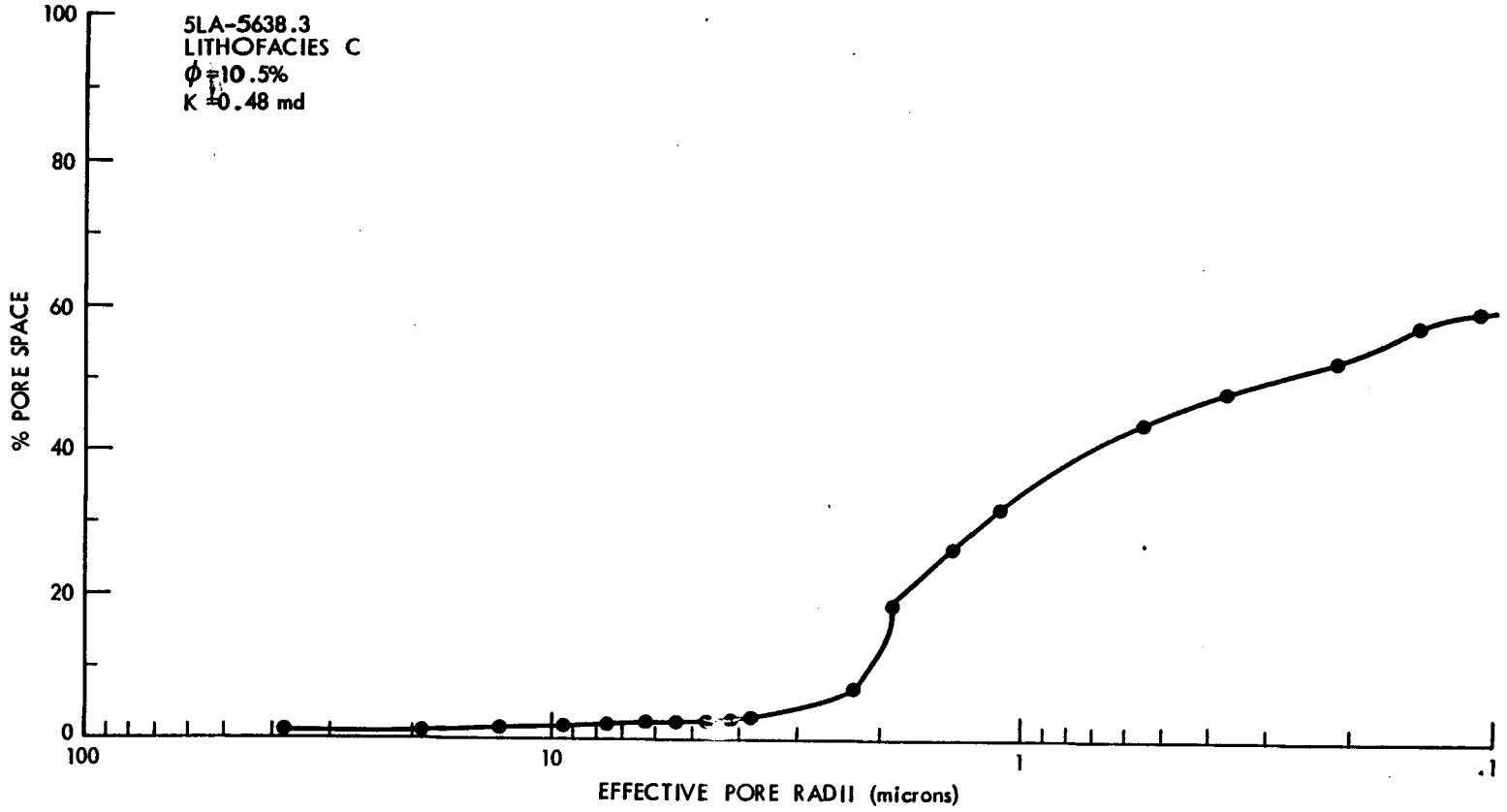
5LA-5638.3
LITHOFACIES C
ϕ =10.5%
K =0.48 md
100
80
60
40
20
0
% PORE SPACE
100
10
1
.1
EFFECTIVE PORE RADII (microns)

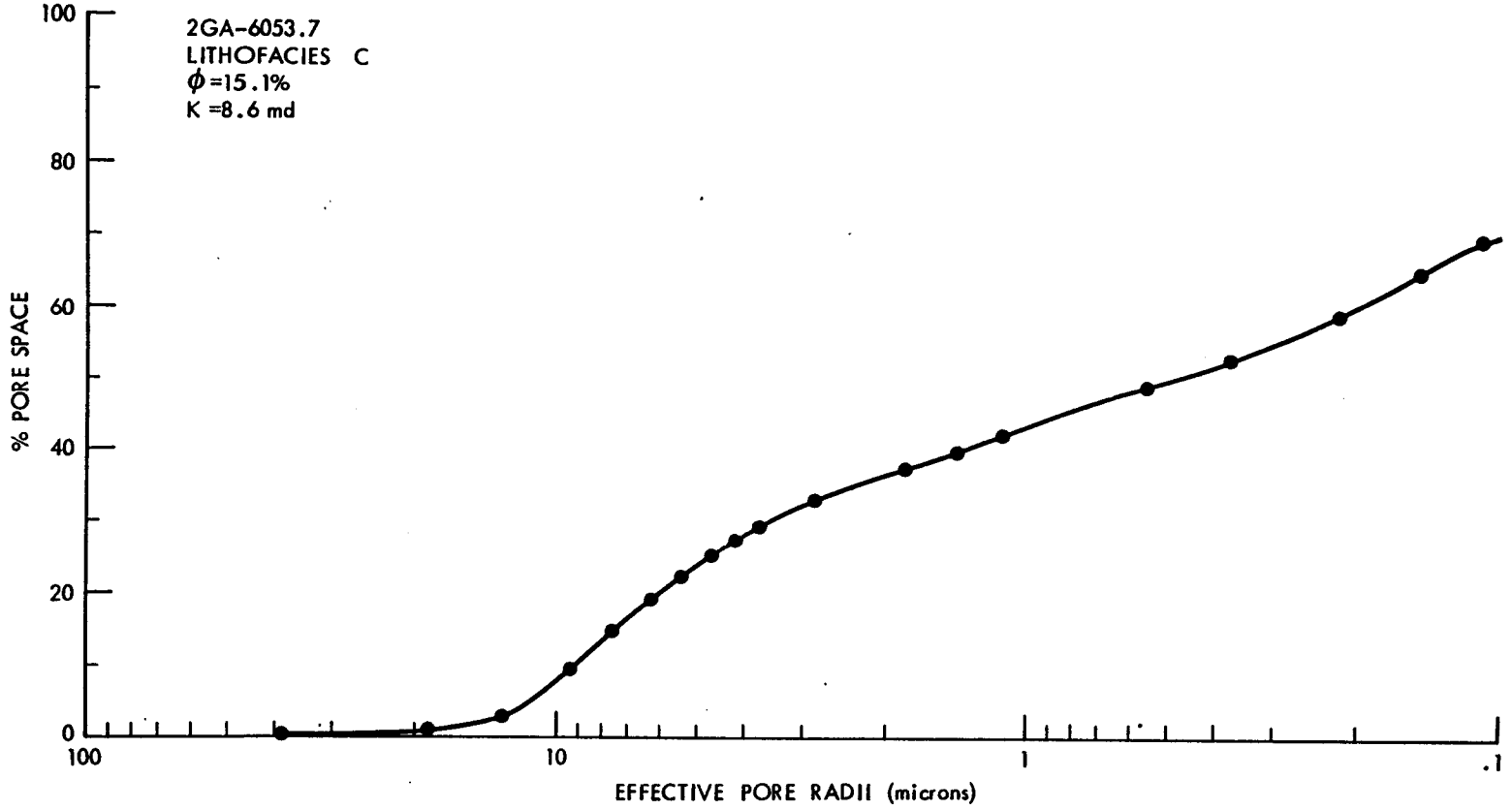
2GA-6053.7
LITHOFACIES C
ϕ=15.1%
K =8.6 md
100
80
60
40
20
0
% PORE SPACE
100
10
1
.1
EFFECTIVE PORE RADII (microns)

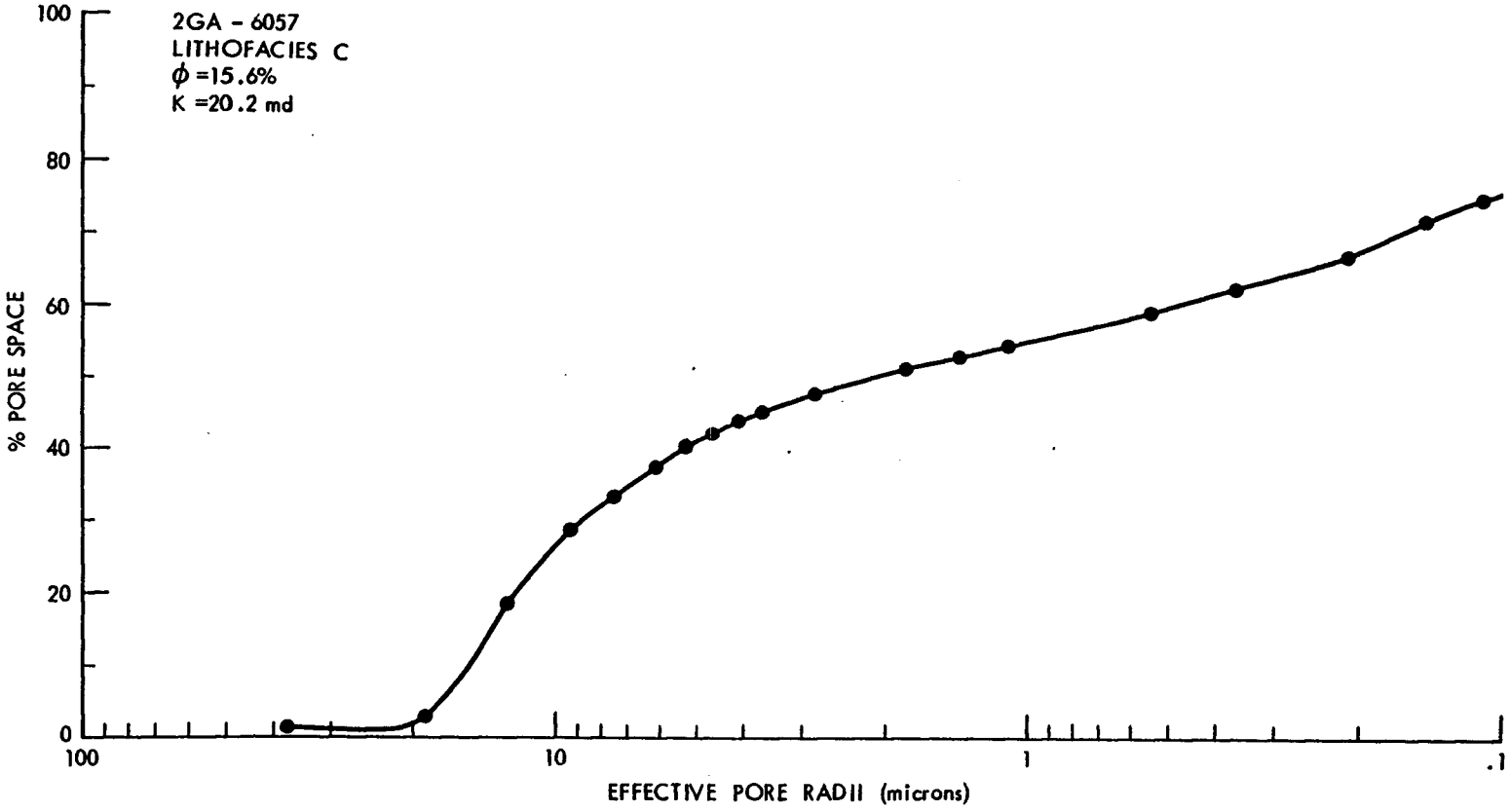
2GA - 6057
LITHOFACIES C
ϕ =15.6%
K =20.2 md
100
80
60
40
20
0
% PORE SPACE
100
10
1
.1
EFFECTIVE PORE RADII (microns)

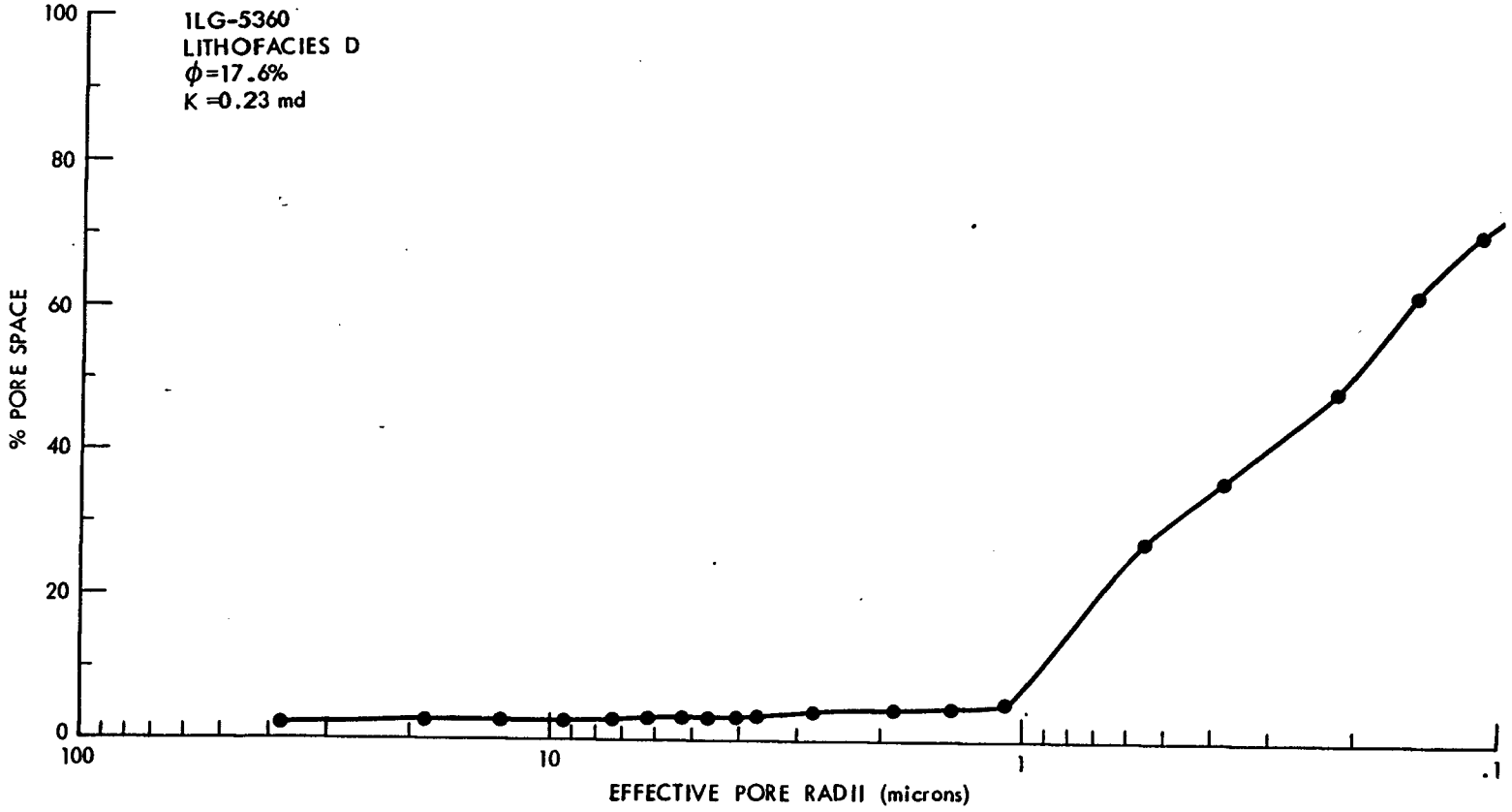
ILG-5360
LITHOFACIES D
ϕ=17.6%
K =0.23 md
100
80
60
40
20
0
% PORE SPACE
100
10
1
.1
EFFECTIVE PORE RADII (microns)

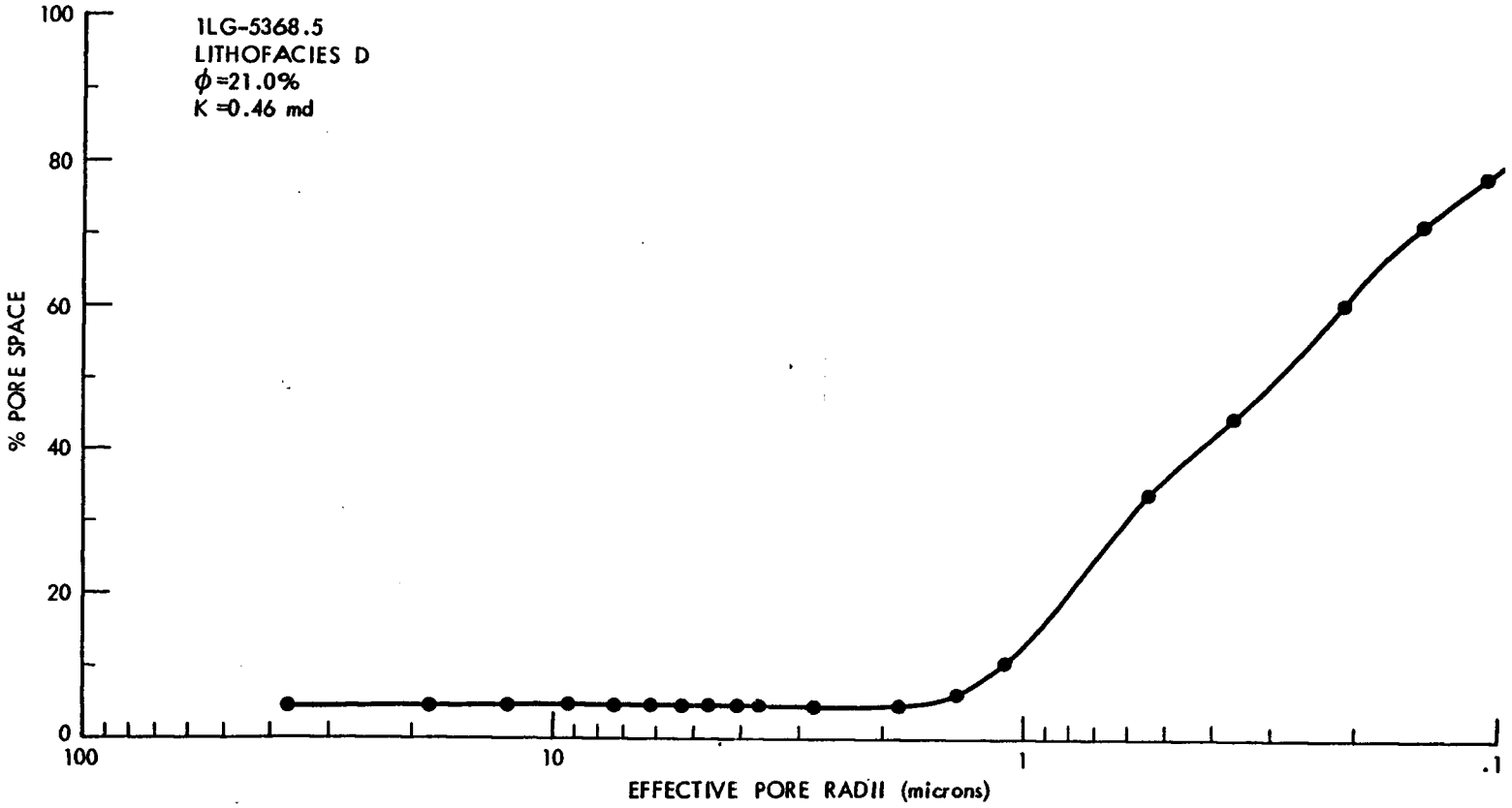
1LG-5368.5
LITHOFACIES D
ϕ=21.0%
K =0.46 md
100
80
60
40
20
0
% PORE SPACE
100
10
1
.1
EFFECTIVE PORE RADII (microns)

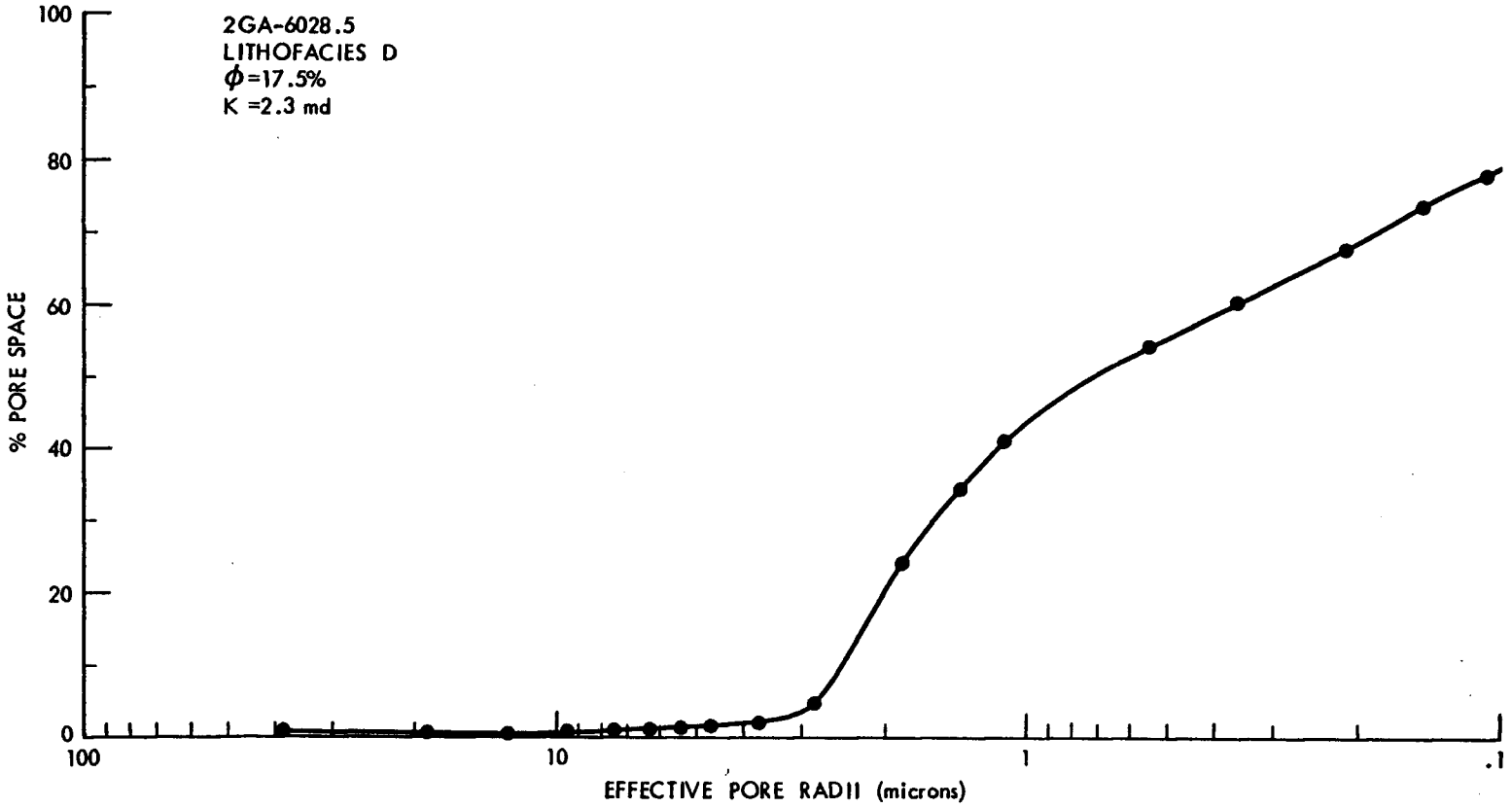
2GA-6028.5
LITHOFACIES D
ϕ=17.5%
K =2.3 md
100
80
60
40
20
0
% PORE SPACE
100
10
1
.1
EFFECTIVE PORE RADII (microns)

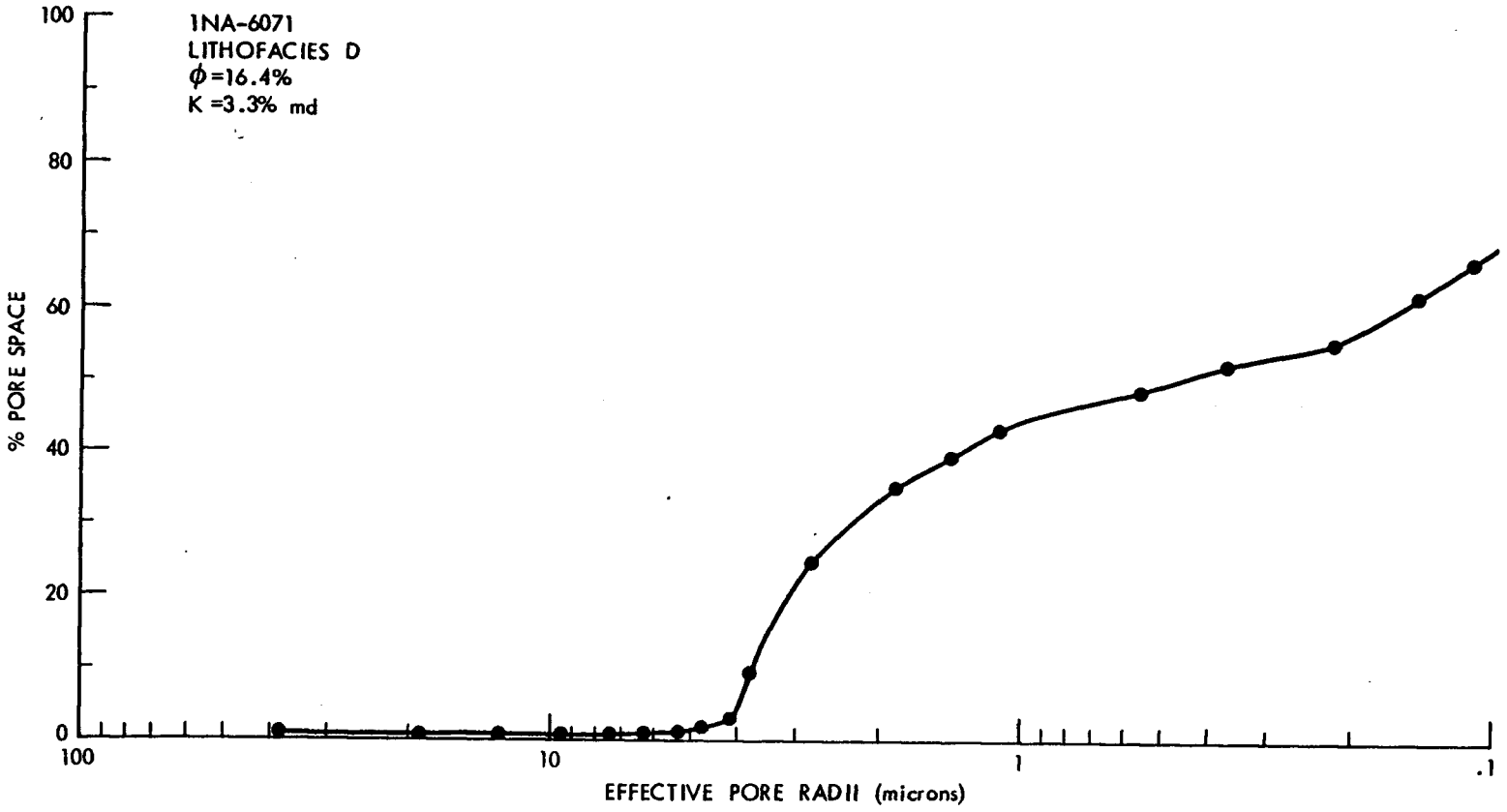
1NA-6071
LITHOFACIES D
ϕ=16.4%
K =3.3% md
100
80
60
40
20
0
% PORE SPACE
100
10
1
.1
EFFECTIVE PORE RADII (microns)

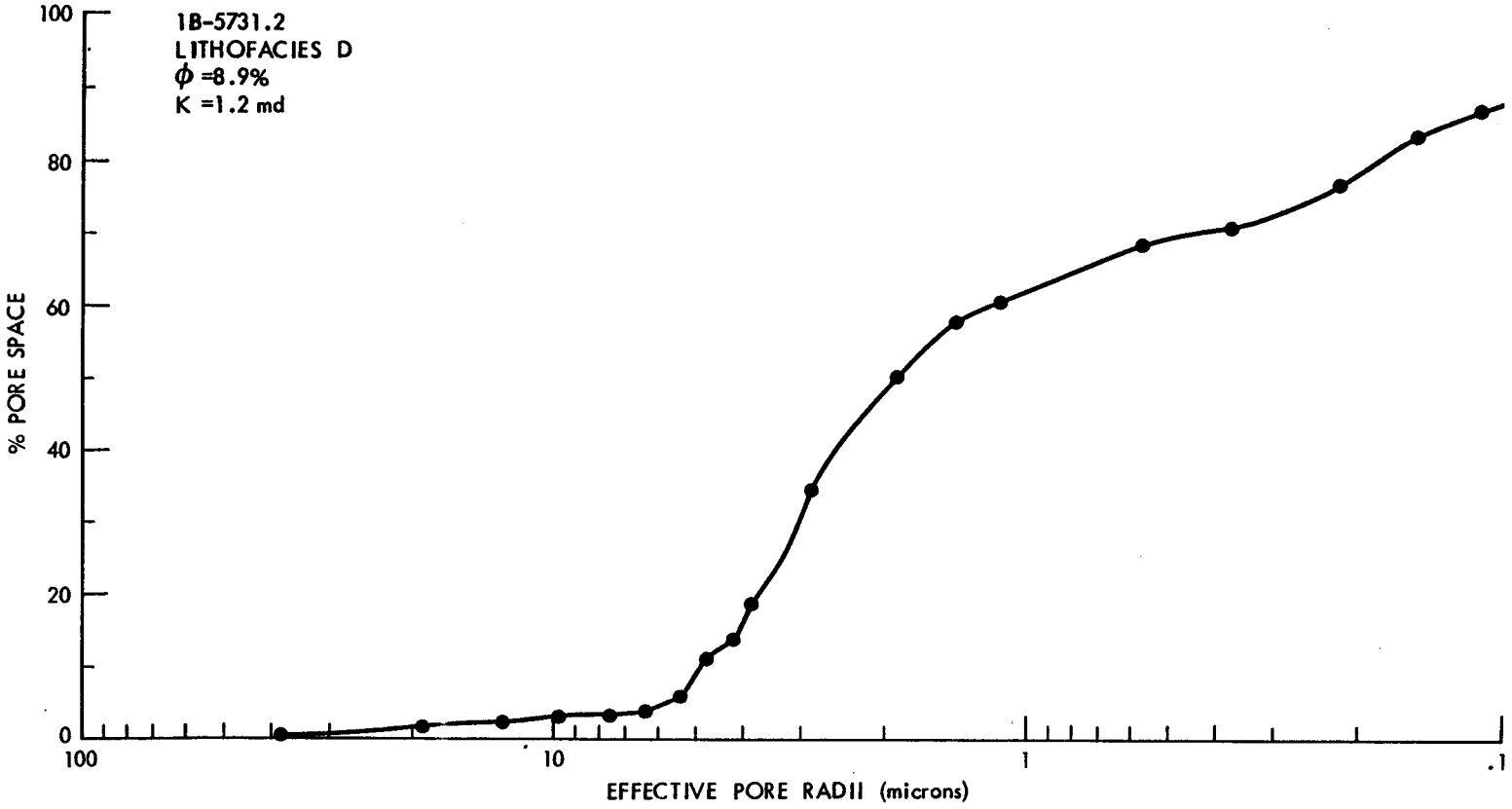
1B-5731.2
LITHOFACIES D
ϕ =8.9%
K =1.2 md
100
80
60
40
20
0
% PORE SPACE
100
10
1
.1
EFFECTIVE PORE RADII (microns)

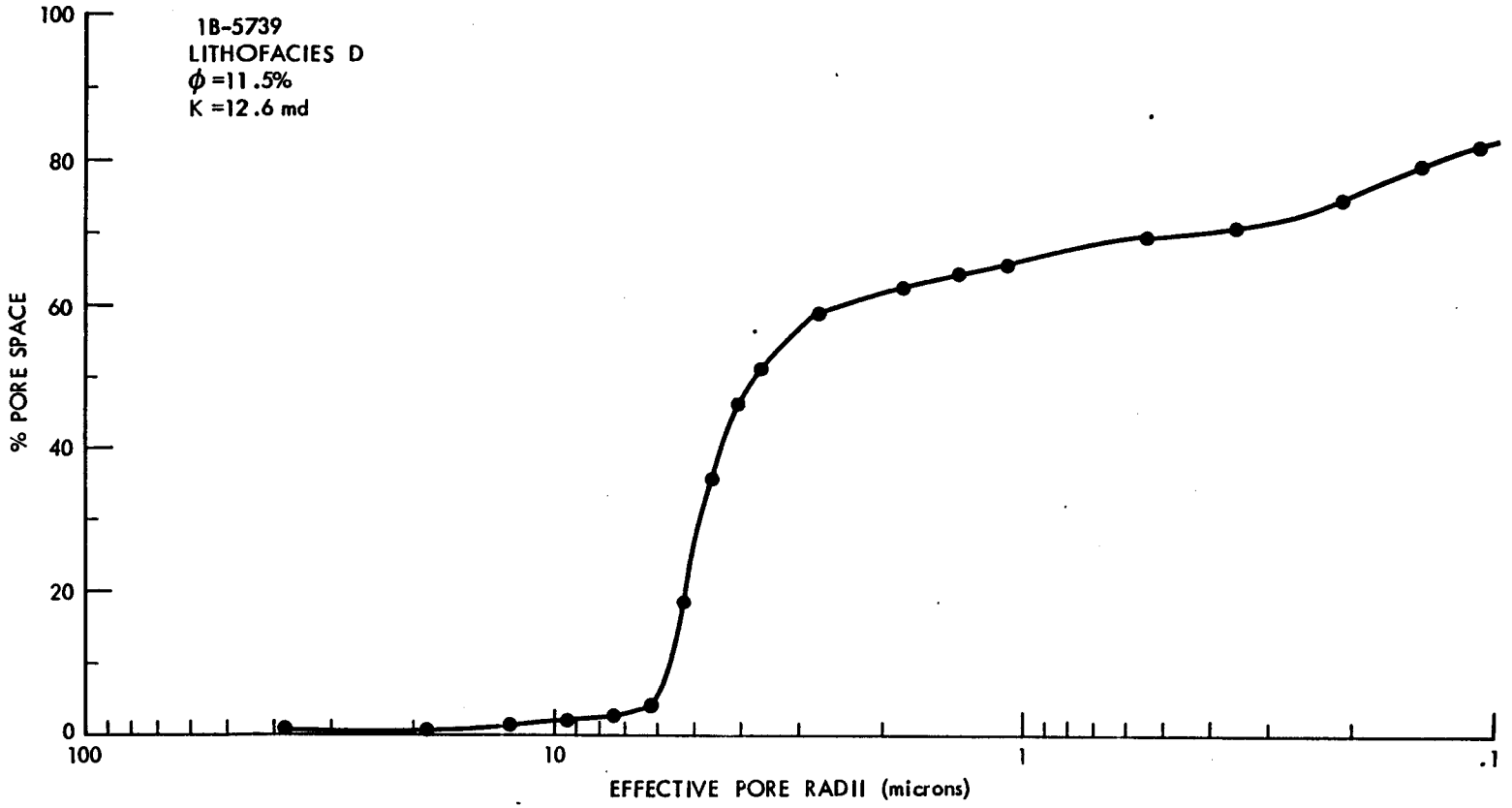
1B-5739
LITHOFACIES D
ϕ =11.5%
K =12.6 md
100
80
60
40
20
0
% PORE SPACE
100
10
1
.1
EFFECTIVE PORE RADII (microns)

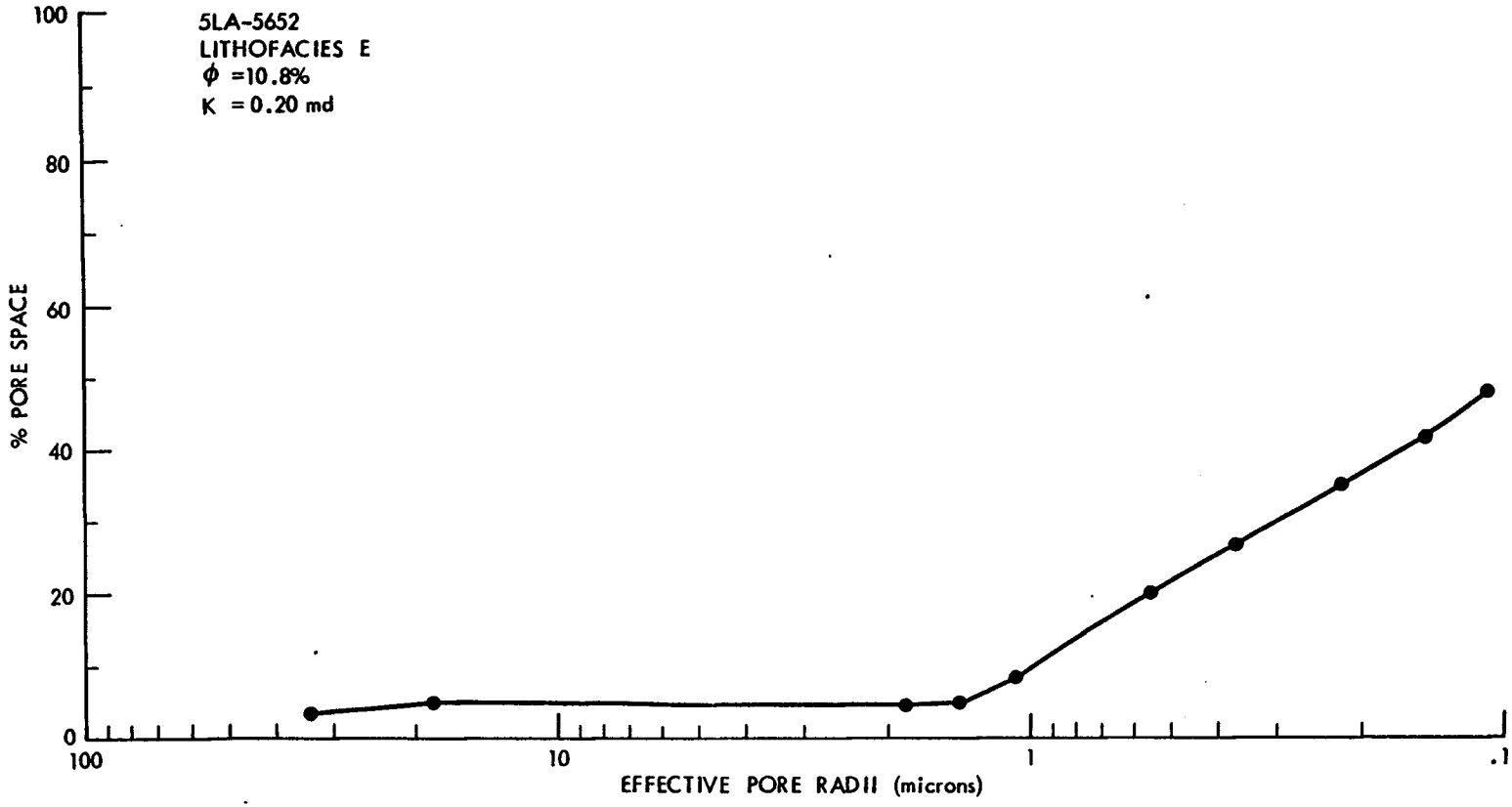
5LA-5652
LITHOFACIES E
ϕ =10.8%
K = 0.20 md
100
80
60
40
20
0
% PORE SPACE
100
10
1
.1
EFFECTIVE PORE RADII (microns)

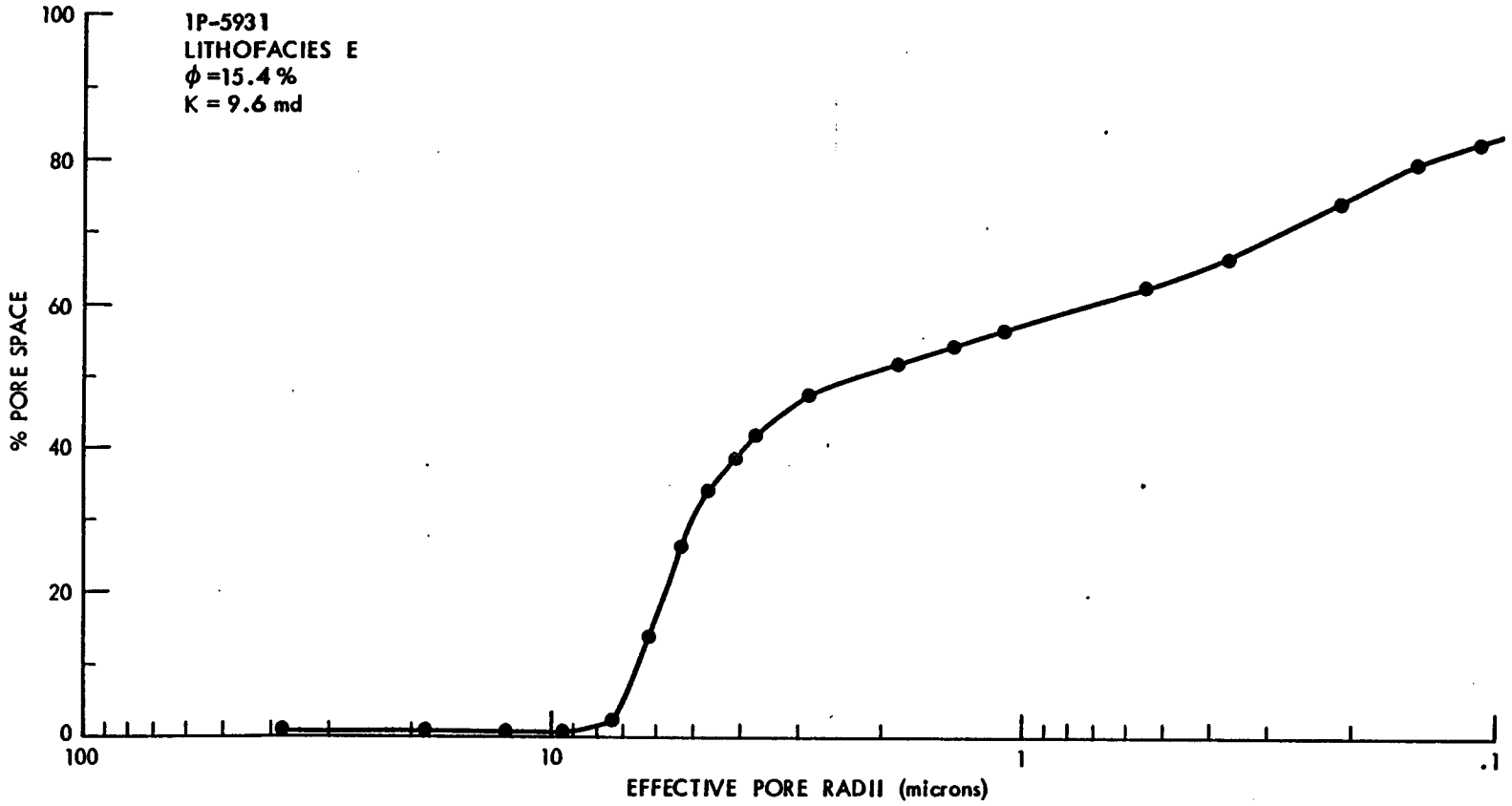
1P-5931
LITHOFACIES E
ϕ =15.4 %
K = 9.6 md
100
80
60
40
20
0
% PORE SPACE
100
10
1
.1
EFFECTIVE PORE RADII (microns)

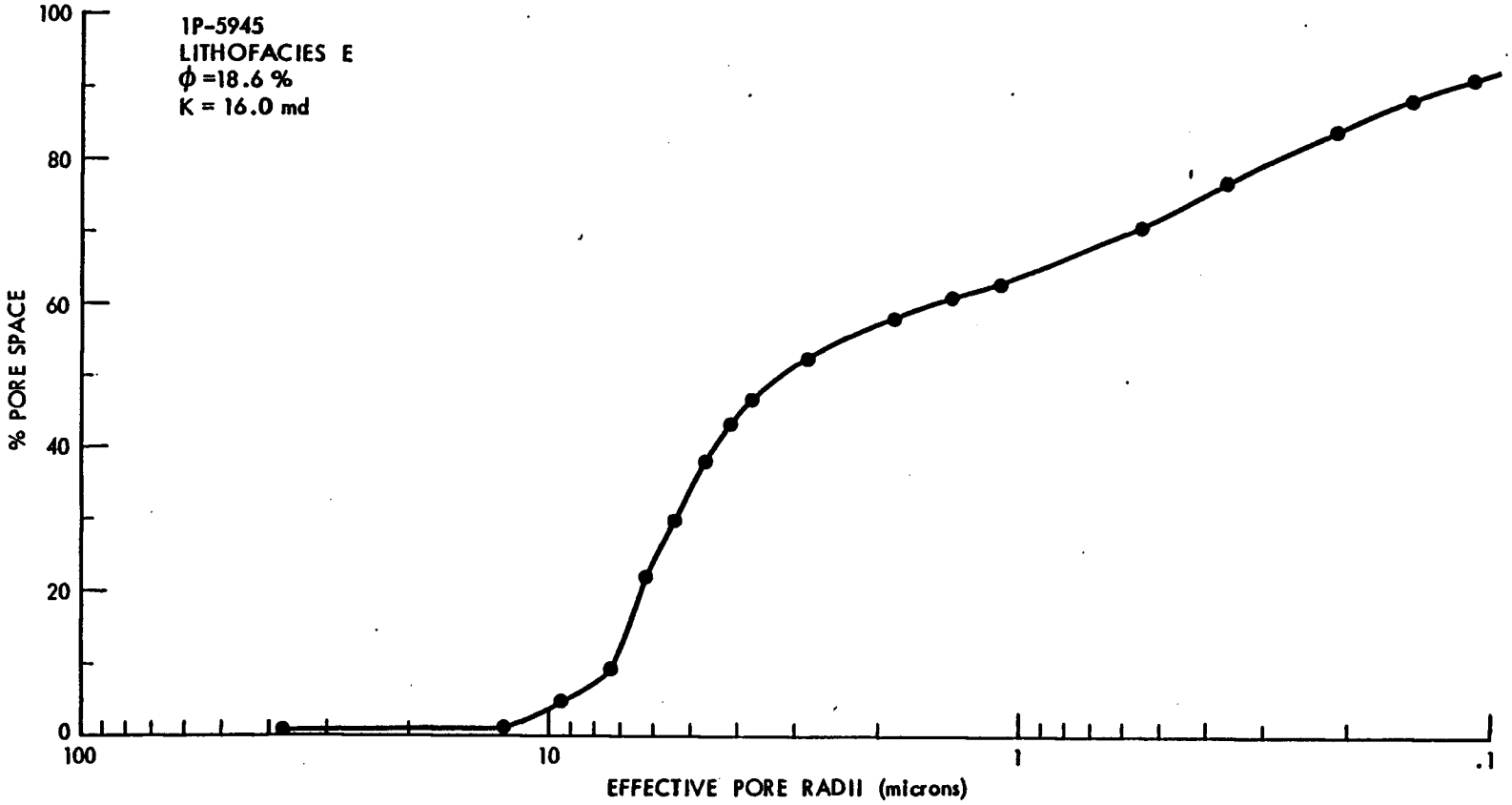
1P-5945
LITHOFACIES E
ϕ =18.6 %
K = 16.0 md
% PORE SPACE
100
80
60
40
20
0
100
10
1
.1
EFFECTIVE PORE RADII (microns)

APPENDIX C

DATA REDUCTION

Sample data is provided to show the process of reduction for microprobe analysis. Equations used to calculate porosity, permeability, and pore size distribution are included here. Statistics related to regression coefficients for porosity and permeabilty are also included.

REDUCTION OF MICROPROBE DATA

Data was taken as counts per 10 seconds in the following sequence: quartz (standard for background), analyzed standard (calcite for Ca, magnesite for Mg, siderite for Fe, rhodochrosite for Mn, strontianite for Sr), 3 to 6 points on sample grains, analyzed standard, and quartz. Average values in counts/sec were calculated. Data was then reduced as follows:

EX. Sample 1NA6064.5a

Ca	N^1	N*	Peak minus Background	$\frac{Im}{I\ Standard}$
Qtz	3.0	3	-	-
Calcite (Standard)	2,464	2,470	2,467	1.000
a (sample grain)	2,402	2,407	2,404	0.9745
Mg				
Qtz	46.6	47	-	-
Magnesite	7,906	8,033	7,986	1.000
a	123.7	124	77	0.0096
Fe				
Qtz	9.1	9	-	-
Siderite	1,775.6	1,779	1,770	1.000
a	17.0	17	8	0.0045
Mn				
Qtz	7.9	8	-	-
Rhodochrosite	1,904.3	1,907	1,899	1.000
a	17.7	18	10	0.0053

*corrected for deadtime at 1000 cts/sec or greater.

INA6064.5a

	K(Im/ISTD)	Beta Factors	K x B (weight fractions)
Ca	.9745	.9999	.9744
Mg	.0096	1.0883	.0104
Fe	.0045	1.0952	.0043
Mn	.0053	1.0970	.0058
	.9939		.9949

Beta factors are corrections calculated for each element/standard (Bence and Albee, 1968). For sample INA6064.5a weight fractions are:

$CaCO_3$ - .9744
$MgCO_3$ - .0104
$FeCO_3$ - .0043
$MnCO_3$ - .0058
.9949

These values were normalized when not close to zero.

Mole fractions were calculated by dividing by molecular weights.

$CaCO_3$ - .9735 = 97.9 mole %
$MgCO_3$ - .0123 = 1.2 mole %
$FeCO_3$ - .0037 = 0.4 mole %
$MnCO_3$ - .0058 = 0.5 mole %
.9946 99.0

CALCULATION OF PETROPHYSICAL PROPERTIES

Effective Porosity By Liquid Saturation

$$\text{Porosity (\%)} = \frac{\text{Fluid weight (grams)} = (\text{saturated plug weight} - \text{dry plug weight})}{\text{Plug length (cm)} \times \text{area (cm}^2\text{)} \times \text{fluid density (gm/cc)}}$$

$$= \frac{\text{Fluid volume (cc)}}{\text{Plug bulk volume (cc)}}$$

Permeability to Brine

Darcy's Law

Permeability (millidarcys) =

$$\frac{Q \times L \times M}{A \times \text{delta } P} \times 1000$$

Q = flow rate (cc/sec) - derived from 3 timings of a measured volume of brine passed through plug.

L = plug length (cm)

M = viscosity of fluid (cp) = 1 (assumed)

A = area of plug (cm^2)

delta P = pressure gradient (atm) - set on Ruska liquid permeameter (generally 1.8 atm.).

Pore Size Distribution

Percent pore space saturated with mercury at each increment of pressure increase is calculated by:

$$\frac{\text{volume mercury injected}}{\text{plug porosity} \times \text{bulk volume}} \times 100$$

This value for each pressure is plotted against pore aperture radius, calculated from pressure by: radius (microns) = $\frac{7.6}{\text{pressure (bars)}}$

(equation from Blatt, et al., 1980, p. 414)

STATISTICS OF POROSITY - PERMEABILITY

Regression coefficients were derived for the porosity (x) and permeability (y) values for each lithofacies. Because of the logarithmic distribution of permeability, these values in millidarcies were converted to the base 10 logarithm prior to calculating the regression coefficients (b's).

The significance of each value was tested by comparing t_s with the critical value t at .001. (Sokal and Rohlf, 1969, p. 423-424).

$$t_s = \frac{(b-0)}{S_b}$$

$$S_b = \frac{S^2Y \cdot X}{\text{sum } X^2}^{\frac{1}{2}} \quad \text{(expression to the } \tfrac{1}{2} \text{ power)}$$

Lithofacies A (population of 13)

$$t_s = \frac{(0.21 - 0)}{5.965} = 0.035$$

t at .001 (11) = 4.37

0.035 is less than 4.437

Lithofacies B (population 27)

$$t_s = \frac{(0.15)}{3.058} = 0.049$$

t at .001 (25) = 3.725

0.049 is less than 3.725

Lithofacies C (population of 19)

$$t_s = \frac{(0.35)}{2.824} \quad 0.124$$

t at .001(17) = 3.965

0.124 is less than 3.965

Lithofacies D (population of 15)

$$t_s = \frac{3.839}{5.893} = 0.651$$

t at .001(13) = 4.221

0.062 is less than 4.587

Lithofacies F (population of 5)

$$t_s = \frac{22.360}{9.866} = 2.266$$

t at .001(3) = 12.924

2.266 is less than 12.924

Given these results it appears that none of the regression coefficients are significantly different from 0. Thus for no lithofacies is the regression significantly deviant from 0 in a positive or negative direction. Further comparison of regression coefficients is unwarranted for these sample populations.